Dynamo Theory

Andrew D. Gilbert

School of Mathematical Sciences, University of Exeter, EX4 4QE, U.K.

Abstract

Dynamo theory concerns the generation of magnetic field from the flow of an electrically conducting fluid, relevant to the magnetic fields of the Earth, Sun, planets, stars and galaxies. The review focusses on fundamental dynamo mechanisms. The induction equation is derived as an approximation from Maxwell's equations and boundary conditions are discussed. Anti-dynamo theorems and upper bounds are considered, followed by discussion of some basic models, the Ponomarenko dynamo and G.O. Roberts dynamo. The application of dynamo theory to the Solar dynamo and the geodynamo is then reviewed, with the introduction of the alpha effect, and the concepts of alpha–squared and alpha–omega dynamos. Finally fast dynamos are considered.

Key words:
Magnetohydrodynamics, magnetic fields, induction equation, dynamo theory, electromagnetism, fluid flow

1 Introduction

Sir Joseph Larmor (1919), at a meeting of the British Association for the Advancement of Science, posed the question 'How could a rotating body such as the Sun become a magnet?' He gave three suggestions of how this might be achieved. In the first he refers to the motion of an electrically conducting fluid, plasma in the case of the Sun, and what happens if this flows through magnetic field lines:

> "Such internal motion induces an electric field acting on the moving matter: and if any conducting path around the Solar axis happens to be open, an electric current will flow round it, which may in turn increase the inducing magnetic field. In this way it is possible for the internal cyclic motion to act after the manner of the cycle of a self-exciting dynamo, and maintain a permanent magnetic field from insignificant beginnings, at the expense of some of the energy of the internal circulation."

This quotation summarises the basic idea of dynamo theory, that in the flow of an electrically conducting fluid magnetic fields may be amplified in the manner of an instability, hence the term *self-exciting*. The explanation requires some seed magnetic field to begin with, but indicates the possibility of growth of field and currents, sapping energy from the fluid motion. The growth will occur until finally the field is strong enough to affect the fluid flow through the Lorentz force. The growth must then saturate, and we are left with an equilibrated magnetohydrodynamic (MHD) system in which the field and flow evolve dynamically on an equal footing.

Such a system has many degrees of freedom, and we are now familiar with the idea that such systems can show complex behaviour. In hydrodynamics, one has only to think of turbulence, or the weather, or just the strange attractor in Lorenz's trio of ordinary differential equations, derived as a truncated model of fluid convection. This complexity is evident in the behaviour of Solar and terrestrial magnetic fields, which show complex structure in space and time, including complete reversals of polarity. This point was well appreciated by Larmor, who remarks that with a fluid mechanical origin changes in the magnetic field can be achieved by a flow causing the rearrangement of the electrical currents through the fluid. On the other hand with an explanation based on the microphysical material properties of the Earth or Sun it would be difficult to account for the observed time-dependence.

We now know that as well as the Earth and Sun, some planets, galaxies and many stars possess magnetic fields, and Larmor's explanation above is generally believed to be correct. However putting it on a firm mathematical footing took many decades, for a number of reasons. First, this explanation is not local, as it requires consideration of how electric currents flow throughout the region containing the conducting fluid. Mathematically, this means the solution of a partial differential equation, the induction equation, in this region with suitable boundary conditions. The Sun and Earth have a high degree of spherical symmetry in terms of their material properties and so the electrical conductivity is essentially a function of radius. Thus any region of conducting fluid will take the form of a sphere or a spherical shell, in which we may approximate the conductivity as a constant. The geometry is thus simple, but then to obtain amplification of magnetic fields, the fluid motion has to be complicated, making solution of the induction equation challenging. This should be contrasted with the situation in the laboratory, where it is not difficult to construct a self-exciting dynamo, without the use of a fluid, by an appropriate arrangement and motion of coils of wire; an attractive thought experiment is the disc dynamo (see Moffatt, 1978; Roberts, 1994). However this results in the electrical conductivity being a complicated function of space, which is unrealistic for an astrophysical dynamo. We shall always have in mind homogeneous fluid dynamos, consisting of a region with simple geometry, containing fluid of constant conductivity.

Secondly, it is very difficult to conduct experiments on such homogeneous fluid dynamos in the laboratory. The Sun and Earth are characterised by large length-scales. To allow a fluid dynamo to function at laboratory or industrial scales, it is necessary to stir a liquid metal, over volumes of the order of 1 m^3 and with velocities of the order of 10 m/s. With considerable expense and engineering expertise it is now becoming possible to achieve growth of magnetic fields using liquid sodium as the conducting fluid (Busse, 2000). Dynamo theory has certainly suffered from a lack of experimental input compared with other areas of fluid dynamics, and these experiments will be very welcome in stimulating future theory and testing ideas, particularly concerning the nonlinear equilibration of dynamos and the role of hydrodynamic turbulence.

However the immediate mathematical problem with developing Larmor's explanation was one of symmetry, or rather the need for symmetry breaking in a fluid dynamo. As we discussed above, the geometry of astrophysical objects is very simple, and this means that the fluid flows required to amplify magnetic fields have to be complicated. Dynamo action, that is the amplification of magnetic fields, cannot be obtained if too much symmetry is imposed on the magnetic field or on the fluid flow. The first result in this direction was obtained by Cowling (1934), who showed that an axisymmetric magnetic field cannot be sustained by fluid motion. This early anti-dynamo theorem suggested that Larmor's idea quoted above was probably doomed, especially since the Earth's field is approximately axisymmetric, with a dipole form. Perhaps it would be only a matter of time before a general result was proved prohibiting dynamo action in all fluid flows in regions of simple geometry.

It was not until the nineteen fifties that positive results in dynamo theory began to emerge. Bullard & Gellman (1954) expressed the dynamo problem in a sphere using a spherical harmonic expansion for the flow and magnetic field. This leads to coupled ordinary differential equations in radius for the field, which after truncation may be solved numerically. Bullard & Gellman (1954) obtained dynamo action in a simple flow, which acted as an important stimulus to dynamo theory even though the results were later discovered to be incorrect: this flow is not a dynamo, and the numerical resolution used was insufficient (Gibson & Roberts, 1969). The first real proofs of dynamo action were obtained by Herzenberg (1958) and Backus (1958), who employed intermittency in space and time respectively to allow mathematical analysis. In Herzenberg's model rotors, that is cylindrical regions of rotating fluid, are imagined embedded in a stationary fluid. If the rotors are small compared to their separation, then at each rotor the magnetic field due to the other is approximately uniform. The problem then becomes tractable, and magnetic field growth may be proved; it was also demonstrated in the laboratory, although using solid metal rotors in a metal block rather than a fluid (Lowes & Wilkinson, 1963, 1968). In Backus (1958) flow fields that are intermittent in time rather than space were introduced. During periods when the whole fluid is at rest the magnetic field decays with higher harmonics, having finer scales, decaying most rapidly. When the fluid motion occurs, this is sufficiently rapid that diffusion may be neglected. With careful tuning, it is possible to focus attention on just a few, large-scale field modes, and with this simplification again dynamo action could be proven.

The results of Backus and Herzenburg are important in establishing rigorously the existence of dynamos in fluid flows. The flows chosen are however rather artificial, and to explain astrophysical magnetic fields it is necessary to develop models closer to realistic convective fluid flows. Such models were developed initially by Parker (1955) who considered plumes and down drafts in the convection zone of the Sun. Hot fluid would rise and twist under the action of the Coriolis effect, leading to lifting and twisting of magnetic field lines. If one averages over many such eddies, one obtains a new transport effect with a coefficient denoted Γ by Parker (1955). This effect, combined with differential rotation, leads to magnetic field growth and travelling waves of dynamo activity, in agreement with Solar observations. These ideas were developed independently by Steenbeck, Krause & Rädler (1966) who used the coefficient α for the same transport effect, a terminology which has stuck to give us the *alpha effect*. At the same time Braginsky (1964a,b) developed related averaging methods for nearly axisymmetric flows and magnetic fields. These averaging ideas are precisely the right tool to use to simplify the dynamo problem. The true flows and magnetic fields are three-dimensional, and so Cowling's anti-dynamo theorem is not applicable. This three-dimensionality would make the induction equation very difficult to solve, but instead it is averaged away at an early stage, to leave much simplified equations which can be solved numerically with moderate effort, or in a few cases analytically.

These averaging ideas were extremely successful and led to a surge of activity in dynamo theory, which continues to this day. Although the fundamental ideas elucidated by Parker (1955) and Steenbeck, Krause & Rädler (1966) explain the basic behaviour of the Solar dynamo, it has proved much more difficult to refine these models, precisely because the underlying motions and magnetic fields are really three-dimensional and complicated. The Solar convection zone is highly turbulent and basic ideas, as to how the dynamo operates and where the magnetic field is located, have been revised in only the last two decades following the results of helioseismology, which probes the fluid motions below the Solar surface. The Earth's dynamo presents special problems, as the fluid flows are dominated by the Coriolis effect, leading to thin boundary layers which are difficult to resolve numerically. Moving further afield, observations from satellites have given information about the magnetic fields of planets and the moons of Jupiter. Magnetic fields of nearby stars have been measured, and some have star spots covering significant portions of their discs.

On a larger scale again, Faraday rotation of polarization planes in the presence of magnetic fields allows measurement of galactic fields, and this has led to the development of dynamo theory based on fluid flow in thin discs, relevant also to accretion discs. Modelling the dynamos in these astrophysical bodies presents serious difficulties for the analysis of all but the most idealised problems; even numerical exploration is very limited and will remain so with foreseeable computer power. On the theoretical side, there has been much interest in fast dynamos, where the field adopts fine-scale structure and grows rapidly in time. The other major theoretical problem concerns the nonlinear equilibration of dynamos, where there remains much uncertainty. What happens when the magnetic field becomes strong enough to suppress or modify convective fluid motions? Finally with dynamo action now established in laboratory experiments, new avenues are opened for theory and computations.

It is impossible in a review such as this to cover all the areas mentioned above in any detail, and the reader will no doubt find many omissions. The focus of this review is on fundamental generation mechanisms, rather than applications and numerical modelling. We begin with basic material, deriving the induction equation from Maxwell's equations, and then discussing anti-dynamo theorems and upper bounds. We go on to consider the Ponomarenko and G.O. Roberts dynamos: these show how generation of field can occur in simple flows and this leads to the introduction of the alpha effect. We survey application to dynamos in the Earth, Sun and galaxies, and discuss convective dynamos. We then return to basic dynamo mechanisms, giving some examples of fast dynamos and highlight the role of Lagrangian chaos in fluid flows. Finally we consider the nonlinear equilibration of dynamos and give a list of some open questions in dynamo theory.

There are many excellent books and reviews that the reader may wish to consult. Books on dynamo theory and MHD include Cowling (1957), Roberts (1967), Moffatt (1978), Parker (1979), Krause & Rädler (1980), Zeldovich, Ruzmaikin & Sokoloff (1983), and the collection Proctor & Gilbert (1994). For reviews of dynamo theory in general see Roberts (1987, 1994) and Roberts & Soward (1992), while for Solar and stellar dynamos see Brandenburg (1994), Weiss (1994) and Spiegel (1994). The special features of the geodynamo are discussed in Soward (1991), Fearn (1994) and Hollerbach (1996). For more information on fast dynamos see Childress (1992), Soward (1994a), Bayly (1994) and the monograph Childress & Gilbert (1995).

2 Governing equations

We begin by setting out Maxwell's equations and discuss their invariance under Lorentz transforms (see, for example, Landau & Lifshitz, 1975). For most astrophysical and geophysical applications, the time scale over which the electromagnetic field evolves is much longer than the time taken for light to cross the system. For example the Sun's field evolves over months and years, and the Earth's over decades and longer time scales. We may therefore approximate Maxwell's equations to obtain the induction equation, in which electromagnetic waves are filtered out and the magnetic field plays a central role. We then discuss boundary conditions and set out the dynamo problem.

Note that in this review we use ∂_x, ∂_y, etc., to denote derivatives, whereas subscripts, whether numbers or the letters x, y, z, denote components of vectors or other labels. We occasionally make reference to Abramowitz & Stegun (1972); for succinctness these references are given in footnotes as AS followed by the section or equation number.

2.1 Maxwell's equations

Maxwell's equations are

$$\nabla \cdot \boldsymbol{E} = \rho/\varepsilon, \tag{2.1}$$

$$\nabla \cdot \boldsymbol{B} = 0, \tag{2.2}$$

$$\nabla \times \boldsymbol{B} = \mu \boldsymbol{J} + \mu\varepsilon \partial_t \boldsymbol{E}, \tag{2.3}$$

$$\nabla \times \boldsymbol{E} = -\partial_t \boldsymbol{B}. \tag{2.4}$$

Here $\boldsymbol{E}$ is the electric field, $\boldsymbol{B}$ the magnetic field, $\boldsymbol{J}$ the electric current, and ρ the electric charge. We will assume here and below that the magnetic permeability μ and the dielectric constant ε are constant, taking their free space values. The speed of light c is defined by $c^{-2} = \varepsilon\mu$. We also have the equation for conservation of charge

$$\partial_t \rho + \nabla \cdot \boldsymbol{J} = 0, \tag{2.5}$$

which may be deduced from (2.1,2.3). We will eventually require a further equation, namely some constitutive relation between the electrical current $\boldsymbol{J}$ and the electromagnetic field, for example Ohm's law, but we defer consideration of this until we have further simplified the equations.

From Maxwell's equations it is possible to isolate the energy and momentum of the electromagnetic field. Suppose we have a continuum distribution of charge with density ρ and velocity $\boldsymbol{v}$. The corresponding current density is $\boldsymbol{J} = \rho\boldsymbol{v}$ and the Lorentz force per unit volume is

$$\boldsymbol{f} = \rho(\boldsymbol{E} + \boldsymbol{v} \times \boldsymbol{B}) = \rho\boldsymbol{E} + \boldsymbol{J} \times \boldsymbol{B}. \tag{2.6}$$

The rate of working of the Lorentz force on the charge distribution is

$$W = \boldsymbol{f} \cdot \boldsymbol{v} = \boldsymbol{E} \cdot \boldsymbol{J}. \tag{2.7}$$

Note that we could have several species of charges, for example ions and electrons, with different (overlapping) densities and velocities, say ρ_α, $\boldsymbol{v}_\alpha$. In this case we would incorporate a sum over the different species labelled by α.

The energy density of the electromagnetic field is given by

$$\mathcal{E} = \tfrac{1}{2}\varepsilon \boldsymbol{E}^2 + \tfrac{1}{2}\mu^{-1}\boldsymbol{B}^2, \tag{2.8}$$

and obeys the energy equation

$$\partial_t \mathcal{E} + \nabla \cdot \boldsymbol{P} = -W \qquad (\boldsymbol{P} = \mu^{-1}\boldsymbol{E} \times \boldsymbol{B}). \tag{2.9}$$

This equation represents conservation of energy; the Poynting vector $\boldsymbol{P}$ gives the flux of energy in the field, while W is the rate of transfer of energy to mechanical degrees of freedom. The momentum of the electromagnetic field may be identified with $c^{-2}\boldsymbol{P}$ and there is a corresponding transport equation

$$c^{-2}\partial_t P_j - \partial_i T_{ij} = -f_j, \tag{2.10}$$

where

$$T_{ij} = \varepsilon(E_i E_j - \tfrac{1}{2}\delta_{ij}\boldsymbol{E}^2) + \mu^{-1}(B_i B_j - \tfrac{1}{2}\delta_{ij}\boldsymbol{B}^2) \tag{2.11}$$

is the electromagnetic, or Maxwell, stress tensor.

2.2 Relativistic invariance and transformation properties

In dynamo theory we are interested in the induction of magnetic fields in a moving, fluid medium. The properties of the medium will be important, in particular its electrical conductivity. As mentioned above, at some point we will need to relate the electrical current $\boldsymbol{J}$ at a point to the local electric field. To do this we need to move into a frame that is comoving with the local fluid velocity $\boldsymbol{u}$ at a point and apply Ohm's law (and possibly derive other physical effects) in this frame. We thus need to know how electric and magnetic fields transform in moving frames, and this is far from clear at the outset. Maxwell's full theory is relativistically invariant, rather than Galilean invariant, and so to derive the transformation laws for the fields we will in this section set up electromagnetic theory using 4-vectors.

Let us consider contravariant 4-vectors with space–time coordinates written $x^\mu = (ct, \boldsymbol{x})$, where Greek indices run from 0 to 3. We also define the metric

$$g_{\mu\nu} = \mathrm{diag}(1, -1, -1, -1) = g^{\mu\nu} \tag{2.12}$$

and the covariant and contravariant derivatives

$$\partial_\mu \equiv \frac{\partial}{\partial x^\mu} = (c^{-1}\partial_t, \nabla), \quad \partial^\mu = (c^{-1}\partial_t, -\nabla). \tag{2.13}$$

Suppose a 4-vector $x^\mu = (ct, \boldsymbol{x})$ is given in a frame S. Then in a frame S' having a velocity $\boldsymbol{u}$ relative to S with aligned axes coincident at $t = 0$, the vector has components $x'^\mu = (ct', \boldsymbol{x}')$ related by the Lorentz transformation

$$x'^0 = \gamma(u)(x^0 - \boldsymbol{x}\cdot\boldsymbol{u}/c), \quad \boldsymbol{x}'_\parallel = \gamma(u)(\boldsymbol{x}_\parallel - x^0\boldsymbol{u}/c), \quad \boldsymbol{x}'_\perp = \boldsymbol{x}_\perp, \tag{2.14}$$

with

$$\gamma(u) = (1 - u^2/c^2)^{-1/2}. \tag{2.15}$$

Here subscripts $\parallel$ and $\perp$ denote components parallel and perpendicular to $\boldsymbol{u}$.

To set up the electromagnetic field in a relativistic form we first define potentials ϕ and $\boldsymbol{A}$ given by

$$\boldsymbol{B} = \nabla\times\boldsymbol{A}, \quad \boldsymbol{E} + \partial_t\boldsymbol{A} = -\nabla\phi \tag{2.16}$$

(using (2.2,2.4)). We can then introduce 4-vectors for the potential and electrical current

$$A^\mu = (\phi, c\boldsymbol{A}), \quad J^\mu = (\rho, \boldsymbol{J}/c). \tag{2.17}$$

The electromagnetic field 4-tensor is defined by

$$F_{\mu\nu} = \partial_\mu A_\nu - \partial_\nu A_\mu \tag{2.18}$$

and contains the electric and magnetic fields as components, explicitly

$$F_{\mu\nu} = \begin{pmatrix} 0 & E_1 & E_2 & E_3 \\ -E_1 & 0 & -cB_3 & cB_2 \\ -E_2 & cB_3 & 0 & -cB_1 \\ -E_3 & -cB_2 & cB_1 & 0 \end{pmatrix}. \tag{2.19}$$

We may also compute $F^{\mu\nu}$ using the form (2.12) of the metric and write these tensors both in a convenient compact notation as

$$F_{\mu\nu} = (\boldsymbol{E}, c\boldsymbol{B}), \quad F^{\mu\nu} = (-\boldsymbol{E}, c\boldsymbol{B}). \tag{2.20}$$

Using this same notation the tensor dual to $F^{\mu\nu}$ is given by

$$F^{*\mu\nu} = \tfrac{1}{2}\varepsilon^{\mu\nu\sigma\tau}F_{\sigma\tau} = (-c\boldsymbol{B}, -\boldsymbol{E}), \quad F^*_{\mu\nu} = (c\boldsymbol{B}, -\boldsymbol{E}), \tag{2.21}$$

(with $\varepsilon^{\mu\nu\sigma\tau}$ the completely anti-symmetric tensor satisfying $\varepsilon^{0123} = 1$) and here electric and magnetic fields become interchanged. The electromagnetic field has two relativistic scalar invariants

$$F_{\mu\nu}F^{\mu\nu} = 2(c^2\boldsymbol{B}^2 - \boldsymbol{E}^2), \quad F_{\mu\nu}F^{*\mu\nu} = -4c\boldsymbol{E}\cdot\boldsymbol{B}. \tag{2.22}$$

Finally, Maxwell's equations become

$$\partial_\mu F^{\mu\nu} = J^\nu/\varepsilon, \quad \partial_\mu F^{*\mu\nu} = 0, \tag{2.23}$$

while conservation of charge (2.5) follows from the antisymmetry of $F^{\mu\nu}$,

$$\partial_\mu J^\mu = 0. \tag{2.24}$$

If the Lorentz gauge $\partial_\mu A^\mu = 0$ is adopted, then we are left with the wave-equation

$$\partial_\mu \partial^\mu A^\nu = J^\nu/\varepsilon. \tag{2.25}$$

The equations (2.9,2.10) for energy and momentum may be summarised in another 4-tensor equation. The electromagnetic stress 4-tensor is

$$T^{\mu\nu} = -\varepsilon(F^{\mu\sigma}F^\nu{}_\sigma - \tfrac{1}{4}g^{\mu\nu}F^{\sigma\tau}F_{\sigma\tau}) \tag{2.26}$$

or explicitly, using obvious notation with $i, j = 1, 2, 3$,

$$T^{\mu\nu} = \begin{pmatrix} \mathcal{E} & c^{-1}P_j \\ c^{-1}P_i & -T_{ij} \end{pmatrix} \tag{2.27}$$

and so incorporates the electromagnetic energy $\mathcal{E}$ (2.8), Poynting vector $\boldsymbol{P}$ (2.9) and Maxwell stress tensor T_{ij} (2.11). Equations (2.9,2.10) amount simply to

$$\partial_\mu T^{\mu\nu} = -f^\nu, \tag{2.28}$$

where $f^\mu = (W/c, \boldsymbol{f})$ is the 4-force acting on the fluid.

From applying the Lorentz transformation (2.14) to the electromagnetic field tensor $F^{\mu\nu}$, we finally obtain how the electric and magnetic fields transform:

$$\boldsymbol{E}'_\parallel = \boldsymbol{E}_\parallel, \qquad \boldsymbol{E}'_\perp = \gamma(u)(\boldsymbol{E}_\perp + \boldsymbol{u}\times\boldsymbol{B}), \tag{2.29}$$

$$\boldsymbol{B}'_\parallel = \boldsymbol{B}_\parallel, \qquad \boldsymbol{B}'_\perp = \gamma(u)(\boldsymbol{B}_\perp - \boldsymbol{u}\times\boldsymbol{E}/c^2), \tag{2.30}$$

$$\rho' = \gamma(u)(\rho - \boldsymbol{J}\cdot\boldsymbol{u}/c^2), \qquad \boldsymbol{J}'_\parallel = \gamma(u)(\boldsymbol{J}_\parallel - \boldsymbol{u}\rho), \quad \boldsymbol{J}'_\perp = \boldsymbol{J}_\perp. \tag{2.31}$$

Note that the transformation properties of $\boldsymbol{E}$ and $\boldsymbol{B}$ are complicated because they form the components of the 4-tensor $F^{\mu\nu}$ rather than parts of individual 4-vectors.

We will not be using the full weight of Maxwell's equations, but a simpler system in which electromagnetic waves are filtered out. The key approximation is that velocities in the system under consideration should be much smaller than the speed of light c. We suppose that the system has typical spatial scale $\mathcal{L}$, time scale $\mathcal{T}$, and velocities $\boldsymbol{u}$ with

$$u \sim \mathcal{V} \equiv \mathcal{L}/\mathcal{T} \ll c, \tag{2.32}$$

where $\sim$ is here used to denote order of magnitude. In this case equation (2.4) gives the estimate

$$E \sim \mathcal{V}B. \tag{2.33}$$

This approximation means that the displacement current $\mu\varepsilon\partial_t\boldsymbol{E} = c^{-2}\partial_t\boldsymbol{E}$ may be dropped from (2.3) as it is negligible, a factor $\mathcal{V}^2/c^2$ smaller than $\nabla \times \boldsymbol{B}$. This leaves us with the *pre-Maxwell equations*

$$\nabla \cdot \boldsymbol{E} = \rho/\varepsilon, \tag{2.34}$$
$$\nabla \cdot \boldsymbol{B} = 0, \tag{2.35}$$
$$\nabla \times \boldsymbol{B} = \mu\boldsymbol{J}, \tag{2.36}$$
$$\nabla \times \boldsymbol{E} = -\partial_t\boldsymbol{B}. \tag{2.37}$$

Using (2.1,2.3) gives the estimates

$$\rho \sim \varepsilon\mathcal{V}B/\mathcal{L}, \quad J \sim B/\mu\mathcal{L}, \tag{2.38}$$

which means that (2.5) may be approximated by

$$\nabla \cdot \boldsymbol{J} = 0, \tag{2.39}$$

and the Lorentz force reduces to

$$\boldsymbol{f} = \boldsymbol{J} \times \boldsymbol{B}. \tag{2.40}$$

The key estimate (2.33) means that the electric field drops out of the electromagnetic energy and the stress tensor, leaving us with

$$\mathcal{E} = \tfrac{1}{2}\mu^{-1}\boldsymbol{B}^2, \quad T_{ij} = \mu^{-1}(B_iB_j - \tfrac{1}{2}\delta_{ij}\boldsymbol{B}^2). \tag{2.41}$$

The energy equation remains unchanged,

$$\partial_t\mathcal{E} + \nabla \cdot \boldsymbol{P} = -W \qquad (\boldsymbol{P} = \mu^{-1}\boldsymbol{E} \times \boldsymbol{B},\ W = \boldsymbol{E} \cdot \boldsymbol{J}), \tag{2.42}$$

but the Poynting vector drops out of (2.10) and this becomes sadly nothing more than a vector identity. In this approximation the electromagnetic field possesses energy, but carries no momentum.

Now we return to Ohm's law. We have in mind a moving fluid with a velocity field $\boldsymbol{u}(\boldsymbol{x}, t)$. At a given point and time, we go into a comoving frame, velocity $\boldsymbol{u}$, where we measure modified fields given by

$$\boldsymbol{E}' = \boldsymbol{E} + \boldsymbol{u} \times \boldsymbol{B}, \quad \boldsymbol{B}' = \boldsymbol{B}, \quad \boldsymbol{J}' = \boldsymbol{J}, \tag{2.43}$$

within the current approximations, using (2.29–2.31) with $\gamma(u) \simeq 1$. In this frame we wish to relate the current to the ambient electric and magnetic fields, and the simplest relation to impose is Ohm's law

$$\boldsymbol{J}' = \sigma \boldsymbol{E}', \tag{2.44}$$

where σ is the electrical conductivity of the medium. Back in the original frame we have

$$\boldsymbol{J} = \sigma(\boldsymbol{E} + \boldsymbol{u} \times \boldsymbol{B}). \tag{2.45}$$

This is Ohm's law in a moving medium, and a key part of the dynamo process: motion across a field can generate a perpendicular current. This relation is used very widely in dynamo theory, but is only an approximation, whose validity depends on the material making up the moving fluid. We will not do so, but at this point one could include other effects. For example the process of ambipolar diffusion, important in galactic dynamos, gives a term of the form $(\boldsymbol{J} \times \boldsymbol{B}) \times \boldsymbol{B}$ on the right-hand side of (2.45) (see, for example, Zweibel, 1988; Brandenburg & Zweibel, 1995). The Hall effect is considered by Galanti, Kleeorin & Rogachevskii (1994), which gives rise to an extra term proportional to $\boldsymbol{B} \times \boldsymbol{J}$.

From Ohm's law (2.45) and the pre-Maxwell equations (2.36,2.37) we may deduce the induction equation

$$\partial_t \boldsymbol{B} = \nabla \times (\boldsymbol{u} \times \boldsymbol{B}) - \nabla \times (\eta \nabla \times \boldsymbol{B}). \tag{2.46}$$

This is the fundamental equation studied in astrophysical and laboratory MHD, and

$$\eta = (\sigma\mu)^{-1} \tag{2.47}$$

is the *magnetic diffusivity*. It is important to note that high conductivity corresponds to low diffusivity and *vice versa*. We must still impose $\nabla \cdot \boldsymbol{B} = 0$, although note that if satisfied at some time t it must be satisfied subsequently, by taking the divergence of (2.46). Equations (2.34,2.45) give the electric charge with $\nabla \cdot (\boldsymbol{u} \times \boldsymbol{B}) = -\rho/\varepsilon$, but this is now decoupled and of little importance to us.

Let the total magnetic energy in a bounded volume V be written as

$$\mathcal{E}_V(t) = \frac{1}{2\mu} \int_V |\boldsymbol{B}|^2 \, dV, \tag{2.48}$$

then using (2.42,2.45) we obtain

$$\partial_t \mathcal{E}_V + \mu^{-1} \int_{\partial V} \boldsymbol{n} \cdot (\boldsymbol{E} \times \boldsymbol{B})\, dS = -\mu\eta \int_V |\boldsymbol{J}|^2\, dV - \int_V \boldsymbol{u} \cdot \boldsymbol{J} \times \boldsymbol{B}\, dV, \quad (2.49)$$

where ∂V is the surface bounding V and $\boldsymbol{n}$ is a field of outward, normal unit vectors. On the right-hand side it may be seen that magnetic energy is lost through Ohmic dissipation (first term) and exchanged with kinetic energy through working by the Lorentz force (second term). The surface integral on the left-hand side represents the Poynting flux of energy out of V.

The induction equation is closely analogous to the vorticity equation. If we assume incompressible flow

$$\nabla \cdot \boldsymbol{u} = 0, \quad (2.50)$$

as we shall do from now on, and constant diffusivity η or conductivity σ in the region under consideration, then we may rewrite (2.46) as

$$\partial_t \boldsymbol{B} + \boldsymbol{u} \cdot \nabla \boldsymbol{B} = \boldsymbol{B} \cdot \nabla \boldsymbol{u} + \eta \nabla^2 \boldsymbol{B}. \quad (2.51)$$

This is similar to the vorticity equation with $\boldsymbol{B}$ replacing vorticity $\boldsymbol{\omega} = \nabla \times \boldsymbol{u}$, and now decoupled from the fluid flow. In the equation are terms representing transport, stretching and diffusion of the magnetic field. In the limit $\eta = 0$ of a perfect conductor ($\sigma = \infty$) the magnetic flux through a material surface is conserved, as similarly are circulations in inviscid fluid flow (see for example, Batchelor, 1967). Mathematically the terms $\boldsymbol{u} \cdot \nabla \boldsymbol{B} - \boldsymbol{B} \cdot \nabla \boldsymbol{u}$ represent a Lie derivative, and indicate that the magnetic field is Lie-dragged in the fluid flow for $\eta = 0$: magnetic vectors evolve like the displacements between infinitessimally close fluid elements. Note one difference between vorticity and magnetic fields, that dissipation at the microscopic level comes from currents $\boldsymbol{J} = \mu^{-1} \nabla \times \boldsymbol{B}$ in the case of magnetic fields, but through the square of the symmetric rate-of-strain tensor $e_{ij} = \frac{1}{2}(\partial_i u_j + \partial_j u_i)$ for fluid flow.

Finally note that if $\boldsymbol{B}$ is written in terms of a magnetic potential $\boldsymbol{B} = \nabla \times \boldsymbol{A}$, then (2.46) may be uncurled to yield

$$\partial_t \boldsymbol{A} = \boldsymbol{u} \times (\nabla \times \boldsymbol{A}) + \eta \nabla^2 \boldsymbol{A} + \nabla F, \quad (2.52)$$

where F is a scalar field reflecting the gauge freedom in defining $\boldsymbol{A}$. Note that uncurling an equation such as this in general only gives a locally defined scalar field F. However in a space for which all closed curves may be continuously contracted to a point, such as a sphere or spherical shell, F may be defined globally (that is, as a single-valued function). In a space that is periodic in one or more directions not all closed curves are contractible, and this requires care in defining such potentials; in dynamo theory a global definition of such a scalar is usually possible provided there is no mean magnetic field in the direction of periodicity.

It is often necessary to consider situations in which the medium undergoes a change in physical properties across a surface S. We consider only the simplest situation in which S is a fixed closed surface. We take there to be no flow across it, $\boldsymbol{n} \cdot \boldsymbol{u} = 0$, where $\boldsymbol{n}$ is a field of outward-pointing normal unit vectors on S. We suppose the discontinuity occurs only in the conductivity σ, or equivalently the diffusivity η, which is much the most important situation in dynamo theory. Except for jumps at such surfaces, we take σ or η to be constant in each region of space from now on.

If we integrate the pre-Maxwell equations (2.34–2.37) over small volumes and contours cutting S, we obtain the jump conditions

$$[\boldsymbol{n} \cdot \boldsymbol{E}] = \rho_S/\varepsilon, \tag{2.53}$$
$$[\boldsymbol{n} \cdot \boldsymbol{B}] = 0, \tag{2.54}$$
$$[\boldsymbol{n} \times \boldsymbol{B}] = \mu \boldsymbol{J}_S, \tag{2.55}$$
$$[\boldsymbol{n} \times \boldsymbol{E}] = 0. \tag{2.56}$$

Here $[\cdot]$ represents the value just outside S minus that just inside, and ρ_S and $\boldsymbol{J}_S$ are possible surface charge and current distributions.

Let subscripts 'i' and 'e' denote values inside and outside S, and to fix ideas suppose that the conductivity inside S is finite and non-zero, $0 < \sigma_{\mathrm{i}} \equiv \sigma < \infty$. The nature of the boundary conditions then depends on the conductivity σ_{e} outside. We will also let V_{i} be the volume inside S, and V_{e} the volume outside, leaving V to represent a general volume, specified in the context used.

If the external conductivity σ_{e} is finite, then it is impossible to maintain a surface current $\boldsymbol{J}_S$. (Such a surface current could only arise from the limit of an external perfect conductor, in which the current $\boldsymbol{J} \to \infty$ just outside S as $\sigma_{\mathrm{e}} \to 0$.) Given $\boldsymbol{J}_S = 0$, we are left with five scalar boundary conditions (2.54–2.56). Of these only four are independent: in the original pre-Maxwell system, if (2.35) is satisfied initially it is subsequently from (2.37) and this dependence is carried over to the boundary conditions.

In the absence of such surface currents, boundary conditions (2.55,2.56) guarantee the continuity of the normal component of the Poynting vector field $\boldsymbol{P}$ across S (see (2.42)), and so the conservation of energy across S. It is useful to write down an equation for the total magnetic energy. The magnetic energy in any volume V is still governed by (2.49), which was derived allowing for variable conductivity. Provided the magnetic field falls off sufficiently quickly at large distances that the surface integral tends to zero as V is enlarged to include all of space, then we obtain

$$\partial_t \mathcal{E}_V = -\mu\eta \int_V |\boldsymbol{J}|^2 \, dV - \int_V \boldsymbol{u} \cdot \boldsymbol{J} \times \boldsymbol{B} \, dV \qquad (V = V_\mathrm{i} \cup V_\mathrm{e}). \tag{2.57}$$

2.4.1 Insulating boundary conditions

A particularly important limit is that of an insulator outside S, for which $\sigma_\mathrm{e} = 0$ or $\eta_\mathrm{e} = \infty$, modelling for example the poorly-conducting mantle outside the Earth's liquid metal core. In this case $\boldsymbol{J} = 0$ in V_e from (2.45) and so $\boldsymbol{B}$ is a potential field, determined from a scalar potential $\boldsymbol{B} = \nabla\chi$ with $\nabla^2\chi = 0$ from (2.35). Any flow $\boldsymbol{u}$ in V_e is irrelevant. Conditions (2.54,2.55) (with $\boldsymbol{J}_S = 0$) require all components of field to be continuous across S,

$$[\boldsymbol{B}] = 0. \tag{2.58}$$

If S is a sphere of radius a and the exterior field is required to decay at infinity, as we shall always assume for insulating boundary conditions, then χ may be written as a spherical harmonic expansion in spherical polar coordinates (r, θ, ϕ),

$$\chi = \sum_{l=1}^{\infty} \sum_{m=-l}^{l} \chi_{lm}(t) \, r^{-l-1} Y_{lm}(\theta, \phi) \qquad (\chi^*_{l,m} = \chi_{l,-m}). \tag{2.59}$$

Here $Y_{lm}(\theta, \phi)$ are spherical harmonics

$$Y_{lm}(\theta, \phi) = (-1)^m \left(\frac{(2l+1)(l-m)!}{4\pi(l+m)!} \right)^{1/2} P_{lm}(\cos\theta) e^{im\phi}, \tag{2.60}$$

normalised so that

$$(Y_{lm}, Y_{l'm'})_{\theta,\phi} = \delta_{ll'}\delta_{mm'}, \quad (f, g)_{\theta,\phi} \equiv \int_{\phi=0}^{2\pi} \int_{\theta=0}^{\pi} \overline{f} g \, \sin\theta \, d\theta \, d\phi. \tag{2.61}$$

The term $l = m = 0$ in (2.59) is omitted to avoid a net flux of $\boldsymbol{B}$ out of S, which is forbidden by (2.35). Note that at large distances

$$\boldsymbol{B} = O(r^{-3}) \qquad (r \to \infty). \tag{2.62}$$

If on the other hand S is the plane $z = 0$, with exterior $z > 0$, then the spatially decaying external potential field is given by

$$\phi = \sum_{m,n} \phi_{mn}(t) \exp(L^{-1}(imx + iny - z\sqrt{m^2 + n^2})) \quad (\phi_{0,0} = 0, \phi^*_{m,n} = \phi_{-m,-n}), \tag{2.63}$$

where we have taken the layer to be periodic in x and y with periodicity length $2\pi L$.

In considering conservation of energy we have to be careful, as in the limit of an insulator the current $\boldsymbol{J}$ and the conductivity $\sigma_\mathrm{e} = (\eta_\mathrm{e}\mu)^{-1}$ tend to zero together in V_e, the region outside S, making the first integral on the right-hand side of (2.57), the Ohmic dissipation, potentially ill-defined. However if we consider the evolution of the magnetic energy in the external region V_e by differentiating (2.48) for $V = V_\mathrm{e}$ with respect to time, and using $\boldsymbol{J} = 0$, (2.36) and (2.37), it may be checked that the rate of change of energy in V_e is equal to the Poynting flux of energy into S, with no contribution from Ohmic dissipation. Since this flux is continuous across S as discussed above, combining it with (2.49) for $V = V_\mathrm{i}$ yields an equation for the total magnetic energy $\mathcal{E}$ in the system

$$\partial_t \mathcal{E}_V = -\mu\eta \int_{V_\mathrm{i}} |\boldsymbol{J}|^2 \, dV - \int_{V_\mathrm{i}} \boldsymbol{u}\cdot\boldsymbol{J}\times\boldsymbol{B} \, dV \qquad (V = V_\mathrm{i} \cup V_\mathrm{e}). \tag{2.64}$$

Here the sources and sinks of energy on the right-hand side are only non-zero inside S, in V_i, whereas the energy $\mathcal{E}_V$ includes that from field inside and outside S.

2.4.2 Perfectly conducting boundary conditions

At the other extreme, the region V_e outside S could be a perfect conductor with $\sigma_\mathrm{e} = \infty$, or equivalently $\eta_\mathrm{e} = 0$. There will then generally be a surface current $\boldsymbol{J}_S$ on S determined by (2.55), which leaves (2.54, 2.56) as the only useful boundary conditions. Obviously a magnetic field can be trapped in the perfect conductor outside S, and will be static if there is no flow, from (2.51) with $\eta_\mathrm{e} = 0$. If however there is no magnetic field outside S initially, then this will remain the case and from (2.45) there must also be no electric field, $\boldsymbol{E} = 0$ outside. Then using $\boldsymbol{n}\cdot\boldsymbol{u} = 0$ on S and (2.45), the boundary conditions (2.54, 2.56) to be applied to the field just inside S become

$$\boldsymbol{n}\cdot\boldsymbol{B} = 0, \quad \boldsymbol{n}\times\boldsymbol{J} = 0 \tag{2.65}$$

in general, or

$$B_z = 0, \quad \partial_z B_x = \partial_z B_y = 0 \tag{2.66}$$

if S is the plane $z = 0$, and

$$B_r = 0, \quad \partial_r(rB_\theta) = \partial_r(rB_\phi) = 0 \tag{2.67}$$

if S is the sphere $r = a$.

For the perfect conductor we again have to treat energy with care, as we have a limiting surface current in a region in which the conductivity tends to infinity, giving an *a priori* ill-defined Ohmic dissipation in (2.57). Here we should use equation (2.49) for a volume $V = V_\mathrm{i}$ lying just inside S, that is, to exclude any surface currents. Since the electric field $\boldsymbol{E}$ must vanish outside S, $\boldsymbol{n} \times \boldsymbol{E}$ must vanish just inside S by (2.56) and so the Poynting flux out of V_i vanishes to leave the energy equation

$$\partial_t \mathcal{E}_{V_\mathrm{i}} = -\mu\eta \int_{V_\mathrm{i}} |\boldsymbol{J}|^2 \, dV - \int_{V_\mathrm{i}} \boldsymbol{u} \cdot \boldsymbol{J} \times \boldsymbol{B} \, dV, \tag{2.68}$$

where V_i is the interior of S. Any surface currents are not implicated in the energy dissipation.

2.5 Definition of a dynamo

We shall first give a very specific definition of a kinematic dynamo and then relax the geometrical framework, while considering the essential features that need to be retained.

Let S be the sphere $r = a$ containing conducting fluid, with volume-preserving flow field $\boldsymbol{u}(\boldsymbol{x}, t)$, conductivity σ and diffusivity η. Suppose all of space outside S is insulating, and that the field decays as $r \to \infty$. From the above discussion we have to solve the induction equation (2.51) with some initial condition and the boundary condition (2.58) that the field be continuous with the external potential field (2.59). We may then evolve the magnetic field in time and measure its energy

$$\mathcal{E}_V(t) = \frac{1}{2\mu} \int_V |\boldsymbol{B}|^2 \, dV \qquad (V = V_\mathrm{i} \cup V_\mathrm{e}). \tag{2.69}$$

The flow $\boldsymbol{u}(\boldsymbol{x}, t)$ is a *dynamo* if, for some initial condition and diffusivity $\eta > 0$, the energy does not tend to zero as $t \to \infty$. We can usually define a dynamo growth rate $\gamma(\eta)$ by

$$\gamma(\eta) = \sup_{\boldsymbol{B}_0} \limsup_{t\to\infty} \frac{1}{2t} \log \mathcal{E}_V(t), \tag{2.70}$$

and say that the flow $\boldsymbol{u}$ is a dynamo if $\gamma(\eta) \geq 0$ for some $\eta > 0$. Here $\boldsymbol{B}_0$ is the initial condition, taken to have finite energy, that is, in L^2.

Note that $\gamma(\eta) = 0$ is the marginal case: in a full nonlinear system with fluid motion coupled through the Lorentz force this would represent a bifurcation from a non-magnetic state with a flow $\boldsymbol{u}$ and $\gamma(\eta) < 0$, to some other state, mediated by magnetic field growth. Our focus at the moment, however, is linear, kinematic dynamo theory. When fully nonlinear dynamos are considered, the flow $\boldsymbol{u}$ is no longer provided and some mechanism is needed to drive a fluid flow, for example convective motion or a prescribed body force. This can introduce complications; for example, for a given driving there may be several possible stable fluid flows $\boldsymbol{u}$, some of which may be dynamos and others not (see Brummell, Cattaneo & Tobias, 2001, discussed in section 6.6).

2.6 Other geometries

The above definition is very natural for astrophysical bodies having spherical symmetry, such as the Earth or Sun. However spherical geometry and insulating boundary conditions are not always easy to handle. Frequently one wishes to consider cylindrical, planar or periodic geometry, and other boundary conditions. In this case it is useful to have some guiding principles as to when a flow is a dynamo. We suggest the following:

I. The total magnetic energy $\mathcal{E}_V(t)$ should always be finite.

II. In the absence of a flow, $\boldsymbol{u} = 0$, the energy $\mathcal{E}_V(t) \to 0$ as $t \to \infty$ for any $\eta > 0$ and any allowable initial condition $\boldsymbol{B}_0$.

III. When the flow is present $\mathcal{E}_V(t)$ does not tend to zero as $t \to \infty$ for some initial condition $\boldsymbol{B}_0$ and some diffusivity $\eta > 0$.

Condition I is designed to eliminate any sources of field at infinity. Condition II is there to avoid possible sources of magnetic excitation from field that is somehow trapped because of the geometry of the system and the boundary conditions. This sometimes may be expressed as a constraint on which initial conditions are allowable, as in the case of periodic boundary conditions discussed below. The problem of the evolution of trapped magnetic fields is a subject in its own right lying largely beyond this review. We only mention that processes such as flux expulsion (R.L. Parker, 1966; Weiss, 1966), topological pumping (Drobyshevski & Yuferev, 1974) and generally the study of magnetoconvection (Proctor & Weiss, 1982; Proctor, 1994) are important in understanding the behaviour of stellar and Solar magnetic fields. In some contexts the issue arises of how a dynamo operates when there is an additional ambient mean field present (Sarson, Jones & Zhang, 1999), an example being possible dynamo action in the moons of Jupiter, which are immersed in Jupiter's magnetic field. The structure of magnetic fields in the presence of a mean field is also used to define the alpha effect; see section 5.1 below.

The geometry discussed above, of a sphere of conducting fluid bounded by an insulator, satisfies I given that the field is required to decay at large distances in the insulator (see (2.59)). In section 3.2 we shall see that in the absence of motion all magnetic fields decay, so that II is also satisfied.

Let us consider briefly how these principles apply to some other geometries. If the flow $\boldsymbol{u}$ is non-zero only inside a sphere S of radius $r = a$ but the conductivity is uniform in all of space, then it is required by I that the field decay at large distances. If the sphere is surrounded by a stationary perfect conductor then to satisfy II there must be no field trapped in the perfect conductor, and so boundary conditions (2.67) must be applied on S.

A commonly used idealisation is to assume space is periodic in 1, 2 or 3 directions. In this case the integral giving the total energy is taken over one fundamental domain V, and Poynting fluxes in any direction of periodicity cancel out in the energy balance equation. For example, in a cylindrical geometry with coordinates (r, θ, z) (as in the Ponomarenko dynamo, sections 4.1 and 4.2) it is natural to take flow and field to be periodic in z. Similarly in a plane layer configuration with $0 \le z \le h$ the geometry may be periodic in x and y, with period $2\pi L$. If the layer is bounded above and below by an insulator the field is required to decay outside at large distances by I. For a perfect conductor outside the layer, the field outside has to be zero by II; in addition the total fluxes through the sides of the periodicity volume,

$$\Phi_1 = \int_{z=0}^{h} \int_{y=0}^{2\pi L} B_1 \, dy \, dz, \quad \Phi_2 = \int_{z=0}^{h} \int_{x=0}^{2\pi L} B_2 \, dx \, dz, \tag{2.71}$$

are constant under the induction equation. The only initial conditions that are therefore allowable for the dynamo problem are those for which these fluxes are zero, to avoid a trapped magnetic field which is forbidden by II. If the flow is periodic in all 3 directions, then there are 3 constant fluxes, and these must all be set to zero for the same reason (Arnold, Zeldovich, Ruzmaikin & Sokoloff, 1982).

Finally we mention that we have assumed we are working with a flow in Euclidean space. However flows and also maps in other spaces are sometimes considered: for example even a uniform steady flow can be a dynamo, if the space chosen is complicated enough (Arnold, Zeldovich, Ruzmaikin & Sokoloff, 1981). All such models are of interest, but have to be assessed carefully as to what they tell us about fundamental dynamo processes in physical space.

3 Decay, anti-dynamo theorems and upper bounds

In this section we explore the basic dynamo geometry of a sphere S containing conducting fluid inside, and an insulator outside. We prove some anti-dynamo theorems, which are of two types. The first restricts the kinds of magnetic field that can be amplified by fluid motion, and the second the classes of fluid motion that allow magnetic field amplification. We also give some upper bounds on growth rates.

First, we introduce the *toroidal–poloidal* decomposition of a magnetic field, which is ideally adapted to spherical geometry and has a Cartesian analogue (Roberts, 1967; Moffatt, 1978). A magnetic field has zero divergence and we write it tentatively in the form (suppressing time-dependence),

$$\boldsymbol{B}(r,\theta,\phi) = \boldsymbol{B}_T + \boldsymbol{B}_P, \quad \boldsymbol{B}_T = \nabla \times (\boldsymbol{r}T), \quad \boldsymbol{B}_P = \nabla \times \nabla \times (\boldsymbol{r}P). \tag{3.1}$$

Here $T(r,\theta,\phi)$ is the *toroidal scalar*, defining the *toroidal component* of $\boldsymbol{B}$,

$$\boldsymbol{B}_T = \hat{\boldsymbol{\theta}}\,(\sin\theta)^{-1}\partial_\phi T - \hat{\boldsymbol{\phi}}\,\partial_\theta T, \tag{3.2}$$

and $P(r,\theta,\phi)$ is the *poloidal scalar*, defining the *poloidal component* of $\boldsymbol{B}$,

$$r\boldsymbol{B}_P = \hat{\boldsymbol{r}}\,L^2 P + \hat{\boldsymbol{\theta}}\,\partial_\theta\partial_r(rP) + \hat{\boldsymbol{\phi}}\,(\sin\theta)^{-1}\partial_\phi\partial_r(rP), \tag{3.3}$$

where L^2 is the angular momentum operator, with

$$-L^2 = (\sin\theta)^{-1}\partial_\theta \sin\theta\,\partial_\theta + (\sin\theta)^{-2}\partial_\phi^2, \quad \nabla^2 = r^{-2}\partial_r r^2\partial_r - r^{-2}L^2. \tag{3.4}$$

The toroidal component $\boldsymbol{B}_T$ has no radial component, but the poloidal component $\boldsymbol{B}_P$ has all three components. Note that a function of r alone can be added to T or P without affecting $\boldsymbol{B}$ in (3.1). Taking the curl interchanges poloidal and toroidal fields, with

$$\mu^{-1}\nabla \times \boldsymbol{B} = \boldsymbol{J} = \boldsymbol{J}_T + \boldsymbol{J}_P, \tag{3.5}$$

$$\mu\boldsymbol{J}_T = -\nabla \times (\boldsymbol{r}\nabla^2 P), \quad \mu\boldsymbol{J}_P = \nabla \times \nabla \times (\boldsymbol{r}T). \tag{3.6}$$

Also there is the important property that

$$\nabla^2\boldsymbol{B} = -\nabla \times \nabla \times \boldsymbol{B} = \nabla \times (\boldsymbol{r}\nabla^2 T) + \nabla \times \nabla \times (\boldsymbol{r}\nabla^2 P). \tag{3.7}$$

Given the scalars T and P, equation (3.1) certainly defines a divergenceless field. The converse is true since

$$L^2 P = \boldsymbol{r}\cdot\boldsymbol{B}, \quad L^2 T = \boldsymbol{r}\cdot\nabla\times\boldsymbol{B}, \tag{3.8}$$

and L^2 may be inverted. Let us consider the T field; the P field is similar. By expanding in spherical harmonics Y_{lm} and using $L^2 Y_{lm} = l(l+1)Y_{lm}$, we obtain

$$T = \sum_{l=1}^{\infty}\sum_{m=-l}^{l} T_{lm}(r)Y_{lm}(\theta,\phi), \quad l(l+1)T_{lm}(r) = (Y_{lm}, \boldsymbol{r}\cdot\boldsymbol{B})_{\theta,\phi} \tag{3.9}$$

(recall (2.61)). The $l = m = 0$ term is not present in $\boldsymbol{r} \cdot \boldsymbol{B}$ because there can be no net flux of $\boldsymbol{B}$ over a sphere, as $\nabla \cdot \boldsymbol{B} = 0$. Correspondingly the above definition of T has a zero average over spheres,

$$\langle T \rangle_{\theta,\phi} = 0. \tag{3.10}$$

Given this, note that $L^2 T = 0$ implies that $T = 0$, and similarly for P.

The insulating boundary conditions (2.58) of continuity of $\boldsymbol{B}$ across the boundary $r = a$ amount to, from (3.2,3.3),

$$[P] = [\partial_r P] = [T] = 0. \tag{3.11}$$

The perfectly conducting boundary conditions (2.65) or (2.67) are satisfied provided $P = \partial_r(rT) = \nabla^2 P = 0$ on the boundary. This assumes there is no field trapped in the perfect conductor, a condition we will assume from now on. However it may be checked from the induction equation that if $B_r = u_r = 0$ on the boundary for all time, then so must $(\nabla^2 \boldsymbol{B})_r$, (as $(\nabla \times (\boldsymbol{u} \times \boldsymbol{B}))_r$ is zero there). But $r(\nabla^2 \boldsymbol{B})_r = L^2 \nabla^2 P$ from (3.7) and so $\nabla^2 P = 0$ automatically. We are left with

$$P = \partial_r(rT) = 0. \tag{3.12}$$

It is also worth briefly noting the Cartesian equivalent of the toroidal–poloidal decomposition. Suppose fluid is confined to a plane layer $0 \leq z \leq h$. Then we may write

$$\boldsymbol{B}(x, y, z) = \boldsymbol{B}_T + \boldsymbol{B}_P, \quad \boldsymbol{B}_T = \nabla \times (\hat{\boldsymbol{z}} T), \quad \boldsymbol{B}_P = \nabla \times \nabla \times (\hat{\boldsymbol{z}} P), \tag{3.13}$$

with

$$\boldsymbol{B}_T = \hat{\boldsymbol{x}}\, \partial_y T - \hat{\boldsymbol{y}}\, \partial_x T, \quad \boldsymbol{B}_T = \hat{\boldsymbol{x}}\, \partial_z \partial_x P + \hat{\boldsymbol{y}}\, \partial_z \partial_y P - \hat{\boldsymbol{z}}\, (\partial_x^2 + \partial_y^2) P. \tag{3.14}$$

The conditions for insulating and perfectly conducting boundaries are, respectively,

$$[P] = [\partial_z P] = [T] = 0, \tag{3.15}$$

and

$$P = \partial_z T = 0. \tag{3.16}$$

3.2 Decay modes

Principle II in section 2.6 above requires that in the absence of fluid flow, $\boldsymbol{u} = 0$, the magnetic energy should decay away. We will check this for a sphere $r = a$ containing stationary conducting fluid, surrounded by an insulator. In this case the field satisfies the diffusion equation $\partial_t \boldsymbol{B} = \eta \nabla^2 \boldsymbol{B}$ with boundary conditions (2.58) matching onto a potential external field $\boldsymbol{B} = \nabla \chi$ (2.59).

In terms of the toroidal–poloidal decomposition (3.1), inside the sphere the scalars T and P themselves obey the diffusion equation by (3.7). Outside, the potential field (2.59) has $\boldsymbol{J} = 0$ and so corresponds to $T = 0$ and $\nabla^2 P = 0$ by (3.5) and (3.6). If we focus on one spherical harmonic, with

$$T = f(r) Y_{lm}(\theta, \phi) e^{\gamma_T t}, \quad P = g(r) Y_{lm}(\theta, \phi) e^{\gamma_P t}, \tag{3.17}$$

then the boundary conditions to be imposed at $r = a$ amount to

$$f = 0, \quad a \partial_r g + (l+1) g = 0 \tag{3.18}$$

from (3.11) and (2.59).

Straightforward calculations (see for example, Moffatt, 1978; Roberts, 1987) give the decaying modes as

$$f(r) = j_l(k_l r/a), \quad g(r) = j_l(k_{l-1} r/a), \tag{3.19}$$

with decay rates

$$\gamma_T = -\eta k_l^2/a^2, \quad \gamma_P = -\eta k_{l-1}^2/a^2. \tag{3.20}$$

Here j_l are spherical Bessel functions [1] and k_l is any zero of j_l. This gives a discrete set of decaying modes. We have $l \geq 1$ only in the toroidal–poloidal decomposition above and so the slowest decaying mode is poloidal, corresponding to $l = 1$ and k_0 as the first zero of j_0, which is π. The corresponding magnetic field is given for $m = 0$ by

$$P = j_1\left(\frac{\pi r}{a}\right) \sqrt{\frac{3}{4\pi}} \cos\theta \, e^{-\gamma_P t}, \quad \gamma_P \equiv \gamma_{\text{decay}} = -\frac{\eta \pi^2}{a^2}, \quad j_1(z) = \frac{\sin z - z \cos z}{z^2}, \tag{3.21}$$

inside $r = a$, and is a decaying dipole; the degeneracy $m = -1, 0, 1$ of this $l = 1$ mode corresponds to the degeneracy in direction of the dipole moment.

Note that the toroidal field is zero outside $r = a$ simply as a consequence of the field being potential there. This means that the order of magnitude of the toroidal field cannot be ascertained directly from outside a planet, such as the Earth, or a star. Only the poloidal field can be observed from $r > a$ and extrapolated down to $r = a$.

The result for the slowest decaying mode $\gamma_{\text{decay}} = -\eta\pi^2/a^2$ also gives a useful inequality. Given any magnetic field defined inside the sphere $r = a$ and matched to a spatially decaying potential field $\boldsymbol{B} = \nabla\chi$ outside, with $[\boldsymbol{B}] = 0$ across the sphere and of course $\nabla \cdot \boldsymbol{B} = 0$ everywhere, we have

$$\int_{V_\mathrm{i}} |\nabla \times \boldsymbol{B}|^2 \, dV \geq \frac{\pi^2}{a^2} \int_V |\boldsymbol{B}|^2 \, dV \qquad (V = V_\mathrm{i} \cup V_\mathrm{e}). \tag{3.22}$$

[1] AS 10.1, 10.1.21

This may be proved by expanding an arbitrary magnetic field in the set of decay modes identified above; we omit the details. This inequality is useful in determining upper bounds on the strength of the flow field needed to overcome diffusive decay; see section 3.5 below.

3.3 Anti-dynamo theorems in periodic Cartesian geometry

The early development of dynamo theory was dominated by *anti-dynamo theorems*, which show that for dynamo action and growing magnetic fields, the field and flow have to be sufficiently complicated, breaking certain symmetries. The most famous of these theorems is that of Cowling (1934), which shows that an axisymmetric magnetic field cannot be maintained by dynamo action. We first discuss two theorems in Cartesian geometry (see, for example, Moffatt, 1978), which much simplifies the argument. We take $\eta > 0$ and always consider incompressible flow, with $\nabla \cdot \boldsymbol{u} = 0$.

Anti-dynamo theorem 1. The first result we prove is the Cartesian version of Cowling's theorem, that a magnetic field $\boldsymbol{B}(x, y, t)$, independent of z, cannot be maintained by dynamo action. In this case the flow must take the form $\boldsymbol{u}(x, y, t)$ as any z-dependence would be transmitted to the magnetic field. With this fluid motion B_z field can be generated from B_x and B_y components, by vertical flows u_z that depend on (x, y). However there is no source for the B_x and B_y components, and this will mean that a dynamo is impossible.

We will consider periodic Cartesian geometry with periodicity $2\pi L$ in x, y and z, letting V denote one periodicity box. To simplify matters, we shall assume a steady flow field $\boldsymbol{u}(x, y)$ and that $\boldsymbol{B}$ takes the form of a normal mode

$$\boldsymbol{B}(x, y, t) = \boldsymbol{b}(x, y)e^{\lambda t} + \text{c.c.}, \quad \gamma = \operatorname{Re}\lambda. \tag{3.23}$$

Here 'c.c.' means the complex conjugate of the previous term. This is put in to give a real field as λ and the eigenfunction $\boldsymbol{b}(x, y)$ will generally be complex, since the right-hand side of the induction equation (2.46) does not represent a self-adjoint operator. We will restrict allowable initial conditions to those with no mean magnetic field in the fundamental volume V (by principle II above in section 2.6). If there is no flow, $\boldsymbol{u} = 0$, and the field is expressed in a Fourier series, it is clear that the slowest decay rate is $\gamma_{\text{decay}} = -\eta/L^2$. Correspondingly we have the inequality (cf. (3.22))

$$\int_V |\nabla \times \boldsymbol{B}|^2 \, dV \geq L^{-2} \int_V |\boldsymbol{B}|^2 \, dV \tag{3.24}$$

for any periodic, zero-mean field $\boldsymbol{B}$ with $\nabla \cdot \boldsymbol{B} = 0$, or similarly for any zero-mean, periodic scalar field ϕ

$$\int_V |\nabla\phi|^2 \, dV \geq L^{-2} \int_V |\phi|^2 \, dV. \tag{3.25}$$

We will show that for any flow $\boldsymbol{u}(x, y)$ and normal mode (3.23), the growth rate is no greater than the slowest decay rate, $\gamma \leq \gamma_{\text{decay}}$, and hence all magnetic field modes decay. Suppose the contrary is true, and we have a normal mode with $\gamma > \gamma_{\text{decay}}$. Since $\nabla \cdot \boldsymbol{B} = \partial_x B_x + \partial_y B_y = 0$, we may write

$$\boldsymbol{B} = \nabla \times (\hat{\boldsymbol{z}} A) + \hat{\boldsymbol{z}} \, B_z = (\partial_y A, -\partial_x A, B_z). \tag{3.26}$$

It is important to note that the potential $A(x, y, t)$ is periodic in x and y because there is no mean field in V. One may check that the three components of the induction equation are satisfied provided that

$$\partial_t A + \boldsymbol{u} \cdot \nabla A = \eta \nabla^2 A, \tag{3.27}$$
$$\partial_t B_z + \boldsymbol{u} \cdot \nabla B_z = ((\partial_y A)\partial_x - (\partial_x A)\partial_y) u_z + \eta \nabla^2 B_z. \tag{3.28}$$

The potential A thus obeys a scalar transport equation with no sources. This potential must therefore decay: to show this multiply (3.27) by $2A$ and rewrite it as

$$\partial_t A^2 + \nabla \cdot (\boldsymbol{u} A^2) = 2\eta \nabla \cdot (A \nabla A) - 2\eta |\nabla A|^2. \tag{3.29}$$

We integrate this, use periodic boundary conditions to discard the surface integral and then apply (3.25) to give

$$\partial_t \int_V A^2 \, dV = -2\eta \int_V |\nabla A|^2 \, dV \leq -2\eta L^{-2} \int_V A^2 \, dV. \tag{3.30}$$

Thus any growing normal mode (3.23) with $\gamma > \gamma_{\text{decay}} = -\eta/L^2$ must have $A \equiv 0$. With A zero, there is no source term in the equation (3.28) and so B_z obeys a scalar transport equation. Repeating the above argument shows that $B_z \equiv 0$. Thus we are left with only the trivial field $\boldsymbol{B} \equiv 0$. We conclude that all normal modes have $\gamma \leq \gamma_{\text{decay}}$.

Anti-dynamo theorem 2. The second result places no restriction on the form of the magnetic field and is that a *planar flow* $\boldsymbol{u} = (u_x(x, y, z, t), u_y(x, y, z, t), 0)$ cannot amplify a magnetic field (Zeldovich, 1957). For this flow, the B_x and B_y components can be forced by the z-dependent flow tilting B_z field; however there is no source term for the vertical B_z component.

We shall only address the simplified form when $\boldsymbol{u}$ is steady, and the magnetic field takes the form of a normal mode, now

$$\boldsymbol{B}(x, y, z, t) = \boldsymbol{b}(x, y, z) e^{\lambda t} + \text{c.c.}, \quad \gamma = \operatorname{Re} \lambda. \tag{3.31}$$

Suppose there is a normal mode with $\gamma > \gamma_{\text{decay}} \equiv -\eta/L^2$. In this planar flow, there is now no source for the vertical field B_z, which obeys (3.28) with $u_z = 0$, and so must be identically zero, by arguing as we did above. $\boldsymbol{B}$ must then take the form $\boldsymbol{B} = \nabla \times (\hat{\boldsymbol{z}}A)$, where the periodic potential $A = A(x, y, z, t)$ obeys (3.27) (given $B_z = 0$) and again can only be zero. We finally obtain only the zero field and so conclude that all normal modes have $\gamma \leq \gamma_{\text{decay}}$.

We see that when too much symmetry is imposed on the flow or the field, the flow has no influence in reducing the decay of normal modes. However these results hide the transient amplification that can and does take place. Mathematically, in the presence of fluid flow, the time-evolution operator in the induction equation is non-normal, and normal modes are not generally orthogonal with respect to the energy or L^2 norm. This allows strong transient amplification of fields before inevitable diffusive decay. For example, while A is transported above as a passive scalar in (3.27), and so cannot grow, the magnetic field $\boldsymbol{B}$ is related to the gradient of A: in an initial value problem $\boldsymbol{B}$ can show transient growth while contours of constant A are pressed close together by the fluid flow, before diffusion takes effect. In the limit $\eta \to 0$ this transient growth becomes more and more long-lived.

We have taken a steady flow and normal mode for the magnetic field above: this is a major simplification and assumes that the normal modes form a complete set. This follows for steady flows from results of hydrodynamic stability theory (see, for example, Childress & Gilbert, 1995, section 9.2). For time-periodic flows or more complex flows, general results have been obtained using functional analysis to show that fields tend to zero and to give bounds on decay rates. Further references may be found in Ivers & James (1984) and Fearn, Roberts & Soward (1988).

Before leaving this section, we note that perhaps the simplest situation in which magnetic field amplification is possible, that is not excluded by the above, is the case of two-dimensional but non-planar fluid flow $\boldsymbol{u}(x, y, t)$ with $u_z \neq 0$ and three-dimensional magnetic field $\boldsymbol{B}(x, y, z, t)$. Examples will be discussed in several sections below, for example section 4.3.

3.4 Anti-dynamo theorems in spherical geometry

The above two results for Cartesian geometry can be translated into spherical geometry; indeed this is where they originated. Spherical geometry introduces a number of complications, which are best dealt with using the toroidal–poloidal decomposition described in section 3.1 above; good sources are Moffatt (1978) and Roberts (1987). We will work within a sphere of radius $r = a$, use insulating boundary conditions and show that for a steady flow all magnetic field modes decay no more slowly than the decay rate in the absence of fluid flow, $\gamma \leq \gamma_{\text{decay}} = -\eta\pi^2/a^2$. To do this we assume we have a normal mode with $\gamma > \gamma_{\text{decay}}$ and show that we are left with only the trivial field $\boldsymbol{B} = 0$.

Anti-dynamo theorem 3. We begin with Cowling's theorem (Cowling, 1934) in the form proved by Braginsky (1964a). From the Cartesian formulation z is replaced by ϕ: an axisymmetric magnetic field $\boldsymbol{B}(r, \theta, t)$ cannot be maintained by a fluid flow (which is necessarily axisymmetric). We use the toroidal–poloidal decomposition for $\boldsymbol{B}$ in (3.1) and similarly for $\boldsymbol{u}$. For fields independent of ϕ, $\boldsymbol{u}_T \times \boldsymbol{B}_T = 0$, and so the toroidal component of $\boldsymbol{u} \times \boldsymbol{B}$ is $\boldsymbol{u}_P \times \boldsymbol{B}_P$, giving the poloidal component of the induction equation as

$$\partial_t \boldsymbol{B}_P = \nabla \times (\boldsymbol{u}_P \times \boldsymbol{B}_P) + \eta \nabla^2 \boldsymbol{B}_P. \tag{3.32}$$

Now we may write $\boldsymbol{B}_P = \nabla \times \boldsymbol{A}_T$ where $\boldsymbol{A}_T = A\hat{\boldsymbol{\phi}}$ is a toroidal field and uncurl the above equation to yield an equation for the ϕ component,

$$\partial_t \boldsymbol{A}_T = \boldsymbol{u}_P \times (\nabla \times \boldsymbol{A}_T) + \eta \nabla^2 \boldsymbol{A}_T. \tag{3.33}$$

There is no contribution from a scalar gradient ∇F here as the problem is independent of ϕ and so $(\nabla F)_\phi = 0$ (cf. (2.52)). Explicitly we obtain for A and B_ϕ,

$$\partial_t A + s^{-1}(\boldsymbol{u}_P \cdot \nabla)(sA) = \eta(\nabla^2 - s^{-2})A, \tag{3.34}$$

$$\partial_t B_\phi + s\boldsymbol{u}_P \cdot \nabla(s^{-1}B_\phi) = \eta(\nabla^2 - s^{-2})B_\phi + s\boldsymbol{B}_P \cdot \nabla\Omega, \tag{3.35}$$

where $s = r\sin\theta$ and $\boldsymbol{u}_T = \hat{\boldsymbol{\phi}}\, s\Omega$, so that $\Omega(r, \theta)$ is the angular velocity of the fluid flow. These equations are analogous to the Cartesian case: A obeys a scalar transport equation with no sources, and B is generated from A by variations in angular velocity, that is differential rotation, often called the *omega effect* for brevity.

Consider first (3.34): if we define a flux function $\chi = sA$, then this is materially transported by

$$\partial_t \chi + \boldsymbol{u}_P \cdot \nabla\chi = \eta D^2 \chi, \tag{3.36}$$

where the Stokes operator D^2 is given by

$$D^2\chi \equiv s(\nabla^2 - s^{-2})(s^{-1}\chi) = (\nabla^2 - 2s^{-1}\nabla s \cdot \nabla)\chi. \tag{3.37}$$

The problem is to show that the right-hand side of (3.36) implies diffusive decay of χ, as it surely must. If this equation is multiplied through by 2χ, it can be written in the form

$$\partial_t \chi^2 + \nabla \cdot (\boldsymbol{u}_P \chi^2) = 2\eta \nabla \cdot (\chi\nabla\chi - \chi^2 s^{-1}\nabla s) - 2\eta|\nabla\chi|^2. \tag{3.38}$$

This holds inside the sphere S of radius $r = a$ with magnetic diffusivity $\eta \equiv \eta_{\mathrm{i}}$, and insulating boundary conditions. Outside the field is potential and so $(\nabla^2 - s^{-2})A = 0$, which similarly amounts to

$$0 = 2\nabla \cdot (\chi\nabla\chi - \chi^2 s^{-1}\nabla s) - 2|\nabla\chi|^2. \tag{3.39}$$

Across $r = a$, $\boldsymbol{u} \cdot \boldsymbol{n} = 0$ and $[\chi] = [\partial_r\chi] = 0$, to guarantee continuity of $\boldsymbol{B}$. If we integrate (3.38) over $V_{\rm i}$, and η times (3.39) over $V_{\rm e}$ then the divergence terms give surface integrals over S which cancel to leave

$$\partial_t \int_{V_{\rm i}} \chi^2\, dV = -2\eta \int_V |\nabla\chi|^2\, dV \qquad (V = V_{\rm i} \cup V_{\rm e}). \tag{3.40}$$

(There is no contribution from the surface integral at infinity since $\chi = O(r^{-1})$ from (2.62)). This equation does not involve the flow $\boldsymbol{u}$ and applies equally in the case of no flow, when we know that the slowest decay rate is $\gamma_{\rm decay} = -\eta\pi^2/a^2$. It therefore follows[2] that for an eigenmode to satisfy $\gamma > \gamma_{\rm decay}$ the field $A = \chi/s$ must be zero and so must $\boldsymbol{B}_P$.

Now there is no source term $s\boldsymbol{B}_P \cdot \nabla\Omega$ in the B_ϕ equation (3.35) above. Let us set $W = s^{-1}B_\phi$, in which case the equation (3.35) may be written

$$\partial_t W + \boldsymbol{u}_P \cdot \nabla W = \eta s^{-1}(\nabla^2 - s^{-2})(sW) = \eta(\nabla^2 + 2s^{-1}\nabla s \cdot \nabla)W. \tag{3.41}$$

Multiplying by $2W$, this can be written as

$$\partial_t W^2 + \nabla \cdot (\boldsymbol{u}_P W^2) = 2\eta\nabla \cdot (W\nabla W + W^2 s^{-1}\nabla s) - 2\eta|\nabla W|^2. \tag{3.42}$$

On $r = a$, $B_\phi = 0$, since there is no toroidal field outside and $[B_\phi] = 0$ (see (3.11)), and so integrating leaves

$$\partial_t \int_{V_{\rm i}} W^2\, dV = -2\eta \int_{V_{\rm i}} |\nabla W|^2\, dV. \tag{3.43}$$

Again this equation does not involve the flow $\boldsymbol{u}$ and so plainly a mode having $\gamma > \gamma_{\rm decay}$ would contradict our results for decay rates. We conclude that all magnetic eigenmodes must have growth rates $\gamma \le \gamma_{\rm decay}$.

Anti-dynamo theorem 4. We now consider the spherical analogue of the second anti-dynamo theorem discussed in Cartesian geometry in the previous section. This showed that a flow on plane surfaces $\boldsymbol{u} = (u_x, u_y, 0)$ cannot maintain any magnetic field. We now replace z by r, so that the theorem becomes that any purely toroidal flow $\boldsymbol{u} = \boldsymbol{u}_T(r, \theta, \phi, t)$, that is flow on spheres with zero radial component, cannot maintain a magnetic field $\boldsymbol{B}(r, \theta, \phi, t)$ (see Elsasser, 1946; Bullard & Gellman, 1954; Backus, 1958; Moffatt, 1978). Again we show that

[2] More formally here, and similarly below, one could derive an inequality analogous to (3.25) from the decay rates (3.20) obtained for the purely diffusive problem (with $\boldsymbol{u} = 0$) and then apply it as in (3.30) above.

for a steady flow and a normal mode, $\gamma \le \gamma_{\rm decay}$. From the induction equation with $\boldsymbol{r}\cdot\boldsymbol{u} = 0$ it may be checked that

$$\partial_t(\boldsymbol{r}\cdot\boldsymbol{B}) + \boldsymbol{u}_T\cdot\nabla(\boldsymbol{r}\cdot\boldsymbol{B}) = \eta\nabla^2(\boldsymbol{r}\cdot\boldsymbol{B}) \tag{3.44}$$

and so $Q \equiv \boldsymbol{r}\cdot\boldsymbol{B} = L^2P$ (see (3.1–3.3)) satisfies an advection–diffusion equation.

From this we may deduce that

$$\partial_t Q^2 + \nabla\cdot(\boldsymbol{u}_T Q^2) = 2\eta\nabla\cdot(Q\nabla Q) - 2\eta|\nabla Q|^2 \tag{3.45}$$

valid inside $V_{\rm i}$ and, outside $\nabla^2 Q = \nabla^2 L^2 P = 0$ (as $\nabla^2 P = 0$ there) and so

$$0 = 2\nabla\cdot(Q\nabla Q) - 2|\nabla Q|^2. \tag{3.46}$$

Across the boundary $[Q] = [\partial_r Q] = 0$ by (3.11). Integrating (3.45) over $V_{\rm i}$ and η times (3.46) over $V_{\rm e}$, and adding to cancel the boundary terms gives

$$\partial_t \int_{V_{\rm i}} Q^2\,dV = -2\eta\int_V |\nabla Q|^2\,dV \qquad (V = V_{\rm i}\cup V_{\rm e}). \tag{3.47}$$

Thus a normal mode with $\gamma > \gamma_{\rm decay}$ must have zero radial field and so zero poloidal scalar P, leaving only toroidal field $\boldsymbol{B} = \boldsymbol{B}_T$. This obeys

$$\partial_t\boldsymbol{B}_T = \nabla\times(\boldsymbol{u}_T\times\boldsymbol{B}_T) + \eta\nabla^2\boldsymbol{B}_T. \tag{3.48}$$

With $\boldsymbol{B}_T = \nabla\times(\boldsymbol{r}T)$ we may uncurl this equation to yield

$$\partial_t(\boldsymbol{r}T) = \boldsymbol{u}_T\times\boldsymbol{B}_T + \eta\nabla^2(\boldsymbol{r}T) + \nabla F = -\boldsymbol{r}(\boldsymbol{u}_T\cdot\nabla T) + \boldsymbol{r}\eta\nabla^2 T + \nabla G, \tag{3.49}$$

where $\nabla G = \nabla F + 2\eta\nabla T$ is some unknown gradient. The θ- and ϕ-components of the equation indicate that G is only a function of r. We may therefore replace ∇G by $\boldsymbol{r}g(r,t)$ to leave

$$\partial_t T + \boldsymbol{u}_T\cdot\nabla T = \eta\nabla^2 T + g(r,t). \tag{3.50}$$

Now T averages to zero over spheres, by equation (3.10), and so multiplying by $2T$ and integrating yields

$$\partial_t\int_{V_{\rm i}} T^2\,dV = -2\eta\int_{V_{\rm i}}|\nabla T|^2\,dV, \tag{3.51}$$

using the condition $T = 0$ on $r = a$. This shows that the toroidal field decays with at least the decay rate $\gamma_{\rm decay}$, and no normal modes exist that decay more slowly.

This concludes our discussion of anti-dynamo theorems. At first sight it looks as though these theorems should generalise not only from Cartesian to spherical geometry but to any orthogonal coordinate system. This is not the case.

The decomposition into toroidal and poloidal fields in spherical and Cartesian geometry has the key property that the diffusive operator ∇^2 maps poloidal field to poloidal and toroidal to toroidal (see (3.7)). This does not carry over to other coordinate systems. For example whereas in spherical geometry with coordinates (r,θ,ϕ) there is no source term for the radial field B_r from B_θ or B_ϕ through the Laplacian, in cylindrical geometry with coordinates (r,θ,z) there is, from B_θ, and this can allow a dynamo to function as we shall see below in sections 4.1 and 4.2.

A question related to anti-dynamo theorems is whether a flow can maintain a magnetic field with a zero poloidal field $P = 0$ (Kaiser, 1995) or a zero toroidal field $T = 0$ everywhere in space (Kaiser, Schmitt & Busse, 1994). In the former case the dynamo is said to be *invisible* as the whole magnetic field exterior to the sphere $r = a$ would be zero. It appears that with 'reasonable' fluid flows such dynamos do not exist.

3.5 Upper bounds

In the absence of fluid flow, $\boldsymbol{u} = 0$, we have seen that field decays, with the slowest decaying mode having $\gamma_{\text{decay}} = -\eta\pi^2/a^2$ in spherical geometry. Since we expect the growth rates of normal modes to behave continuously as we increase the flow $\boldsymbol{u}$ from zero, it is clear that we will need to reach some finite strength of flow before dynamo action can occur, with $\gamma \geq 0$. There are a number of upper bound results which make this precise. In each case we consider the energy equation in the form

$$\mu\partial_t\mathcal{E}_V = -\eta\int_{V_{\rm i}}|\nabla\times\boldsymbol{B}|^2\,dV - \int_{V_{\rm i}}\boldsymbol{u}\cdot(\nabla\times\boldsymbol{B})\times\boldsymbol{B}\,dV \qquad (V = V_{\rm i}\cup V_{\rm e}), \quad (3.52)$$

from (2.64), and give an upper bound on the term which involves the flow field $\boldsymbol{u}$. We shall work in spherical geometry with insulating boundary conditions, but there are analogues in Cartesian geometry.

Upper bound 1. For the first upper bound (Childress, 1969) we let $u_{\max}$ be the maximum value of $|\boldsymbol{u}|$ in the domain V and use the Cauchy–Schwartz inequality and then inequality (3.22) to establish that

$$\begin{aligned} -\int_{V_{\rm i}}\boldsymbol{u}\cdot(\nabla\times\boldsymbol{B})\times\boldsymbol{B}\,dV &\leq u_{\max}\left(\int_{V_{\rm i}}|\nabla\times\boldsymbol{B}|^2\,dV\right)^{1/2}\left(\int_{V_{\rm i}}|\boldsymbol{B}|^2\,dV\right)^{1/2} \\ &\leq \frac{a u_{\max}}{\pi}\int_{V_{\rm i}}|\nabla\times\boldsymbol{B}|^2\,dV. \end{aligned} \quad (3.53)$$

Putting this expression back in (3.52) shows that

$$\mu\partial_t\mathcal{E}_V \leq \left(\frac{a u_{\max}}{\pi} - \eta\right)\int_{V_{\rm i}}|\nabla\times\boldsymbol{B}|^2\,dV \quad (3.54)$$

and so growth can only occur when $\eta \le a u_{\max}/\pi$, or equivalently when the *magnetic Reynolds number*

$$R = a u_{\max}/\eta \ge \pi. \tag{3.55}$$

This dimensionless parameter measures the strength of the flow field, compared with the effect of diffusion, and is a key parameter in MHD. It is defined as a velocity scale multiplied by a length scale, divided by the magnetic diffusivity; its precise definition depends on the problem at hand. The above bound is based only on the magnitude of velocity. However magnetic fields are intensified not through motion so much as through stretching, by the term $\boldsymbol{B} \cdot \nabla \boldsymbol{u}$ in (2.51), and this is brought out in the next bound.

Upper bound 2. The next bound of Backus (1958) (see also Proctor, 1977) makes the role of stretching explicit, but requires the additional *no slip* condition that $\boldsymbol{u} = 0$ on the boundary S of V_{i}. First write $(\nabla \times \boldsymbol{B}) \times \boldsymbol{B} = \boldsymbol{B} \cdot \nabla \boldsymbol{B} - \nabla \frac{1}{2}|\boldsymbol{B}|^2$ and integrate by parts to show that

$$\int_{V_{\mathrm{i}}} \boldsymbol{u} \cdot (\nabla \times \boldsymbol{B}) \times \boldsymbol{B} \, dV = \int_{V_{\mathrm{i}}} B_i B_j \partial_i u_j \, dV. \tag{3.56}$$

Now $B_i B_j \partial_i u_j = B_i B_j e_{ij}$ where $e_{ij} = \frac{1}{2}(\partial_i u_j + \partial_j u_i)$ is the symmetric rate-of-strain tensor. If $e_{\max}$ is the largest eigenvalue of this tensor in the volume V, at any time, then

$$-\int_{V_{\mathrm{i}}} \boldsymbol{u} \cdot (\nabla \times \boldsymbol{B}) \times \boldsymbol{B} \, dV \le e_{\max} \int_{V_{\mathrm{i}}} |\boldsymbol{B}|^2 \, dV. \tag{3.57}$$

Putting this back in (3.52) and applying (3.22) then shows that the energy satisfies

$$\mu \partial_t \mathcal{E}_V \le (e_{\max} - \eta \pi^2/a^2) 2\mu \mathcal{E}_V. \tag{3.58}$$

A necessary condition for growth is that

$$R = a^2 e_{\max}/\eta \ge \pi^2, \tag{3.59}$$

giving a new definition of the magnetic Reynolds number R. Note also that for a normal mode, $\mathcal{E}_V$ grows at a rate 2γ and so the above inequality gives a bound on the growth rate,

$$\gamma \le e_{\max}(1 - \pi^2/R), \tag{3.60}$$

with the above definition of R.

These are necessary conditions, but far from sufficient: it is clear they do not capture the requirement that the fluid flow be sufficiently complicated, especially in view of the toroidal flow anti-dynamo theorem 4 above. Another upper bound has been derived by Roberts (1967, p. 75), while Busse (1975) and Roberts (1987) give a bound on the magnitude of the poloidal flow needed to overcome the toroidal flow anti-dynamo theorem.

4 Laminar dynamos

We now move on to discuss some working kinematic dynamos, in which flows are given and shown to amplify magnetic fields. There are two matters we should note: first there are very few elementary examples in this field, perhaps unsurprisingly in view of the anti-dynamo theorems and the 40–50 year gap between Larmor's suggestion and the first working examples. Secondly we will now become more cavalier about the geometry. The above discussion is for a sphere of conducting fluid surrounded by an insulator, for example modelling the Earth's liquid iron core surrounded by the largely insulating mantle. Few models can be embedded naturally in this geometry, and we will now generally consider spatially periodic situations, but with an eye on the principles stated in section 2.6 above as to what constitutes a dynamo. This will allow us to understand fundamental dynamo mechanisms without the distraction of geometrical complications.

4.1 Ponomarenko dynamo

Perhaps the simplest dynamo is that of Ponomarenko (1973) in which the given flow is written in cylindrical polar coordinates (r, θ, z) as

$$\boldsymbol{u} = \begin{cases} \hat{\boldsymbol{\theta}}\, r\Omega + \hat{\boldsymbol{z}}\, U & (r < a), \\ \mathbf{0} & (r > a), \end{cases} \tag{4.1}$$

where the angular velocity Ω and axial velocity U are constants. This flow is depicted in figure 1(a). Plainly there is solid body rotation inside and outside the cylinder $r = a$, and solid body motion alone cannot give a dynamo, by upper bound 2 above. The dynamo is therefore intimately connected with the discontinuity of the flow at $r = a$. A magnetic Reynolds number can also be defined, for example as

$$R = a\sqrt{a^2\Omega^2 + U^2}/\eta; \tag{4.2}$$

however we will not formally non-dimensionalise this problem. It is useful also to define the parameter $\chi = U/a\Omega$, which determines the pitch of the helical motion.

At first sight this is a bizarre flow, with a vortex sheet at $r = a$, a highly unstable configuration. Nonetheless it forms the basis of ongoing dynamo experiments being conducted in Riga, Latvia, and in which dynamo action has recently been detected (see, for example, Gailitis & Freiberg, 1980; Gailitis, 1993; Gailitis et al., 2000). These involve a vessel depicted schematically in figure 1(b) leading, at a basic level of approximation, to flows that are piecewise constant in radius.

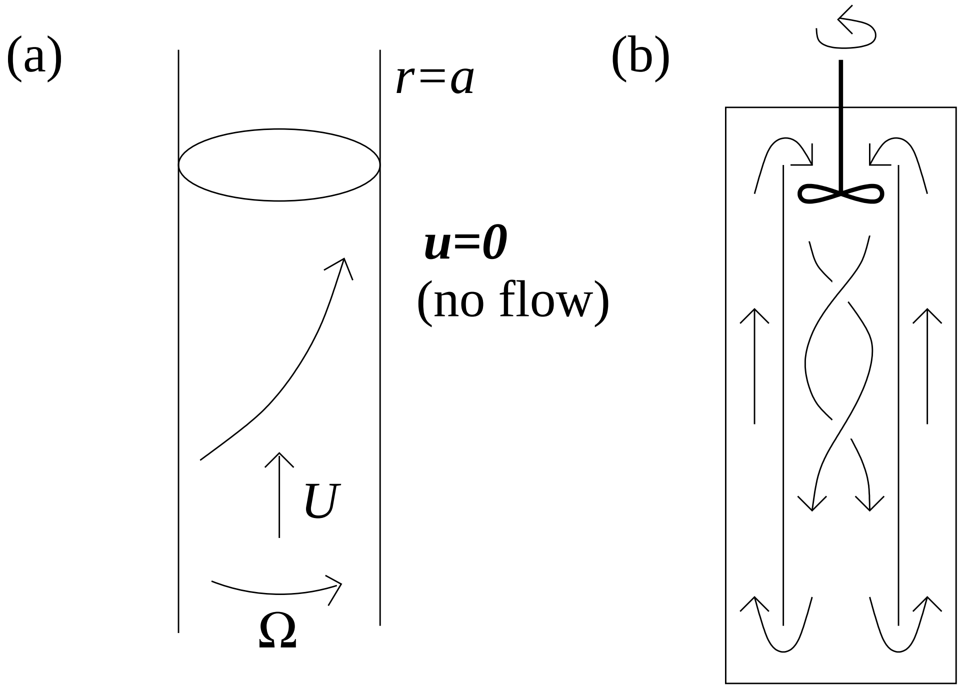

Fig. 1. (a) The Ponomarenko dynamo flow field, and (b) a highly schematic picture of the Riga dynamo experiment. Liquid sodium is driven round a vessel by a propeller as shown.

To obtain growth rates we consider a normal mode $\boldsymbol{B} = \boldsymbol{b}(r)e^{\lambda t+im\theta+ikz}$. There is no stretching in the system except at $r = a$. The induction equation in $r < a$ or $r > a$ simplifies to the form

$$p^2 b_r = (\Delta_m - r^{-2})b_r - 2imr^{-2}b_\theta, \tag{4.3}$$
$$p^2 b_\theta = (\Delta_m - r^{-2})b_\theta + 2imr^{-2}b_r, \tag{4.4}$$
$$p^2 b_z = \Delta_m b_z, \tag{4.5}$$

where $\Delta_m = \partial_r^2 + r^{-1}\partial_r - m^2r^{-2}$ is the horizontal Laplacian operator. Vertical diffusion and motion are absorbed into the definition of the constant p, which takes two values: inside $r = a$, $p = p_\mathrm{i}$ and outside $p = p_\mathrm{e}$, where

$$\eta p_\mathrm{i}^2 = \lambda + im\Omega + ikU + \eta k^2, \quad \eta p_\mathrm{e}^2 = \lambda + \eta k^2 \qquad (\mathrm{Re}\, p_\mathrm{i}, \mathrm{Re}\, p_\mathrm{e} \geq 0). \tag{4.6}$$

We must impose $\nabla \cdot \boldsymbol{B} = 0$, which amounts to

$$\partial_r b_r + r^{-1}b_r + imr^{-1}b_\theta + ikb_z = 0. \tag{4.7}$$

The solution is also subject to $[\boldsymbol{B}] = [\boldsymbol{n} \times \boldsymbol{E}] = 0$ across $r = a$, although of these five jump conditions only four are independent (see section 2.4).

To solve these equations define $b_\pm = b_r \pm ib_\theta$, which obey

$$p^2 b_\pm = \Delta_{m\pm1} b_\pm, \tag{4.8}$$

with $p = p_{\rm i}$ or $p_{\rm e}$. These are satisfied by modified Bessel functions [3],

$$b_\pm = A_\pm I_{m\pm1}(rp_{\rm i})/I_{m\pm1}(ap_{\rm i}), \quad b_z = A_z I_m(rp_{\rm i})/I_m(ap_{\rm i}) \quad (r < a), \tag{4.9}$$
$$b_\pm = A_\pm K_{m\pm1}(rp_{\rm e})/K_{m\pm1}(ap_{\rm e}), \quad b_z = A_z K_m(rp_{\rm e})/K_m(ap_{\rm e}) \quad (r > a), \tag{4.10}$$

building in the condition that $[\boldsymbol{B}] = 0$ and correct behaviour at the origin and infinity. The three constants, $A_\pm$, A_z, are fixed by imposing $\nabla\cdot\boldsymbol{B} = 0$ in the two regions and the continuity of electric field $[\boldsymbol{n}\times\boldsymbol{E}] \equiv [\boldsymbol{n}\times(\eta\nabla\times\boldsymbol{B}-\boldsymbol{u}\times\boldsymbol{B})] = 0$ across $r = a$, which gives two conditions,

$$\eta[\partial_r b_\theta] + [u_\theta]b_r(a) = 0, \quad \eta[\partial_r b_z] + [u_z]b_r(a) = 0, \tag{4.11}$$

or, bearing in mind that $[\cdot]$ represents the value as $r \to a^+$ minus that as $r \to a^-$,

$$\eta[\partial_r b_\theta] - a\Omega b_r(a) = 0, \quad \eta[\partial_r b_z] - Ub_r(a) = 0. \tag{4.12}$$

Of this total of four conditions only three are independent. It turns out that the fastest way to proceed (Ponomarenko, 1973) is to note that (4.7) and $[\boldsymbol{B}] = 0$ imply that $[\partial_r b_r] = 0$: this, with the first electric field condition in (4.12), gives two independent equations

$$2\eta[\partial_r b_\pm] = \pm ia\Omega(b_+(a) + b_-(a)). \tag{4.13}$$

Using these with (4.9), (4.10) and (4.6), straightforwardly gives the dispersion relation as two simultaneous equations for $p_{\rm i}$ and $p_{\rm e}$

$$2\eta S_+S_- = ia\Omega(S_+ - S_-), \quad p_{\rm i}^2 = p_{\rm e}^2 + \eta^{-1}(im\Omega + ikU), \tag{4.14}$$

where

$$S_\pm = p_{\rm i} I'_{m\pm1}(ap_{\rm i})/I_{m\pm1}(ap_{\rm i}) - p_{\rm e} K'_{m\pm1}(ap_{\rm e})/K_{m\pm1}(ap_{\rm e}). \tag{4.15}$$

The dispersion relation has to be studied numerically for general parameter values. Despite its complexity it is probably the simplest exact solution we have in dynamo theory! Fortunately some of the asymptotic approximations used in this and other models give rather more manageable formulae.

The above formulae do simplify significantly when $m\Omega + kU = 0$ and so the field lines are aligned with the shear across $r = a$. In this case $p_{\rm i} = p_{\rm e} = p$, say, and the Bessel functions reduce to [4]

$$S_\pm = (aI_{m\pm1}(ap)K_{m\pm1}(ap))^{-1}. \tag{4.16}$$

The dispersion relation becomes the single equation

$$2\eta = ia^2\Omega(I_{m-1}(ap)K_{m-1}(ap) - I_{m+1}(ap)K_{m+1}(ap)), \tag{4.17}$$

[3] AS 9.6
[4] AS 9.6.15, 9.6.26

or, with more manipulation,

$$i\eta p = am\Omega(I_m(ap)K'_m(ap) + I'_m(ap)K_m(ap)). \tag{4.18}$$

This again cannot be solved in general; however approximate formulae can be obtained in the limit of large magnetic Reynolds number (4.2). Informally think of the limit $\eta \to 0$ for fixed flow field and geometry and in this limit it turns out that $ap \to \infty$. Substituting asymptotic expansions for Bessel functions[5] $I_m(z)$ and $K_m(z)$ for large $z = ap$ in (4.17) or (4.18) then gives

$$p = (im\Omega/2a\eta)^{1/3}, \tag{4.19}$$

and so the complex and real growth rates (neglecting the small term $-\eta k^2$ in (4.6)) are, for growing modes,

$$\lambda \simeq \eta p^2 = \eta\left(\frac{im\Omega}{2a\eta}\right)^{2/3}, \quad \gamma = \operatorname{Re}\lambda = \frac{\eta^{1/3}}{2}\left(\frac{|m|\Omega}{2a}\right)^{2/3}. \tag{4.20}$$

These are correct for fixed a, Ω, U, m and k, in the limit of small η, and so, in non-dimensional terms, for the Ponomarenko dynamo at large magnetic Reynolds number R (4.2).

The real growth rate γ in (4.20) increases as a function of wave number m and to find out which is the fastest growing mode we need a formula that is uniformly valid for m large in (4.18). Using expansions for Bessel functions[6] $I_m(mz)$, $K_m(mz)$ with $z = ap/m$ and $m \gg 1$ gives eventually

$$\lambda = \eta\left(\frac{im\Omega}{2a\eta}\right)^{2/3} - \frac{\eta m^2}{a^2}(1+\chi^{-2}), \quad \gamma = \frac{\eta^{1/3}}{2}\left(\frac{|m|\Omega}{2a}\right)^{2/3} - \frac{\eta m^2}{a^2}(1+\chi^{-2}) \tag{4.21}$$

(recalling that $\chi = U/a\Omega$ and $m\Omega + kU = 0$). The fastest growing modes are given by

$$|m| = (6(1+\chi^{-2}))^{-3/4}\left(\frac{a^2\Omega}{2\eta}\right)^{1/2}, \quad \gamma = 6^{-3/2}\Omega(1+\chi^{-2})^{-1/2}. \tag{4.22}$$

Thus at large magnetic Reynolds number the maximum growth of magnetic field occurs on the order of the turn-over time-scale Ω^{-1} or a/U, independent of the magnetic diffusivity η. This makes this dynamo a *fast dynamo*, which we shall discuss later; however the fields amplified are of rather small scale, of order $a/R^{1/2}$ in this limit.

[5] AS 9.7.1–6
[6] AS 9.7.7–11

Some further comments are in order. First of all note that the growth rate is zero if m is zero, or if k is zero (since $m\Omega = -kU$). If m is zero $\boldsymbol{B} = \boldsymbol{B}(r, z, t)$ is axisymmetric and cannot be maintained by anti-dynamo theorem 3. If $k = 0$ the magnetic field is independent of z and falls foul of anti-dynamo theorem 1. In addition note that we have set $m\Omega + kU = 0$, and that flows with $\Omega = 0$ or $U = 0$ cannot be dynamos by anti-dynamo theorems 2 and 4 respectively. Secondly note that all the generation is located at the discontinuity in the flow field. The dynamo is a boundary phenomenon, and the above growth rates at large R can be obtained by a boundary layer analysis (Roberts, 1987; Gilbert, 1988). The mechanism involves diffusion of B_θ field to give radial field, and the stretching out of radial field at the discontinuity to regenerate B_θ field. This will be seen more clearly in the next section when we smooth out the discontinuity.

Similar generation of field at discontinuities occurs in the rotor dynamo of Herzenberg (1958) and the experimental dynamos of Lowes & Wilkinson (1963, 1968), the latter using solid metal rotors embedded in a conducting block. Obviously further work can be done in tuning the Ponomarenko model for the experimental configuration depicted in figure 1(b), for example optimising the geometry so as to minimise the critical magnetic Reynolds number, allowing an outer vacuum region, and requiring the instability to be absolute rather than convective (Gailitis & Freiberg, 1980).

4.2 Smooth Ponomarenko dynamo

In the above discontinuous Ponomarenko dynamo, the generation is hidden in a thin layer of infinite shear. More relevant to astrophysical and geophysical fluid dynamics would generally be the smooth flow

$$\boldsymbol{u} = \hat{\boldsymbol{\theta}}\, r\Omega(r) + \hat{\boldsymbol{z}}\, U(r), \tag{4.23}$$

which we consider next. The fundamental issue here is: how do swirling, helical flows generate magnetic fields? Such flows can occur in convection and other instabilities, and are a very natural building block of dynamos in astrophysical flows.

For this example there are no obvious exact solutions and we have to assume a limit of large magnetic Reynolds number R to obtain approximate analytical results (Gilbert, 1988; Ruzmaikin, Sokoloff & Shukurov, 1988a), or study examples of flows numerically (Solovyev, 1985, 1987). We shall use a dimensionless version of the induction equation, non-dimensionalised using a scale of the flow and a velocity scale, written in the form

$$\partial_t \boldsymbol{B} + \boldsymbol{u} \cdot \nabla \boldsymbol{B} = \boldsymbol{B} \cdot \nabla \boldsymbol{u} + \varepsilon \nabla^2 \boldsymbol{B}, \tag{4.24}$$

where $\varepsilon^{-1} = R$ is a magnetic Reynolds number. To recover dimensional results we simply replace ε by η.

We may put $\boldsymbol{B} = \boldsymbol{b}(r)e^{\lambda t + im\theta + ikz}$ to obtain from the induction equation

$$(\lambda + im\Omega(r) + ikU(r))b_r = \varepsilon((\Delta_{m,k} - r^{-2})b_r - 2imr^{-2}b_\theta), \tag{4.25}$$
$$(\lambda + im\Omega(r) + ikU(r))b_\theta = r\Omega'(r)b_r + \varepsilon((\Delta_{m,k} - r^{-2})b_\theta + 2imr^{-2}b_r), \tag{4.26}$$
$$(\lambda + im\Omega(r) + ikU(r))b_z = U'(r)b_r + \varepsilon\Delta_{m,k}b_z, \tag{4.27}$$

where now we set $\Delta_{m,k} = \partial_r^2 + r^{-1}\partial_r - m^2r^{-2} - k^2$ as the full Laplacian operator. Again we have coupling terms between b_r and b_θ because of diffusion in cylindrical geometry, and also generation of b_θ and b_z from b_r by differential rotation $\Omega'(r)$ and axial shear $U'(r)$ respectively. We shall seek a magnetic mode localised near any given radius $r = a$, and to obtain growth rates we expand all spatial quantities in powers of $\varepsilon^{1/3} \ll 1$, setting

$$m = \varepsilon^{-1/3}M, \quad k = \varepsilon^{-1/3}K, \quad r = a + \varepsilon^{1/3}s, \quad \partial_r = \varepsilon^{-1/3}\partial_s. \tag{4.28}$$

We have chosen this wave number scaling to obtain the most useful results. We scale the growth rate as

$$\lambda = \varepsilon^{-1/3}\lambda_0 + \lambda_1 + \varepsilon^{1/3}\lambda_2 + \cdots, \tag{4.29}$$

and for the field,

$$b_r = \varepsilon^{1/3}b_{r0}(s) + \cdots, \quad b_\theta = b_{\theta0}(s) + \cdots, \quad b_z = b_{z0}(s) + \cdots. \tag{4.30}$$

These expansions are then substituted into the induction equation (4.25–4.27), and $\Omega(r)$ and $U(r)$ are also Taylor-expanded about $r = a$.

The first two orders in the expansion simply fix

$$\lambda_0 + iM\Omega(a) + iKU(a) = 0, \tag{4.31}$$
$$iM\Omega'(a) + iKU'(a) = 0, \quad \lambda_1 = 0. \tag{4.32}$$

Of these three conditions the second is crucial, and is that magnetic field lines must be aligned with the shear in the flow at this radius. This may be thought of as a resonance condition. Physically, for a given M and K, as we move away from this critical radius, the pitch of the stream lines changes and this enhances diffusion of this particular normal mode, as we discuss further below.

At the next order we obtain the equations for b_r and b_θ (dropping b_z, which can always be reconstructed from the condition $\nabla \cdot \boldsymbol{B} = 0$), and these can be written compactly as

$$(c_0 + ic_2s^2 - \partial_s^2)b_{r0} = -2iMa^{-2}b_{\theta0}, \tag{4.33}$$
$$(c_0 + ic_2s^2 - \partial_s^2)b_{\theta0} = a\Omega'(a)b_{r0}, \tag{4.34}$$

which are coupled parabolic cylinder equations, with

$$c_0 = \lambda_2 + M^2/a^2 + K^2, \quad 2c_2 = M\Omega''(a) + KU''(a). \tag{4.35}$$

These coupled differential equations can be rewritten as

$$\mathcal{P}_+\mathcal{P}_-b_{r0} = 0, \quad \mathcal{P}_\pm = (c_0 \pm d + ic_2 s^2 - \partial_s^2), \quad d = (-2iM\Omega'(a)/a)^{1/2}. \tag{4.36}$$

The operators $\mathcal{P}_+$ and $\mathcal{P}_-$ commute so that the solution for b_{r0} is a linear combination of solutions to the two equations $\mathcal{P}_\pm b_{r0} = 0$ or, in canonical form[7],

$$(\partial_\sigma^2 - (\tfrac{1}{4}\sigma^2 + c_\pm))b_{r0} = 0, \quad \sigma = s(4ic_2)^{1/4}, \quad c_\pm = (c_0 \pm d)/(4ic_2)^{1/2}. \tag{4.37}$$

Solutions that decay for $s \to \pm\infty$ exist only if $c_\pm = -j - \frac{1}{2}$ for $j = 0, 1, 2, \ldots$, and this gives eigenvalues of the original dynamo problem.[8]

Untangling all the previous changes of variable and expansions gives finally leading order growth rates,

$$\gamma = \operatorname{Re}\lambda \simeq \mp\sqrt{\frac{\varepsilon|m\Omega'(a)|}{a}} - (j + \tfrac{1}{2})\sqrt{\varepsilon|m\Omega''(a) + kU''(a)} - \varepsilon(m^2/a^2 + k^2) \tag{4.38}$$

(Gilbert, 1988; Ruzmaikin, Sokoloff & Shukurov, 1988a). These growth rates were determined for $m, k = O(\varepsilon^{-1/3})$, but in fact are valid for all m and k. This scaling (4.28) was chosen as it gives the richest formula for γ and includes the case of maximum growth rate $\gamma = O(\varepsilon^{1/3})$. It is equally valid for $m = O(1)$, except that the last term in the equation (4.38) is now subdominant, and $\gamma = O(\varepsilon^{1/2})$. For $m > O(\varepsilon^{-1/3})$, growth rates are negative. The eigenfunctions take the form of a (complex) Gaussian multiplied by a Hermite polynomial

$$b_r, b_\theta, b_z \propto \mathrm{He}_j(\sigma)e^{-\sigma^2/4}. \tag{4.39}$$

In the equation for the growth rate (4.38), the first term, with the lower sign, represents amplification of field through the interaction of differential rotation and diffusion in cylindrical geometry (cf. (4.25), (4.26)). The second term is always negative and represents enhanced diffusion: although the shear in the flow and the field are aligned at $r = a$ because of the condition (4.32), as we move away from $r = a$ the pitch of the stream lines changes, and the flow begins to advect field across lines of constant field, increasing the effect of diffusion. The final term is simply what is left from molecular diffusion of field in this geometry, with the flow playing no role.

7 AS 19.1.2
8 AS 19.13.1

As in the discontinuous Ponomarenko dynamo, field decays if $m = 0$ or $k = 0$ in keeping with anti-dynamo theorems 3 and 1. The first case is obvious, for the second note that if $k = 0$ then by the resonance condition (4.32), we have $m\Omega'(a) = 0$ and again there is no positive term in (4.38). Note also that if there is no axial flow, $U(r) \equiv 0$, there is no dynamo as we then have $m = 0$ from (4.32), and in this case the enhanced diffusion caused by the motion leads to the mechanism of flux expulsion (R.L. Parker, 1966; Weiss, 1966) by which field is removed from regions of closed stream lines in the plane on a time scale of order $\varepsilon^{-1/3}$.

Interestingly the first two terms in (4.38) possess the same scaling with m and ε. For dynamo action at small ε it is required that the sum of these two terms be positive for $j = 0$, and this can be rearranged (using also (4.32)) as the geometrical condition that

$$r \left| \frac{\Omega''(r)}{\Omega'(r)} - \frac{U''(r)}{U'(r)} \right| \equiv r \left| \frac{d}{dr} \log \left| \frac{\Omega'(r)}{U'(r)} \right| \right| < 4, \tag{4.40}$$

at the given radius $r = a$. This condition states (roughly) that the rate of change of pitch of the stream lines should not be too great: if it is then the enhanced diffusion will dominate over the regeneration of field, and the flow will not be a dynamo for small ε. An example of a family of flows that satisfies this condition is spiral Couette flows, for which $\nu\nabla^2\boldsymbol{u} = 0$,

$$\Omega(r) = a + br^{-2}, \quad U(r) = c + d\log r, \tag{4.41}$$

and the left-hand side of (4.40) is 2 (assuming b and d are non-zero). Dynamo action can occur at any radius, at sufficiently large magnetic Reynolds number $R = \varepsilon^{-1}$. On the other hand in spiral Couette–Poiseuille flows, for which $\nu\nabla^2\boldsymbol{u} - \nabla P = 0$ with a constant axial pressure gradient $P = pz$, we have

$$\Omega(r) = a + br^{-2}, \quad U(r) = c + d\log r + pr^2/4\nu, \tag{4.42}$$

and not all radii support dynamo action at large R. These flows have been studied numerically (Solovyev, 1985, 1987).

The smooth Ponomarenko dynamo is the simplest example of a class of smooth flows that defeat the anti-dynamo theorems. In this dynamo the flow lies on cylindrical surfaces, whereas the anti-dynamo theorems 2 and 4 rule out flows on planes and spheres. The key point is that in a cylindrical geometry B_θ field, parallel to the stream surfaces, can diffuse to give perpendicular, B_r field. This, together with shear, which regenerates B_θ from B_r, gives a closed dynamo loop and can amplify field. In spherical and planar geometry there is no analogous process by which diffusion generates poloidal field from toroidal. The field structure is given schematically in figure 2, which shows spiralling tubes of field (top row) for $m = 1$ and $m = 2$. The tubes have a roughly fish-like cross section (bottom row), and the trailing fins of the fish are a result

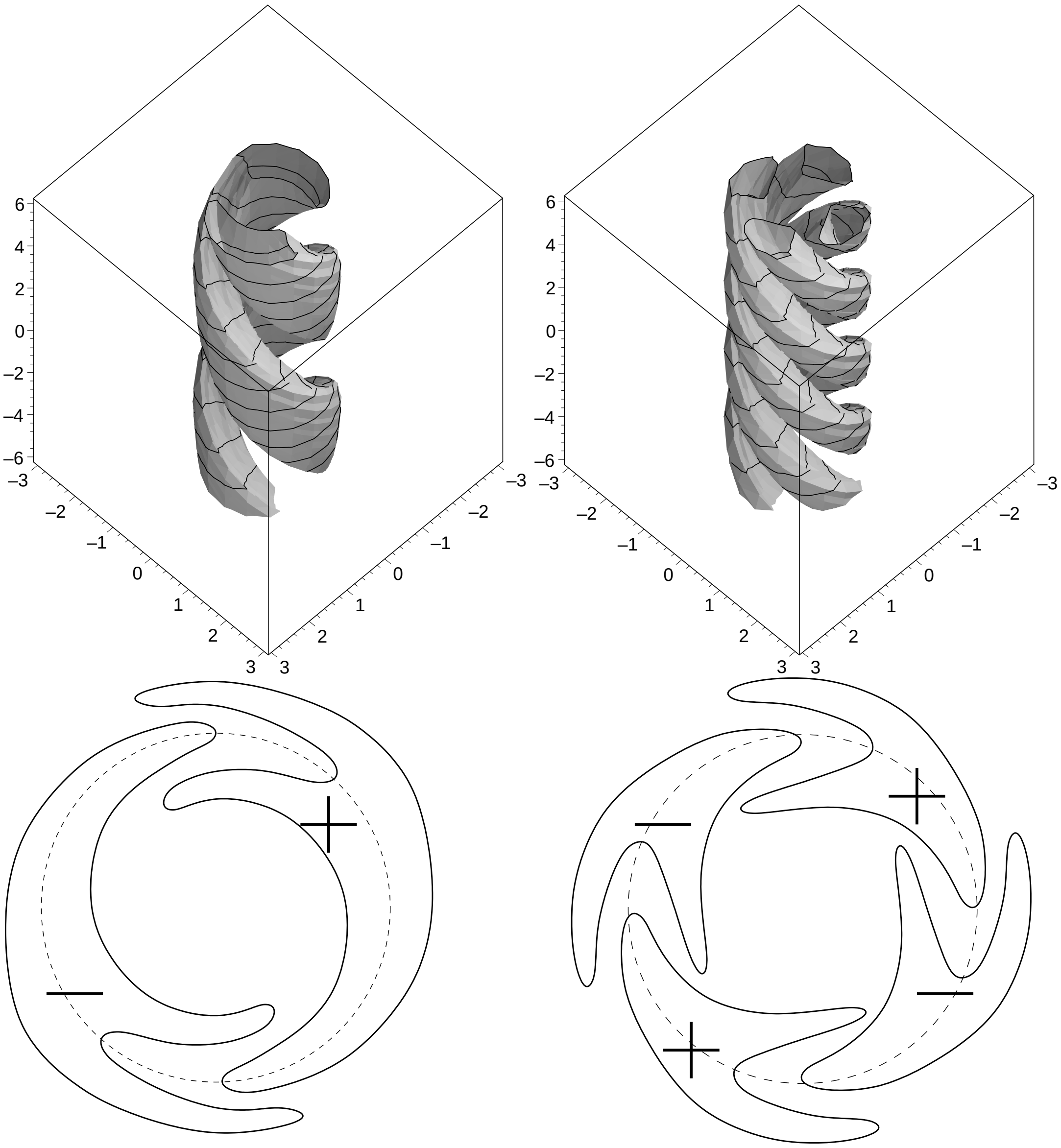

Fig. 2. Magnetic field in the Ponomarenko dynamo at large magnetic Reynolds number $R = \varepsilon^{-1}$ forms spiralling tubes of field localised near the radius $r = a$ for which $m\Omega'(a) + kU'(a) = 0$. The bottom row shows a cross section of the tubes, while the top row shows the three-dimensional structure of the field for $m = 1$ modes (left) and $m = 2$ modes (right). The tubes indicate regions of high field strength $|\boldsymbol{B}|$ and the field is largely directed along the tubes, that is along the spirals of constant $m\theta + kz$ in three dimensions.

of the pitch changing with radius, reducing the radial scale and enhancing diffusion, as mentioned above.

The Ponomarenko mechanism may also be thought of as the first of a number of generic dynamo mechanisms, here amplifying field for flows in which the stream lines lie on closed surfaces. These will arise for general flows of the form $\boldsymbol{u}(x, y)$ in Cartesian coordinates, for example in convection near to onset (Matthews, 1999; Ponty, Gilbert & Soward, 2001), or of the form $\boldsymbol{u}(r,\theta)$ in spherical polar coordinates (r,θ,ϕ) (for example, Dudley & James, 1989). Asymptotic growth rates have been found in these cases (Gilbert & Ponty, 2000) and agreement obtained with simulations of Plunian, Marty & Alemany (1999) of flows modelling nuclear reactor cores. Other applications include modelling of galactic jets (Shukurov & Sokoloff, 1993). A very general framework for such approximations has been given by Soward (1990), and some results on dynamo saturation, with dynamical feedback on the flow field through the Lorentz force, may be found in Bassom & Gilbert (1997) and Dobler, Shukurov & Brandenburg (2002). A related family of dynamos was introduced by Lortz (1968), and involves a helical coordinate system in which the dynamo problem can be reduced to a finite set of ordinary differential equations; see for example Chen & Milovich (1984) and Benton (1979a,b).

Ponomarenko dynamo flows are helical: the *helicity density*

$$h = \boldsymbol{u}\cdot\nabla\times\boldsymbol{u} = 2U\Omega + r(U\Omega' - U'\Omega) \tag{4.43}$$

(Moffatt, 1969) is generally non-zero. This gives some indication of the complexity of the flow and will play an important role when we shortly consider large-scale fields. However it is hard to make a more concrete connection at this point, as some helical flows will satisfy (4.40) and others will not. If a flow does not satisfy this condition, with $r|(\log|\Omega'/U'|)'| > 4$ for all radii, then it appears that for all small C^2 perturbations to the flow for which the stream lines remain on surfaces, the flow will remain a non-dynamo, at least at large R. This opens the question of more general perturbations, which could introduce regions of chaotic particle paths into the flow; flows with Lagrangian chaos will be considered when we discuss fast dynamos in section 6 below.

4.3 G.O. Roberts dynamo: multiple scale analysis

The smooth Ponomarenko dynamo shows that dynamo action can occur in a laminar flow, in which spiral stream lines form a single eddy. The fields are localised about stream surfaces. As a next step in complexity we consider laminar, spatially periodic flows; these might for example model convective cells. This introduces two additional elements that we have not yet considered. First a spatially periodic flow will generally have stagnation points. Secondly there is the possibility to generate large-scale fields that span many cells, and to consider transport effects governing such fields, important in modelling dynamo action in convection and turbulence.

The flow field we consider is a member of the family of *ABC flows* (Beltrami,

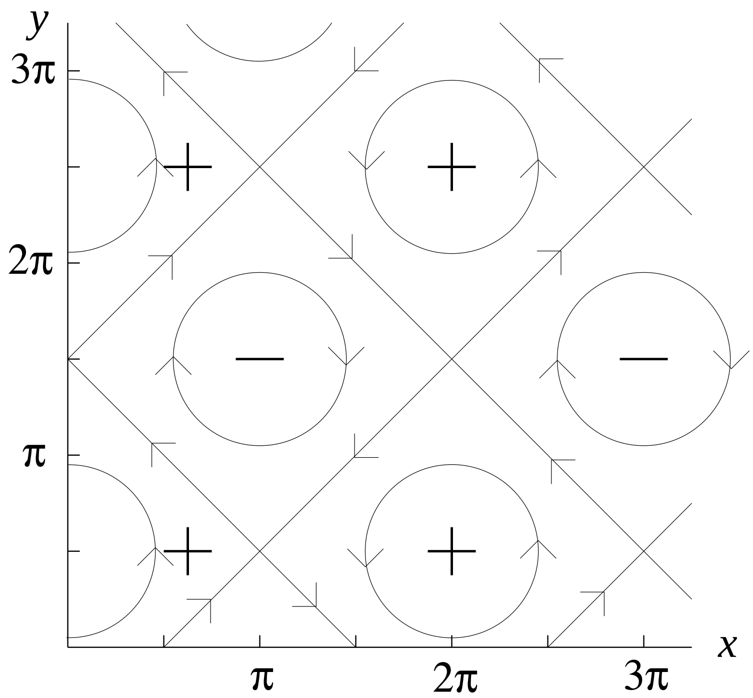

Fig. 3. The G.O. Roberts flow field in (4.45). The + and − signs show the direction of the motion in z, with $u_z = 0$ on the network of separatrices.

1889; Arnold, 1965; Childress, 1970)

$$\boldsymbol{u} = (\mathcal{C}\sin z + \mathcal{B}\cos y, \mathcal{A}\sin x + \mathcal{C}\cos z, \mathcal{B}\sin y + \mathcal{A}\cos x). \tag{4.44}$$

These have the *Beltrami property* that $\nabla \times \boldsymbol{u} = k\boldsymbol{u}$ for a constant k; here $k = 1$. If $\mathcal{C} = 0$ and $\mathcal{A} = \mathcal{B} = 1$, the flow is independent of z,

$$\boldsymbol{u} = (\cos y, \sin x, \sin y + \cos x) = (\partial_y\psi, -\partial_x\psi, \psi), \quad \psi = \sin y + \cos x, \tag{4.45}$$

and has the cellular structure shown in figure 3. This and similar flows are considered numerically by G.O. Roberts (1970) and analytically by Childress (1967, 1970) and G.O. Roberts (1972). We will follow their analysis in a low Reynolds number limit for a large-scale field, using standard multiple-scale asymptotic analysis.

The above flows are already non-dimensionalised and so we will use the induction equation in the form

$$\partial_t\boldsymbol{B} = \nabla \times (\boldsymbol{u} \times \boldsymbol{B}) + R^{-1}\nabla^2\boldsymbol{B}, \quad \nabla \cdot \boldsymbol{B} = 0, \tag{4.46}$$

where R is the magnetic Reynolds number based on the scale of the cells and magnitude of the flow, and is now taken to be small, $R \ll 1$.

We consider a magnetic field $\boldsymbol{B}$ that depends both on the scale $\boldsymbol{x} = (x, y, z)$ of the cellular flow, but also on a larger scale $\boldsymbol{x} = O(R^{-2})$. Diffusion of field across a single cell occurs on a short time-scale $t = O(R)$, and diffusion on scale $\boldsymbol{x} = O(R^{-2})$ over times $t = O(R^{-3})$. We therefore set $t = R\tau$, $\boldsymbol{x} = R^{-2}\boldsymbol{X}$, $t = R^{-3}T$ and replace

$$\partial_t = R^{-1}\partial_\tau + R^3\partial_T, \quad \nabla = \nabla_{\boldsymbol{x}} + R^2\nabla_{\boldsymbol{X}}, \quad \boldsymbol{B} = \boldsymbol{B}_0 + R\boldsymbol{B}_1 + \cdots \tag{4.47}$$

in the induction equation, with $\boldsymbol{B}_j = \boldsymbol{B}_j(\boldsymbol{x}, \tau, \boldsymbol{X}, T)$.

On the small scales $(\boldsymbol{x}, \tau)$, we will require that fields $\boldsymbol{B}_j$ are periodic in space and time, and this means the imposition of solvability conditions that will eventually govern the behaviour of field on large scales $(\boldsymbol{X}, T)$. The velocity field may be taken to be any flow that is strictly periodic in $(\boldsymbol{x}, \tau)$ and has zero mean over these fast variables, $\langle \boldsymbol{u} \rangle = 0$.

From the induction equation at the first few orders we have

$$\begin{aligned}
&(\partial_\tau - \nabla_{\boldsymbol{x}}^2)\boldsymbol{B}_0 = 0, && (4.48)\\
&(\partial_\tau - \nabla_{\boldsymbol{x}}^2)\boldsymbol{B}_1 = \nabla_{\boldsymbol{x}} \times (\boldsymbol{u} \times \boldsymbol{B}_0), && (4.49)\\
&(\partial_\tau - \nabla_{\boldsymbol{x}}^2)\boldsymbol{B}_2 = \nabla_{\boldsymbol{x}} \times (\boldsymbol{u} \times \boldsymbol{B}_1) + 2\nabla_{\boldsymbol{x}} \cdot \nabla_{\boldsymbol{X}}\boldsymbol{B}_0, && (4.50)\\
&(\partial_\tau - \nabla_{\boldsymbol{x}}^2)\boldsymbol{B}_3 = \nabla_{\boldsymbol{x}} \times (\boldsymbol{u} \times \boldsymbol{B}_2) + \nabla_{\boldsymbol{X}} \times (\boldsymbol{u} \times \boldsymbol{B}_0) + 2\nabla_{\boldsymbol{x}} \cdot \nabla_{\boldsymbol{X}}\boldsymbol{B}_1, && (4.51)\\
&(\partial_\tau - \nabla_{\boldsymbol{x}}^2)\boldsymbol{B}_4 = \nabla_{\boldsymbol{x}} \times (\boldsymbol{u} \times \boldsymbol{B}_3) + \nabla_{\boldsymbol{X}} \times (\boldsymbol{u} \times \boldsymbol{B}_1) + 2\nabla_{\boldsymbol{x}} \cdot \nabla_{\boldsymbol{X}}\boldsymbol{B}_2 && \\
&\qquad\qquad\qquad\qquad - (\partial_T - \nabla_{\boldsymbol{X}}^2)\boldsymbol{B}_0, && (4.52)
\end{aligned}$$

and from $\nabla \cdot \boldsymbol{B} = 0$,

$$\begin{aligned}
\nabla_{\boldsymbol{x}} \cdot \boldsymbol{B}_0 &= 0, && (4.53)\\
\nabla_{\boldsymbol{x}} \cdot \boldsymbol{B}_1 &= 0, && (4.54)\\
\nabla_{\boldsymbol{X}} \cdot \boldsymbol{B}_0 + \nabla_{\boldsymbol{x}} \cdot \boldsymbol{B}_2 &= 0. && (4.55)
\end{aligned}$$

At leading order in (4.48) the only solution that is periodic in the fast variables $(\boldsymbol{x}, \tau)$ is a constant field, and so $\boldsymbol{B}_0 = \boldsymbol{B}_0(\boldsymbol{X}, T)$ depends only on large space and time scales (and (4.53) is satisfied automatically). At the next order the equation (4.49) for $\boldsymbol{B}_1$ is a diffusion equation, forced by the periodic function on the right-hand side, and may be solved using Fourier series. Note first that $\nabla_{\boldsymbol{x}} \times (\boldsymbol{u} \times \boldsymbol{B}_0) = \boldsymbol{B}_0 \cdot \nabla_{\boldsymbol{x}}\boldsymbol{u}$ as $\boldsymbol{B}_0$ is uniform on the small scales. If we write

$$\boldsymbol{u} = \sum_{\boldsymbol{k},\omega} \hat{\boldsymbol{u}}_{\boldsymbol{k},\omega} e^{i\boldsymbol{k}\cdot\boldsymbol{x} - i\omega\tau} \qquad (\hat{\boldsymbol{u}}_{\boldsymbol{k},\omega} = \hat{\boldsymbol{u}}^*_{-\boldsymbol{k},-\omega},\ \boldsymbol{k} \cdot \hat{\boldsymbol{u}}_{\boldsymbol{k},\omega} = 0), \tag{4.56}$$

of which the above ABC flows are special cases, then (4.49) may be solved in terms of Fourier modes of $\boldsymbol{B}_1$ as

$$\hat{\boldsymbol{B}}_{1,\boldsymbol{k},\omega} = (k^2 - i\omega)^{-1}(i\boldsymbol{k} \cdot \boldsymbol{B}_0)\hat{\boldsymbol{u}}_{\boldsymbol{k},\omega}. \tag{4.57}$$

The flow thus drives a small-scale field $\boldsymbol{B}_1$, by churning up the large-scale field $\boldsymbol{B}_0$.

The equations (4.50,4.51) for $\boldsymbol{B}_2$ and $\boldsymbol{B}_3$ could be solved in a similar manner. These equations also have solvability conditions, that the right-hand sides must be zero when averaged over the fast scales $(\boldsymbol{x}, \tau)$, so that in Fourier space the factor $k^2 - i\omega$ is non-zero for all terms present and $\partial_\tau - \nabla_{\boldsymbol{x}}^2$ may be inverted. These conditions for (4.50,4.51) are satisfied automatically, using the facts that $\langle \boldsymbol{u} \rangle = 0$, $\langle \boldsymbol{B}_0 \rangle = \boldsymbol{B}_0$, and $\langle \nabla_{\boldsymbol{x}}(\cdot) \rangle = 0$ for any quantity $(\cdot)$. However the solvability of equation (4.52) for $\boldsymbol{B}_4$ gives the evolution of the large-scale field as

$$\partial_T \boldsymbol{B}_0 = \nabla_{\boldsymbol{X}} \times \langle \boldsymbol{u} \times \boldsymbol{B}_1 \rangle + \nabla_{\boldsymbol{X}}{}^2 \boldsymbol{B}_0, \quad \nabla_{\boldsymbol{X}} \cdot \boldsymbol{B}_0 = 0; \tag{4.58}$$

the latter condition follows from averaging (4.55).

The key term here is the *mean electromotive force* or *mean emf*,

$$\bar{\boldsymbol{\mathcal{E}}} \equiv \langle \boldsymbol{u} \times \boldsymbol{B}_1 \rangle, \tag{4.59}$$

which may be written, using (4.56,4.57) and averaging over space and time, as

$$\bar{\boldsymbol{\mathcal{E}}} = \sum_{\boldsymbol{k},\omega} \frac{(i\boldsymbol{k} \cdot \boldsymbol{B}_0)(\hat{\boldsymbol{u}}^*_{\boldsymbol{k},\omega} \times \hat{\boldsymbol{u}}_{\boldsymbol{k},\omega})}{k^2 - i\omega}. \tag{4.60}$$

To simplify this expression note first that by incompressibility $\boldsymbol{k}$ and $\hat{\boldsymbol{u}}_{\boldsymbol{k},\omega}$ are perpendicular and so $\hat{\boldsymbol{u}}^*_{\boldsymbol{k},\omega} \times \hat{\boldsymbol{u}}_{\boldsymbol{k},\omega}$ is parallel to $\boldsymbol{k}$. We may therefore write

$$\hat{\boldsymbol{u}}^*_{\boldsymbol{k},\omega} \times \hat{\boldsymbol{u}}_{\boldsymbol{k},\omega} = k^{-2} \hat{H}(\boldsymbol{k},\omega) i\boldsymbol{k}, \quad \hat{H}(\boldsymbol{k},\omega) = \hat{\boldsymbol{u}}^*_{\boldsymbol{k},\omega} \cdot i\boldsymbol{k} \times \hat{\boldsymbol{u}}_{\boldsymbol{k},\omega}. \tag{4.61}$$

Here $\hat{H}(\boldsymbol{k},\omega)$ is the contribution to the helicity per unit volume of the fluid flow from the mode $(\boldsymbol{k},\omega)$,

$$H = \langle \boldsymbol{u} \cdot \nabla \times \boldsymbol{u} \rangle = \sum_{\boldsymbol{k},\omega} \hat{H}(\boldsymbol{k},\omega). \tag{4.62}$$

One can easily check that $\hat{H}(\boldsymbol{k},\omega)$ is real and that $\hat{H}(\boldsymbol{k},\omega) = \hat{H}(-\boldsymbol{k},-\omega)$. With a little further simplification (combining the contributions from modes $(\boldsymbol{k},\omega)$ and $(-\boldsymbol{k},-\omega)$) we may write the mean emf as

$$\bar{\mathcal{E}}_m = \alpha_{mn} B_{0n}, \quad \alpha_{mn} = -\sum_{\boldsymbol{k},\omega} \frac{k_m k_n \hat{H}(\boldsymbol{k},\omega)}{k^4 + \omega^2}. \tag{4.63}$$

This is an important result: the mean emf is written as a tensor α_{mn} multiplying the large-scale field.

The generation of a mean emf by small-scale fluid flow is known as the *alpha effect* and was first introduced by Parker (1955) and Steenbeck, Krause & Rädler (1966). We will discuss it further in section 5.1 below. For the G.O.

Roberts flow (4.45) the alpha tensor may be computed as

$$\boldsymbol{\alpha} \equiv (\alpha_{mn}) = \alpha \boldsymbol{I}_2, \quad \alpha = -1, \quad \boldsymbol{I}_2 \equiv \begin{pmatrix} 1 & 0 & 0 \\ 0 & 1 & 0 \\ 0 & 0 & 0 \end{pmatrix}. \tag{4.64}$$

With this alpha effect now written down explicitly, the mean field satisfies

$$\partial_T \boldsymbol{B}_0 = \nabla_{\boldsymbol{X}} \times (\boldsymbol{\alpha} \cdot \boldsymbol{B}_0) + {\nabla_{\boldsymbol{X}}}^2 \boldsymbol{B}_0, \quad \nabla_{\boldsymbol{X}} \cdot \boldsymbol{B}_0 = 0. \tag{4.65}$$

Consider a large-scale field mode $\boldsymbol{B}_0 = \boldsymbol{\beta} e^{iKZ+\Lambda T}$ with $\boldsymbol{\beta} \cdot \hat{\boldsymbol{z}} = 0$, and $\nabla_{\boldsymbol{X}} \times \boldsymbol{B}_0 = \pm K \boldsymbol{B}_0$; this has growth rate

$$\Lambda = \mp K - K^2. \tag{4.66}$$

The field modes and the corresponding vector potentials are, up to translation in Z, given by

$$\boldsymbol{B}_0 = (\pm \sin KZ, \cos KZ, 0), \quad \boldsymbol{A}_0 = \pm K^{-1} (\pm \sin KZ, \cos KZ, 0). \tag{4.67}$$

We see that from (4.66) that the G.O. Roberts flow, which has positive fluid helicity density $h = \boldsymbol{u} \cdot \boldsymbol{\omega}$, amplifies large-scale magnetic fields having negative *magnetic helicity density* $h_{\mathrm{M}} = \boldsymbol{A} \cdot \boldsymbol{B}$.

If the flow is rewritten in dimensional units with

$$\boldsymbol{u} = u_0 (\cos ky, \sin kx, \sin ky + \cos kx), \quad R = u_0/\eta k, \tag{4.68}$$

and the induction equation used with η replacing R^{-1}, then the result is that large-scale modes of wave number q have growth rates

$$\gamma = \pm \alpha q - \eta q^2, \quad \alpha = -u_0^2/\eta k = -R u_0. \tag{4.69}$$

The fastest growing mode has

$$q_{\max} = -\alpha/2\eta = kR^2/2, \quad \gamma_{\max} = \alpha^2/4\eta = R^3 k u_0/4. \tag{4.70}$$

This example highlights the role of fluid helicity in dynamo theory. The alpha effect, a transport effect that at large scales dominates over diffusion, is given by a weighted sum over the helicity of the fluid flow. We will discuss alpha effects further below in section 5.1. Helicity has a topological interpretation in terms of the linkage of vorticity lines for $h = \boldsymbol{u} \cdot \boldsymbol{\omega}$ in a fluid, or magnetic field lines for $h_M = \boldsymbol{A} \cdot \boldsymbol{B}$ (Woltjer, 1958; Moffatt, 1969; Moffatt & Ricca, 1992).

If the alpha tensor vanishes completely, for example in mirror-symmetric flows for which $\hat{H}(\boldsymbol{k}, \omega) = 0$, it is possible to rescale and pick up an eddy diffusivity term as a transport effect involving second derivatives of $\boldsymbol{B}_0$. This term can be negative for suitable choices of flows and magnetic Reynolds numbers, corresponding again to the destabilisation of field at large scales (Kraichnan, 1976a; Lanotte, Noullez, Vergassola & Wirth, 1999); see also Kazantsev (1967). A transport effect analogous to the alpha effect can also occur in forced fluid flows (Frisch, She & Sulem, 1987): in this case the averaging is taken over Reynolds stresses and large-scale helical fluid flows can be destabilised.

The above theory involves the limit of low magnetic Reynolds number, and it is important to note that this is based on the scale of the periodic flow field, not on the scale of the magnetic field itself. Indeed to contain the fastest growing mode given above, the whole system needs to have a scale of order $L = q_{\max}^{-1}$, and so a Reynolds number based on this scale would be $R_L = u_0 L/\eta = 2R^{-1}$. This diverges in the limit we are taking and shows, first that there is no contradiction with the upper bounds derived in section 3.5 above, and secondly that these dynamos are not particularly efficient for small R. The motion $\boldsymbol{u}$ has only a weak effect on the field $\boldsymbol{B}_0$, as small-scale diffusion is so dominant, and thus only large-scale fields can be sustained by this mechanism.

The G.O. Roberts flow forms the basis of dynamo experiments taking place in Karlsruhe, Germany (Busse, 2000; Tilgner, 2000; Stieglitz & Müller, 2001). To obtain a suitable two-scale flow liquid sodium is constrained to flow in a series of pipes and helical channels, which mimic the flow depicted in figure 3 for finite ranges of z and $x^2 + y^2$. The height of the apparatus is approximately 1 metre, diameter 2 metres and it contains 52 helical cells. Dynamo action has been observed experimentally and has been studied in detail numerically: the field adopts a configuration that within the limitations of the finite geometry may be identified with a large-scale helical mode.

Finally, it is possible to extend the above theory for low magnetic Reynolds number to include dynamical effects, if the underlying flow is viscous and driven by a prescribed body force (Krause & Rädler, 1980; Krause & Meinel, 1988; Gilbert & Sulem, 1990). In this case the alpha tensor (4.63) becomes a nonlinear function of the mean field. If the forcing, in the absence of magnetic field, is chosen to drive the G.O. Roberts flow, equation (4.65) becomes (after a suitable rescaling from $\boldsymbol{B}_0$ to $\bar{\boldsymbol{B}}$, say)

$$\partial_T \bar{B}_x = -\alpha_0 \partial_Z (\bar{B}_y (\bar{B}_y^2 + 1)^{-2}) + \partial_Z^2 \bar{B}_x, \quad \partial_T \bar{B}_y = \alpha_0 \partial_Z (\bar{B}_x (\bar{B}_x^2 + 1)^{-2}) + \partial_Z^2 \bar{B}_y. \tag{4.71}$$

Here α_0 is the value of the alpha coefficient in the kinematic regime when $\bar{\boldsymbol{B}}$ is weak. When this system is simulated beginning with a seed magnetic field, initially the kinematically most unstable field mode grows. However as nonlinear interactions become important the magnetic energy is driven to the

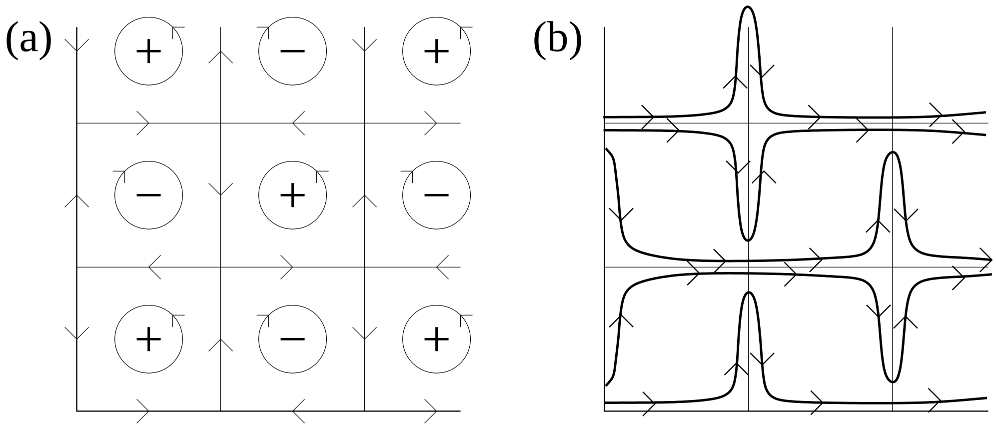

Fig. 4. The G.O. Roberts flow field written in the form (4.72). (a) shows stream lines. (b) shows the steady state with a uniform imposed x-directed magnetic field, $\bar{b}_x = 1$, $\bar{b}_y = 0$ with $\varepsilon \ll 1$. Magnetic field lines are shown, which are also lines of constant scalar a.

largest scales of the system, through a series of meta-stable states, in what is known as an *inverse cascade* (Gilbert & Sulem, 1990). Such cascades have been observed in MHD turbulence (Pouquet, Frisch & Léorat, 1976) and in other nonlinear dynamos (see for example, Brandenburg, 2001).

4.4 G.O. Roberts dynamo for large R

We studied the G.O. Roberts dynamo when the Reynolds number R, based on the scale of the cells in the flow, is small. In this limit only large-scale magnetic field modes are destabilised and growth rates tend to zero. It is natural to consider also the opposite limit of asymptotically large R, as we did for the smooth Ponomarenko dynamo in section 4.2. The dynamo has been studied numerically by G.O. Roberts (1970) and in this limit by Childress (1979), Anufriyev & Fishman (1982), Perkins & Zweibel (1987) and Soward (1987). For large R a Ponomarenko dynamo will also generally occur in the closed stream lines of each cell of the network depicted in figure 3 whenever a criterion analogous to (4.40) is satisfied (Soward, 1990; Gilbert & Ponty, 2000). We will now however consider the possibility of large-scale fields: at high R magnetic modes tend to localise on stream surfaces and so large-scale modes must be localised on the network of hyperbolic stagnation points and separatrices shown in figure 3.

It is first convenient to rotate axes and rescale space, and so write the flow in the form

$$\boldsymbol{u} = (\sin x \cos y, -\cos x \sin y, \sqrt{2}\,\sin x \sin y) = (\partial_y \psi, -\partial_x \psi, K\psi), \qquad (4.72)$$

with

$$\psi = \sin x \sin y, \quad K = \sqrt{2}. \tag{4.73}$$

We will solve the induction equation in the dimensionless form

$$\partial_t \boldsymbol{B} = \nabla \times (\boldsymbol{u} \times \boldsymbol{B}) + \varepsilon \nabla^2 \boldsymbol{B}, \quad \nabla \cdot \boldsymbol{B} = 0, \tag{4.74}$$

with $\varepsilon \equiv R^{-1} \ll 1$ now. We note the minor point that the rescaling of space implies a redefinition of the magnetic Reynolds number, and that now $\nabla \times \boldsymbol{u} = \sqrt{2}\boldsymbol{u}$. The flow is shown in figure 4(a).

To obtain growth rates we will follow Childress (1979) and again use an alpha effect to make progress. We divide the magnetic field into a mean and a fluctuating part, simultaneously taking out a normal mode in z and t,

$$\boldsymbol{B}(x, y, z, t) = (\bar{\boldsymbol{b}} + \boldsymbol{b}'(x, y))e^{\lambda t + ikz}, \quad \langle \boldsymbol{b}' \rangle = 0. \tag{4.75}$$

Here $\langle \cdot \rangle$ denotes an average over x and y and $\bar{\boldsymbol{b}}$ is a constant which we refer to as the mean field. Averaging the induction equation and solenoidal condition (4.74) gives

$$(\lambda + \varepsilon k^2)\bar{\boldsymbol{b}} = ik\hat{\boldsymbol{z}} \times \langle \boldsymbol{u} \times \boldsymbol{b}' \rangle, \quad ik\hat{\boldsymbol{z}} \cdot \bar{\boldsymbol{b}} = 0, \tag{4.76}$$

using $\langle \partial_x(\cdot) \rangle = \langle \partial_y(\cdot) \rangle = 0$ and $\langle \boldsymbol{u} \rangle = 0$. The fluctuating, zero-mean parts of these equations are

$$\begin{aligned} (\lambda + \varepsilon k^2)\boldsymbol{b}' = (\partial_x, \partial_y, ik) \times (\boldsymbol{u} \times \bar{\boldsymbol{b}} + \boldsymbol{u} \times \boldsymbol{b}') \qquad & (4.77) \\ - ik\hat{\boldsymbol{z}} \times \langle \boldsymbol{u} \times \boldsymbol{b}' \rangle + \varepsilon(\partial_x^2 + \partial_y^2)\boldsymbol{b}', & \\ (\partial_x, \partial_y, ik) \cdot \boldsymbol{b}' = 0. \qquad & (4.78) \end{aligned}$$

These equations are exact and we see a similar structure to the previous multiple scales framework. The mean field $\bar{\boldsymbol{b}}$ is driven by a mean emf $\bar{\boldsymbol{\mathcal{E}}} = \langle \boldsymbol{u} \times \boldsymbol{b}' \rangle$. The fluctuating field $\boldsymbol{b}'$ is governed by a linear equation with a source term from transport and stretching of the mean field.

We fix $\varepsilon \ll 1$ and consider the limit of small, positive k, that is of fields with large-scale dependence on z. (For $k = 0$ the magnetic field is independent of z and so cannot be a dynamo by anti-dynamo theorem 1.) Assuming that the combination $\lambda + \varepsilon k^2$ is small as $k \to 0$ with ε fixed (verified later in (4.102)), the leading order approximation to (4.77) is

$$0 = (\partial_x, \partial_y, 0) \times (\boldsymbol{u} \times \bar{\boldsymbol{b}} + \boldsymbol{u} \times \boldsymbol{b}') + \varepsilon(\partial_x^2 + \partial_y^2)\boldsymbol{b}', \quad (\partial_x, \partial_y, 0) \cdot \boldsymbol{b}' = 0. \tag{4.79}$$

This is just the steady induction equation for $\boldsymbol{b}'$ in the presence of a given, constant mean field $\bar{\boldsymbol{b}}$. The fluctuating field $\boldsymbol{b}'$ generated will depend linearly on $\bar{\boldsymbol{b}}$ and so the mean emf can be written

$$\bar{\mathcal{E}}_m = \alpha_{mn}\bar{b}_n, \quad \boldsymbol{\alpha} = \alpha \boldsymbol{I}_2, \tag{4.80}$$

where $\boldsymbol{\alpha}$ is the alpha tensor. Since $\bar{b}_z = 0$ from (4.76), only the 2×2 block of (x, y)-components of the $\boldsymbol{\alpha}$ tensor is relevant, and this block is isotropic, which follows from the symmetries of the flow $\boldsymbol{u}$. For example, the flow is invariant under rotation through $\pi/2$ about the axis $x = y = \pi/2$. All the symmetries of the flow are evident from figure 4 but a more formal discussion is given in Gilbert (1992) and section 5.5 of Childress & Gilbert (1995).

The framework is now very similar to that of anti-dynamo theorem 1 in section 3.3 above, except that there is an imposed constant mean field $\bar{\boldsymbol{b}}$ maintaining magnetic energy in the system. We decompose the full magnetic field in the form

$$\boldsymbol{b} = \nabla \times (\hat{\boldsymbol{z}} a) + \hat{\boldsymbol{z}}\, b_z = (\partial_y a, -\partial_x a, b_z), \tag{4.81}$$

where the scalar potential a incorporates the mean field $\bar{\boldsymbol{b}}$, and may be written in the form

$$a(x, y) = a'(x, y) + \bar{a}(x, y), \quad \bar{a} = (y - \pi/2)\bar{b}_x - (x - \pi/2)\bar{b}_y, \quad \langle a' \rangle = 0. \tag{4.82}$$

Here $a'(x, y)$ is required to be periodic in space, and the definition of $\bar{a}$ is such as to make a zero at the centre $(\pi/2, \pi/2)$ of the *primary cell* $0 \leq x, y \leq \pi$ in the development below. The steady equations (4.79) for a and b_z are (using $u_z = K\psi$)

$$\boldsymbol{u} \cdot \nabla a = \varepsilon \nabla^2 a, \tag{4.83}$$

$$\boldsymbol{u} \cdot \nabla b_z = -K \boldsymbol{u} \cdot \nabla a + \varepsilon \nabla^2 b_z \tag{4.84}$$

(cf. (3.27), (3.28)).

The equation for a governs a scalar with a prescribed mean gradient in the flow $\boldsymbol{u}$, and so is of interest in the theory of scalar transport (Rosenbluth, Berk, Doxas & Horton, 1987; Shraiman, 1987; Soward, 1987). For example let us take $\bar{b}_x = 1$, $\bar{b}_y = 0$, and then we can interpret the results in two ways. First, the problem is one of the steady state of a uniform x-directed field in this flow field, in which case the field lines (projected down on the (x, y)-plane) of constant a are shown schematically in figure 4(b). For small ε the field is expelled from the recirculating eddies and sits in boundary layers along the separatrices. In this case we are interested in computing the alpha effect, with

$$\alpha = \langle \hat{\boldsymbol{x}} \cdot \boldsymbol{u} \times \boldsymbol{b} \rangle = \langle b_z u_y \rangle - K \langle b_y \psi \rangle \qquad (\bar{\boldsymbol{b}} = \hat{\boldsymbol{x}}) \tag{4.85}$$

(using (4.72)). Replacing $b_y = -\partial_x a$ in the last term and integrating by parts gives

$$\alpha = \langle b_z u_y \rangle + K \langle a u_y \rangle \qquad (\bar{\boldsymbol{b}} = \hat{\boldsymbol{x}}). \tag{4.86}$$

Secondly, we can interpret the field lines (without arrows) in figure 4(b) as contours of constant passive scalar a in a steady state obtained by imposing a uniform gradient in y. In this case the quantity of interest is the net flux of scalar in the $-y$-direction, down the gradient, which gives the effective diffusivity κ of the scalar in this flow field,

$$\kappa = -\langle a u_y \rangle \qquad (\bar{a} = y - \pi/2). \tag{4.87}$$

The second term of (4.86) appears in (4.87) for κ, and in fact the first term is also closely related, as we shall see.

To make further progress we assume that the magnetic field is confined to boundary layers along the network of separatrices as shown in figure 4. Inside the eddies the field is suppressed by the process of flux expulsion. Let us focus on one boundary layer, $0 \le x \le \pi$ and $y = 0$. Here we replace coordinates (x, y) by (s, ψ) with $s = x$. It then follows that $\partial_x = \partial_s - u_y \partial_\psi$ and $\partial_y = u_x \partial_\psi$. We assume that the scale of the field is $\varepsilon^{1/2}$ in the ψ coordinate, but of order unity in s. In this region $u_x = O(1)$ and $u_y = O(\varepsilon^{1/2})$ and, at leading order, equations (4.83,4.84) become

$$q\partial_s a = \varepsilon q^2 \partial_\psi^2 a, \tag{4.88}$$
$$q\partial_s b_z = \varepsilon q^2 \partial_\psi^2 b_z - Kq\partial_s a, \tag{4.89}$$

where $q = (u_x^2 + u_y^2)^{1/2} \simeq u_x \simeq \sin x = \sin s$ is the fluid velocity on this separatrix. A further transformation to *von Mises coordinates*,

$$\sigma = \int_0^s q\, ds = 1 - \cos s, \quad \xi = \varepsilon^{-1/2}\psi, \tag{4.90}$$

leaves us with

$$\partial_\sigma a = \partial_\xi^2 a, \tag{4.91}$$
$$\partial_\sigma b_z = \partial_\xi^2 b_z - K\partial_\sigma a, \tag{4.92}$$

a heat diffusion equation for a and a similar but forced equation for b_z.

This is correct for the separatrix $0 \le x \le \pi$, $y = 0$, for which $0 \le \sigma \le 2$, but can be extended all the way around the boundary of the primary cell $0 \le x, y \le \pi$, with $0 \le \sigma \le 8$, as depicted in figure 5(a). For example, q is replaced by u_y on $2 \le \sigma \le 4$. After one traversal of the primary cell we must identify $a(0, \xi) = a(8, \xi)$ and $b_z(0, \xi) = b_z(8, \xi)$. At the corners that connect the separatrices, the boundary layers thicken to be of width $\varepsilon^{1/4}$ in x and y and diffusion is subdominant to advection, with the result that the fields a and b_z are continuous at $\sigma = 0$, 2, 4 and 6 (see Childress, 1979, for further discussion). In the eddies a is constant as there is no magnetic field, and in view of (4.82) $a = 0$ in the centre of the primary cell.

Looking at the symmetries evident in figures 4 and 5, and bearing in mind

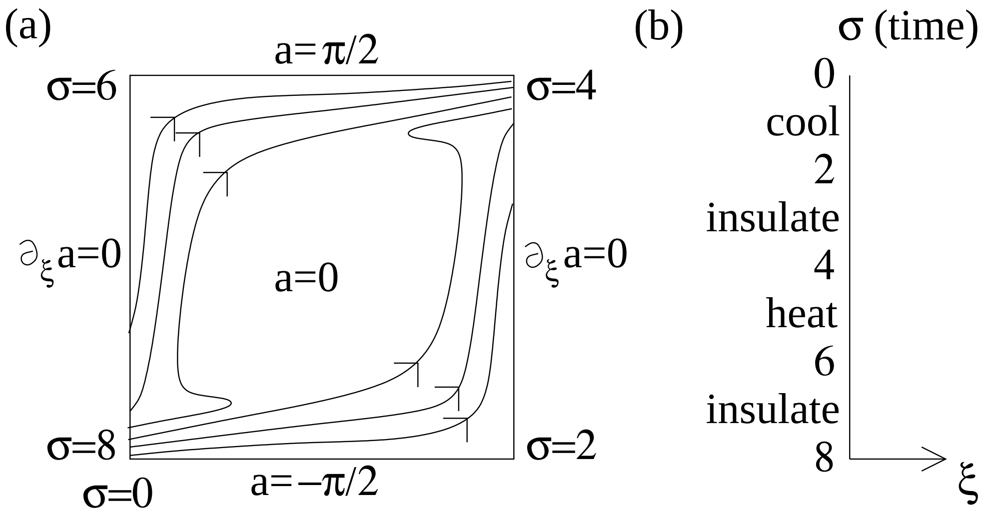

Fig. 5. Magnetic boundary layers in the G.O. Roberts flow field. (a) boundary conditions in the cellular geometry. (b) the boundary layer problem as a heated, cooled and insulated semi-infinite rod.

that $\bar{a} = y - \pi/2$, the boundary conditions on a and b_z are

$$a(\sigma, 0) = -\pi/2, \qquad b_z(\sigma, 0) = 0 \qquad (0 \le \sigma \le 2), \tag{4.93}$$
$$\partial_\xi a(\sigma, 0) = 0, \qquad b_z(\sigma, 0) = 0 \qquad (2 \le \sigma \le 4), \tag{4.94}$$
$$a(\sigma, 0) = \pi/2, \qquad b_z(\sigma, 0) = 0 \qquad (4 \le \sigma \le 6), \tag{4.95}$$
$$\partial_\xi a(\sigma, 0) = 0, \qquad b_z(\sigma, 0) = 0 \qquad (6 \le \sigma \le 8), \tag{4.96}$$

and that a, b_z tend to zero for large ξ, that is, towards the centre of the primary cell. With these boundary conditions, we note that given a solution $a(\sigma, \xi)$ of (4.91), then the corresponding solution to (4.92) for b_z is just $b_z = \frac{1}{2} K \xi \partial_\xi a$.

The problem for a takes the form of a diffusion equation (4.91) with σ, the coordinate around the primary cell, taking the role of time and spatial coordinate $\xi \ge 0$. The boundary conditions correspond to cooling the end of a semi-infinite bar to temperature $a = -\pi/2$ for time $0 \le \sigma \le 2$, insulating it for $2 \le \sigma \le 4$, heating the end to $a = \pi/2$ for $4 \le \sigma \le 6$, insulating it for $6 \le \sigma \le 8$, and then repeating this process; see figure 5(b). What is required is the periodic solution in time, corresponding to a periodic solution in σ around the primary cell. This can be solved by the Weiner–Hopf technique and is discussed in Soward (1987). A key quantity that emerges from the analysis is

$$\int_0^\infty a(\sigma, \xi)\, d\xi = -\frac{\pi}{2} G \quad (2 \le \sigma < 4), \qquad \int_0^\infty a(\sigma, \xi)\, d\xi = \frac{\pi}{2} G \quad (6 \le \sigma < 8), \tag{4.97}$$

with

$$G = 2\sqrt{\frac{2}{\pi}} \sum_{n=0}^{\infty} \frac{(-1)^n}{\sqrt{2n+1}} \simeq 1.0655. \tag{4.98}$$

The integrands in (4.97) are constants as σ varies over the ranges given (using

(4.91), (4.94) and (4.96)), and correspond to the total heat in the bar during periods of time when the end is insulated.

Now we need to obtain κ (4.87) and α (4.86). The average $\langle au_y\rangle$ is dominated by the boundary layers corresponding to $2 \leq \sigma \leq 4$ and $6 \leq \sigma \leq 8$, which give equal contributions. On $2 \leq \sigma \leq 4$, $q = u_y$ and also $q\,dx\,dy = ds\,d\psi$. Thus $au_y\,dx\,dy = a\,ds\,d\psi = \varepsilon^{1/2}a\,ds\,d\xi$. Now the integral of a over ξ is given above in (4.97) and is a constant on this separatrix, which is of length π in s. Thus we obtain

$$\langle au_y\rangle \equiv \pi^{-2}\int_0^\pi\int_0^\pi au_y\,dx\,dy = 2\pi^{-1}\varepsilon^{1/2}\int_0^\infty a\,d\xi = -\varepsilon^{1/2}G. \tag{4.99}$$

We also require $\langle b_z u_y\rangle$ for α in (4.86). Now

$$\int_0^\infty b_z\,d\xi = \int_0^\infty \tfrac{1}{2}K\xi\partial_\xi a\,d\xi = -\tfrac{1}{2}K\int_0^\infty a\,d\xi, \tag{4.100}$$

using integration by parts, and so $\langle b_z u_y\rangle = -\frac{1}{2}K\langle au_y\rangle$.

Finally we obtain the results for the alpha effect and effective scalar diffusivity,

$$\alpha = -\tfrac{1}{2}K\varepsilon^{1/2}G, \quad \kappa = \varepsilon^{1/2}G. \tag{4.101}$$

For a passive scalar, the flux through molecular diffusion is ε, and so the transport through boundary layers represents an enhancement of diffusion. As far as magnetic fields are concerned, the alpha effect given implies a growth rate for large-scale field modes of wave number k, with

$$\lambda \simeq \mp\tfrac{1}{2}K\varepsilon^{1/2}Gk - \varepsilon k^2 \tag{4.102}$$

from (4.76) and (4.80), the lower sign corresponding to modes of negative magnetic helicity. The last term is of course subdominant. Reassuringly, $K \neq 0$ is required for dynamo action, in keeping with anti-dynamo theorem 2 above.

The physical mechanism amplifying the field may be seen from figure 4. Given mean field $\bar{\boldsymbol{b}}$ in the x-direction, the flow draws out tongues of field along the separatrices in the y-direction. The upward and downward flows are such as to lift $+y$-directed field in the tongues up in the z-direction, while pushing down $-y$-directed field. If the $\bar{b}_x$ field depends on a large scale as $\bar{b}_x = \cos kz$, the effect of the generation and motion of y-field is to reinforce the field component $\bar{b}_y = \sin kz$. This corresponds to a magnetic mode of negative helicity.

This mechanism, identified by G.O. Roberts (1970), only lifts field a distance of order $\varepsilon^{1/2}$ in z. The reinforcement of large-scale fields is rather poor for small ε, and indeed the growth rate (4.102) increases as the scale in z is reduced, by increasing k. The form of the growth rate (4.102) suggests that the maximum growth rate is $\lambda_{\max} = O(1)$, achieved at $k_{\max} = O(\varepsilon^{-1/2})$. However this is not a firm estimate, and further analysis has been done by Soward (1987) to show that the maximum growth rate is

$$\lambda_{\max} = O\left(\frac{\log\log\varepsilon^{-1}}{\log\varepsilon^{-1}}\right), \quad k_{\max} = O\left(\frac{\varepsilon^{-1/2}}{\sqrt{\log\varepsilon^{-1}}}\right). \tag{4.103}$$

This analysis involves a rather more delicate treatment of the boundary layers in which the vertical z-dependent structure of the field now intrudes.

The maximum growth rates for the G.O. Roberts dynamo decrease only very slowly as $\varepsilon \to 0$ and so this dynamo is very close to being a fast dynamo, for which $\lambda_{\max}$ would remain of order unity as $\varepsilon \to 0$. The dynamo can be made into a fast dynamo by modifying the flow so as to introduce singularities at the hyperbolic stagnation points (Soward, 1987); these have the effect of tearing fluid elements apart in a finite time at the corners of the cells.

Further studies of the alpha effect and scalar transport in space-periodic steady flows $\boldsymbol{u}(x, y)$ may be found in Childress & Soward (1989) and Soward & Childress (1990). In a numerical study of a space-periodic flow (Plunian, Marty & Alemany, 1999), modelling the core of a nuclear reactor, there is a competition between Ponomarenko modes, localised on closed stream surfaces, and G.O. Roberts modes, localised on the network of separatrices. A similar competition is found in simulations of dynamo action in convection and driven fluid flows (Ponty, Gilbert & Soward, 2001); see section 5.4 below.

5 The alpha effect and dynamo modelling

In this section we leave systematic asymptotic analysis of dynamos, and discuss dynamo modelling and the magnetic fields of the Sun, Earth and galaxies. We return to the more mathematical topic of fast dynamos in section 6 below.

5.1 The alpha effect

We first met the alpha effect while studying the G.O. Roberts dynamo. Using dimensional quantities, we may write down a general expression involving a weighted sum of the helicity in the modes of the flow field,

$$\alpha_{mn} = -\eta \sum_{\boldsymbol{k},\omega} \frac{k_m k_n \hat{H}(\boldsymbol{k}, \omega)}{\eta^2 k^4 + \omega^2}, \tag{5.1}$$

which is valid when the magnetic Reynolds number $R = u_0/k\eta$ based on the scale of the small-scale flow is small. In a continuum limit of wave vectors $(\boldsymbol{k}, \omega)$

and when the small-scale flow is isotropic, the tensor is isotropic, involving an integral over the *helicity spectrum* $\hat{H}(k,\omega)$,

$$\boldsymbol{\alpha} = \alpha \boldsymbol{I}, \quad \alpha = -\frac{\eta}{3}\int \frac{k^2 \hat{H}(k,\omega)}{\eta^2 k^4 + \omega^2}\, dk\, d\omega \tag{5.2}$$

(Moffatt, 1978). We also met the alpha effect for large R in the G.O. Roberts (1970) flow, but this was closely connected with the geometry of the separatrices, and unsurprisingly no formulae are known for general flows.

An alpha effect also appears in the theory of Braginsky (1964a,b) in which a magnetic field is dominated by a strong axisymmetric component, and this is maintained by a flow with strong toroidal and weak poloidal components. In this theory the magnetic Reynolds number is large, and the non-axisymmetric parts of the flow and field, while not dominant, mean that the anti-dynamo theorems 3 and 4 do not apply. We will not develop this theory here; see for example Moffatt (1978), Soward (1990), Braginsky (1994) and references therein.

The idea of the alpha effect has been extremely important in the development of dynamo theory. While analysis of dynamo models such as those of Backus (1958), Herzenberg (1958), Lortz (1968), G.O. Roberts (1970) and Ponomarenko (1973) show that in principle dynamo action can occur, the fluid flows proposed are far from those in astrophysical bodies. However the alpha effect involves averaging over small-scale flows, which could include turbulent convection. This new transport effect can both short-circuit detailed study of fluid flows and also bypass the anti-dynamo theorems. The introduction of this effect by Parker (1955), Braginsky (1964a,b) and Steenbeck, Krause & Rädler (1966) represented a breakthrough in the modelling of real astrophysical dynamos.

An alpha effect may be argued on general grounds as follows (see, for example, Moffatt, 1978; Krause & Rädler, 1980). Consider a situation in which there is a magnetic field $\bar{\boldsymbol{B}}$ on large scales L, and turbulence $\boldsymbol{u}$ on small scales l. We write the full magnetic field as $\boldsymbol{B} = \bar{\boldsymbol{B}} + \boldsymbol{B}'$ and take $\langle \boldsymbol{B}' \rangle = \langle \boldsymbol{u} \rangle = 0$, where $\langle \cdot \rangle$ represents an average over scales intermediate between L and l. Then the induction equation may be separated into a mean and a fluctuating part,

$$\partial_t \bar{\boldsymbol{B}} = \nabla \times \bar{\boldsymbol{\mathcal{E}}} + \eta \nabla^2 \bar{\boldsymbol{B}}, \qquad \bar{\boldsymbol{\mathcal{E}}} = \langle \boldsymbol{u} \times \boldsymbol{B}' \rangle, \tag{5.3}$$

$$\partial_t \boldsymbol{B}' = \nabla \times (\boldsymbol{u} \times \bar{\boldsymbol{B}}) + \nabla \times (\boldsymbol{u} \times \boldsymbol{B}' - \langle \boldsymbol{u} \times \boldsymbol{B}' \rangle) + \eta \nabla^2 \boldsymbol{B}'. \tag{5.4}$$

The equation for $\boldsymbol{B}'$ is linear, with a source term involving $\bar{\boldsymbol{B}}$. Plainly $\boldsymbol{B}'$ and so the emf $\bar{\boldsymbol{\mathcal{E}}}$ are linear functionals of $\bar{\boldsymbol{B}}$. If the field $\bar{\boldsymbol{B}}$ is of large scale then an expansion of the form

$$\bar{\mathcal{E}}_i = \alpha_{ij} \bar{B}_j + \beta_{ijk} \partial_k \bar{B}_j + \cdots \tag{5.5}$$

is suggested. Here the alpha tensor α_{ij} and the *eddy diffusion tensor* β_{ijk} are in fact *pseudo-tensors*.

Without being too formal, we recall that vectors (and tensors) may be classified according to how they transform under mirror inversion $M : \boldsymbol{r} \to -\boldsymbol{r}$. This transformation has Jacobian $\boldsymbol{\mathcal{J}} = \partial(M(\boldsymbol{r}))/\partial(\boldsymbol{r}) = -\boldsymbol{I}$. Vectors are called *polar* if under mirror inversion they transform by multiplication by $\boldsymbol{\mathcal{J}} = -\boldsymbol{I}$, so that they change sign; such vectors transform 'in the natural way' under M. Vectors are called *axial* if they transform by multiplication by $-\boldsymbol{\mathcal{J}} = \boldsymbol{I}$, so that they do not change sign.

Similar definitions apply to tensors; a tensor is really a *pseudo-tensor* if it acquires an extra factor of -1 when it transforms in the natural manner under mirror inversion. In particular ε_{ijk} is a pseudo-tensor, and thus so is the binary operation $\times$ and the operator $\nabla\times$. Since electrical current is a polar vector, corresponding to the velocity of individual charged particles and $\nabla\times\boldsymbol{B} = \mu\boldsymbol{J}$, it follows that the magnetic field is an axial vector. Plainly then, the mean emf $\bar{\boldsymbol{\mathcal{E}}} = \langle \boldsymbol{u} \times \boldsymbol{B}' \rangle$ is a polar vector, and so the tensor $\boldsymbol{\alpha}$ relating $\bar{\boldsymbol{\mathcal{E}}}$ (polar) to $\bar{\boldsymbol{B}}$ (axial) in (5.5) above is a pseudo-tensor.

The (second rank) alpha tensor $\boldsymbol{\alpha}$ is a property of the underlying fluid flow $\boldsymbol{u}$, and for this pseudo-tensor to be non-zero it is necessary that $\boldsymbol{u}$ should itself fail to be invariant under mirror inversion. The flow should thus lack *parity invariance*, and the simplest way this can occur is if the flow possess helicity $H = \langle \boldsymbol{u} \cdot \nabla \times \boldsymbol{u} \rangle$, another pseudo-scalar. The flow can still be isotropic and homogeneous: indeed one can imagine a box full of isotropic homogeneous turbulence, helical in nature, generated by small propellers locally imparting helicity to the turbulent eddies (Moffatt, 1978). Note that the third rank tensor $\boldsymbol{\beta}$ need not be zero for a parity invariant flow, as it could take the form $\beta_{ijk} = \beta\varepsilon_{ijk}$ where β is a scalar rather than a pseudo-scalar.

Thus the connection between the alpha effect and helicity may be firmly cemented. The most natural way a flow can fail to be parity invariant is if it possesses helicity, and helicity can arise very naturally in rotating convecting bodies through the Coriolis term in the equation of motion. This tends to impart rotation to diverging or converging masses of fluid, for example in convective plumes, and so to create correlations between vertical flow $\boldsymbol{u}$ and vertical vorticity $\boldsymbol{\omega} = \nabla \times \boldsymbol{u}$. Helicity however is not absolutely crucial to the alpha effect. One can write down flows for which all modes lack helicity, $\hat{H}(\boldsymbol{k}, \omega) = 0$, but for which an alpha effect can arise (at higher order than (5.1)) as the flow lacks parity invariance; see Frisch, She & Sulem (1987) and Gilbert, Frisch & Pouquet (1988).

The above general formulae for the alpha effect are limited to low R. Another approach is to study random, isotropic, homogeneous flows $\boldsymbol{u}(\boldsymbol{x}, t)$ varying on a time scale τ and length scale l. In the limit of a short correlation time $\tau u/l \ll 1$,

$$\alpha_{ij} = \alpha\delta_{ij}, \quad \beta_{ijk} = \beta\varepsilon_{ijk}, \tag{5.6}$$

with

$$\alpha = -\tfrac{1}{3}\tau\langle \boldsymbol{u} \cdot \nabla \times \boldsymbol{u}\rangle, \quad \beta = \tfrac{1}{3}\tau\langle |\boldsymbol{u}|^2\rangle \tag{5.7}$$

(Steenbeck, Krause & Rädler, 1966). Again there is a clear connection between the alpha effect and the helicity of the flow. The derivation of these formulae requires ensemble-averaging over random flows, which raises a number of issues of how ensemble averages may differ from typical realisations (for example, Hoyng, 1988; Zeldovich, Molchanov, Ruzmaikin & Sokoloff, 1988; Childress & Gilbert, 1995). However these formulae appear to work well and the tensors have been computed numerically in random flows by Kraichnan (1976b).

The quantity α in (5.7) has the dimensions of velocity and β of diffusivity, and so for modelling of, for example, the Solar dynamo it is natural to estimate $\alpha \sim \mathcal{V}H$ and $\beta \sim \mathcal{L}\mathcal{V}$ where $\mathcal{V} = \mathcal{L}/\mathcal{T}$ and $\mathcal{T}$ are typical velocity and time scales in the Solar convection zone, and H is now some dimensionless measure of how helical the flow is. Molecular diffusion η would then be negligible compared with β as in the Sun the magnetic Reynolds number $R = \mathcal{L}\mathcal{V}/\eta$ is very large. Obviously α may also vary in space, depending on the strength of the flow and the level of helicity, and we will discuss this further in section 5.3 below.

Let us however suppose for the moment that we are working in an infinite fluid flow and that α and β are constants. Then, as we found above for the G.O. Roberts flow, magnetic modes have growth rates

$$\lambda \simeq \mp\alpha k - (\beta + \eta)k^2, \tag{5.8}$$

where k is the wave number and the upper sign is for positive magnetic helicity, the lower for negative. This represents an α^2-*dynamo* as in a magnetic mode with, say, $\boldsymbol{k} = k\hat{\boldsymbol{z}}$, it is solely the alpha effect that is responsible for generating x-field from y-field and *vice versa*. This will be contrasted with $\alpha\omega$-dynamos below.

Note that if $\alpha \sim \mathcal{V}H$ and $\beta \sim \mathcal{L}\mathcal{V}$ with $H = O(1)$, $R \gg 1$ then it is clear that the most unstable magnetic modes will have length scale $1/k \sim \mathcal{L}$ and growth rate $\lambda \sim \mathcal{T}^{-1}$. These scales are independent of molecular diffusion, being based only on the length and time scales of the flow. However none of the analytical models we have considered in section 4 for large R have this property! The discontinuous Ponomarenko dynamo (section 4.1) has growth rates of order $\mathcal{T}^{-1}$, and so does the G.O. Roberts cellular flow, to within logarithmic terms. However the magnetic fields amplified are on very small scales, of order $R^{-1/2}\mathcal{L}$. The smooth Ponomarenko dynamo has maximum growth rates of order $R^{-1/3}\mathcal{T}^{-1}$ on spatial scales of order $R^{-1/3}\mathcal{L}$.

Of the dynamos we have met, none amplify fields at spatial scales $\mathcal{L}$ on time scales $\mathcal{T}$. The reason is that diffusion is playing a crucial role in the amplification processes so far identified, in generating field components transverse to stream surfaces (most clearly seen in the smooth Ponomarenko dynamo of section 4.2). For large R this mechanism becomes weak on large scales: large-scale modes grow slowly and the maximum growth rates occur for small-scale modes. We will take up this topic again when we discuss fast dynamos below in section 6; for the present we simply note that to obtain fast amplification of large-scale fields a smooth flow $\boldsymbol{u}$ must have regions of chaotic stream lines, rather than laminar stream surfaces.

Our focus has been on kinematic dynamo theory, in which the alpha effect is solely a functional of the flow field $\boldsymbol{u}$. However as a magnetic field grows, it will begin to affect the flow through the Lorentz force $\boldsymbol{J} \times \boldsymbol{B}$, and in a simple two-scale picture, it can do so either by generating large-scale flows, or by changing the small-scale flow $\boldsymbol{u}$. In the latter case it will modify the alpha effect, which will now be a function of $\bar{\boldsymbol{B}}$, as will other transport effects, including eddy diffusion and magnetic buoyancy. A typical alpha effect might be, for example,

$$\alpha = \alpha_0/(1 + c|\bar{\boldsymbol{B}}|^2/B_{\text{eq}}^2) \qquad (\mu^{-1}B_{\text{eq}}^2 \equiv \rho\boldsymbol{u}^2), \tag{5.9}$$

where c is a constant. This formula reflects the notion that the alpha effect will be suppressed when the magnetic energy density of the mean field $\frac{1}{2}\mu^{-1}|\bar{\boldsymbol{B}}|^2$ is comparable with the kinetic energy density $\frac{1}{2}\rho\boldsymbol{u}^2$. Similar forms can be obtained analytically in certain limits, as mentioned above equation (4.71). We refer the reader to the books of Moffatt (1978) and Krause & Rädler (1980) for references and discussion. The advantage of this modelling is that it allows dynamos to be constructed and simulated, building in many interesting and important physical effects, but without reference to the detailed and difficult fluid mechanics of highly turbulent flows interacting with magnetic fields. The corresponding disadvantage is that there is little to guide the choices of these transport effects, which in general are inhomogeneous, anisotropic and, of course, nonlinear in $\bar{\boldsymbol{B}}$.

In the early nineties it was pointed out that the quenching of the alpha effect written above should not really depend so much on the large-scale field $\bar{\boldsymbol{B}}$ and the corresponding Lorentz force $\bar{\boldsymbol{J}} \times \bar{\boldsymbol{B}}$ but instead on the Lorentz force for the fluctuating fields $\boldsymbol{J}' \times \boldsymbol{B}'$, which can be many times larger if the magnetic Reynolds number is large (Cattaneo & Vainshtein, 1991; Vainshtein & Cattaneo, 1992; Vainshtein, Parker & Rosner, 1993; Gruzinov & Diamond, 1996). The reason is that to reconnect magnetic field the scales need to be reduced to $O(R^{-1/2})$ and if this is done by drawing out loops of field, then this may lead to a much enhanced Lorentz force, with $\boldsymbol{B}' \sim R^{1/2}\bar{\boldsymbol{B}}$. The alpha effect suggested by Vainshtein & Cattaneo (1992) then takes the form

$$\alpha = \alpha_0/(1 + cR|\bar{\boldsymbol{B}}|^2/B_{\text{eq}}^2), \tag{5.10}$$

the extra factor of R meaning that the alpha effect is strongly suppressed for rather weak large-scale fields. This form has been supported by numerical simulations for large R by Cattaneo & Hughes (1996) and Brandenburg (2001).

Since R is extremely large in many astrophysical bodies, for example the Sun, this leads to many questions about how the dynamo can operate there, from the traditional viewpoint of modelling the Solar dynamo as an $\alpha\omega$-dynamo, which we introduce below. These issues, of the strength and time scale of the Solar field, remain to be resolved. Also unclear is the dependence of the alpha effect on the hydrodynamic Reynolds number, which is also extremely large in astrophysical objects, and the role of boundary conditions (Blackman & Field, 2000; Brandenburg & Dobler, 2001; Vishniac & Cho, 2001; Brandenburg, Dobler & Subramanian, 2002).

5.2 Alpha omega dynamos and dynamo waves

The alpha effect introduces a term $\langle \boldsymbol{u} \times \boldsymbol{B}' \rangle = \alpha \bar{\boldsymbol{B}}$ into the induction equation, in the simplest, isotropic case in which α is a scalar constant. This can amplify magnetic fields on its own, as above, or interact with differential rotation to give *dynamo waves* (Parker, 1955; Moffatt, 1978). Let us drop the overline, and let $\boldsymbol{B}$ denote the mean field in this section only; then the induction equation with an alpha effect becomes

$$\partial_t \boldsymbol{B} = \nabla \times (\boldsymbol{u} \times \boldsymbol{B} + \alpha \boldsymbol{B}) + \eta \nabla^2 \boldsymbol{B}, \quad \nabla \cdot \boldsymbol{B} = 0. \tag{5.11}$$

Consider a flow of the form $\boldsymbol{u} = U\hat{\boldsymbol{y}}$ and field $\boldsymbol{B} = B\hat{\boldsymbol{y}} + \boldsymbol{B}_P$, with $\boldsymbol{B}_P = \nabla \times (A\hat{\boldsymbol{y}})$ (cf. (3.26)), and U, B and A all independent of y. The induction equation then becomes

$$\partial_t A = \alpha B + \eta \nabla^2 A, \tag{5.12}$$
$$\partial_t B = \hat{\boldsymbol{y}} \cdot \nabla \times (\alpha \boldsymbol{B}_P) + \boldsymbol{B}_P \cdot \nabla U + \eta \nabla^2 B \tag{5.13}$$

(cf. (3.27), (4.84)). We now have in mind η as a turbulent diffusivity, neglecting the molecular value at large R. The relative magnitude of the two source terms on the right-hand side of (5.13) is given by

$$\frac{\boldsymbol{B}_P \cdot \nabla U}{\nabla \times (\alpha \boldsymbol{B}_P)} = O\left(\frac{\mathcal{L}|\nabla U|}{\alpha}\right). \tag{5.14}$$

If this ratio is small, then the $\boldsymbol{B}_P \cdot \nabla U$ term may be neglected and we return to an α^2-dynamo, with U playing no role. If the ratio is large, then the $\alpha \boldsymbol{B}_P$ terms may be dropped in the second equation (5.13) but αB retained in (5.12) to give an $\alpha\omega$-dynamo. Here the U generates a strong toroidal field component B from $\boldsymbol{B}_P$, while the alpha effect, necessary to avoid antidynamo theorem 2, regenerates $\boldsymbol{B}_P$. Assuming a constant ∇U as well as α, the dispersion relation for magnetic modes,

$$\boldsymbol{B} \propto e^{i\boldsymbol{k}\cdot\boldsymbol{r}+\lambda t}, \quad \hat{\boldsymbol{y}}\cdot\boldsymbol{k} = 0, \tag{5.15}$$

in an $\alpha\omega$-dynamo is

$$\lambda = \pm(i\alpha\boldsymbol{k}\cdot\hat{\boldsymbol{y}}\times\nabla U)^{1/2} - \eta k^2. \tag{5.16}$$

The presence of a fully complex frequency indicates the presence of waves and their direction of propagation is crucial in comparing with observations (Parker, 1955; Yoshimura, 1975).

Suppose we have a growing mode, with the upper sign taken so that $\operatorname{Re}\lambda > 0$, and let us take the fastest growing mode so that $\boldsymbol{k}$ is parallel or anti-parallel to $\hat{\boldsymbol{y}} \times \nabla U$. Then, bearing in mind (5.15) we see that if $\operatorname{Im}\lambda > 0$ the mode propagates in the $-\boldsymbol{k}$-direction. The sign of $\operatorname{Im}\lambda$ is the same as the sign of $\alpha\boldsymbol{k}\cdot\hat{\boldsymbol{y}}\times\nabla U$, and so we see that a growing dynamo mode propagates in the direction $-\alpha\hat{\boldsymbol{y}}\times\nabla U$. In spherical geometry with ϕ replacing y and (r,θ) replacing (x,z), this becomes $-\alpha\hat{\boldsymbol{\phi}}\times\nabla\Omega$, where $\Omega(r,\theta)$ is the angular velocity. Here the flow U and dominant magnetic field B are toroidal. Note however that if there is also a strong poloidal flow $\boldsymbol{u}_P$, which we have excluded, then the direction can be changed, simply by advection of the magnetic field.

5.3 The Solar dynamo

The above theory of $\alpha\omega$-dynamos is immediately relevant to the Sun. The Sun shows an 11-year dynamo cycle, although the period is strictly 22 years, with polarity changing at each half-cycle. This is evident in the distribution of Sun spots. Although these appear irregularly in space and time, when plotted as a function of latitude against time in a *butterfly diagram* (for example, Moffatt, 1978; Weiss, 1994) waves of Sun spot activity are evident, originating at latitudes of roughly 25°–30°, and then propagating equator-wards in both hemispheres. The above modelling then suggests an $\alpha\omega$-dynamo wave with these fields breaking through the surface because of magnetic buoyancy (Parker, 1955).

The toroidal field (given by B in the above analysis) is not directly visible from outside the Sun, but there is evidence that there is a strong coherent field in the Sun because of the Hale polarity laws. Regions of strong magnetic activity on the Sun's surface appear in pairs of opposite polarity, angled to lines of constant latitude. The magnetic polarities of the leading regions (in the sense of the rotation of the Sun) have, almost without exception, the same sign in the Northern hemisphere, and the opposite sign in the Southern. All the signs are reversed each dynamo cycle. This suggests two opposing and very coherent belts of field deeper in the Sun which propagate equator-wards, to be replaced by new, oppositely oriented fields each dynamo cycle.

The traditional view of the Solar dynamo was that it is of $\alpha\omega$ type, with $\alpha > 0$ in the Northern hemisphere and $\alpha < 0$ in the Southern, and $\partial\Omega/\partial r < 0$ throughout the convection zone, to give the correct equator-ward migration of Sun spots (for example, Moffatt, 1978; Parker, 1979; Krause & Rädler, 1980). Numerical simulations showed waves, and the parameters can be adjusted to give an 11-year dynamo cycle matching the observations. There are many open questions however.

The alpha effect is usually thought to arise because of the influence of convection and the Coriolis effect. For example at the base of a rising plume of hot fluid the fluid flow will be convergent and so will tend to rotate under the action of the Coriolis effect, giving Parker's famous picture of rising twisted loops of field, and helicity $\boldsymbol{u}\cdot\boldsymbol{\omega}$. However as a plume rises to the top of the convection zone it will expand, the flow will become divergent, and the rotation and helicity will be reversed. Thus it is not clear what the sign of α should be in each hemisphere, although by symmetry it should certainly be odd about the equator. Similarly on the surface of the Sun the angular velocity increases from the poles to the equator. In a rotating fluid sphere such as the Sun there is a tendency for motion to be independent of a coordinate along the axis of rotation, in so far as the Taylor–Proudman Theorem applies, in which case this would suggest that $\partial\Omega/\partial r > 0$ inside the Sun.

These concerns with the functioning of the Solar dynamo came to the fore with the numerical simulations of convection in spherical geometry by Gilman & Miller (1981), Gilman (1983) and Glatzmaier (1984, 1985a,b). These studies did not include an alpha effect nor eddy diffusion, thus avoiding the modelling problems mentioned above. The simulations gave flows with $\partial\Omega/\partial r > 0$, in agreement with the surface rotation of the Sun but in contradiction to the theoretical framework. Together with this went a robust *pole-ward* migration of magnetic fields. As a possible resolution of this paradox, these authors suggested that the Solar magnetic field might instead be generated at the base of the convection zone, at about 70% of the Solar radius, where convection overshoots into the stably stratified, radiative interior.

At about the same time, direct information about the internal structure of the Sun was becoming available through the science of helioseismology, involving the inversion of frequencies of the five-minute oscillations of the Solar surface. The rotation of the Sun leads to the splitting of frequencies between Eastward and Westward travelling modes of oscillation and so to information about the profile of differential rotation inside the Sun. The results (see for example Brown *et al.*, 1989; Dziembowski, Goode & Libbrecht, 1989; Gough, Sekii & Stark, 1996) are shown schematically in figure 6. In the convection zone

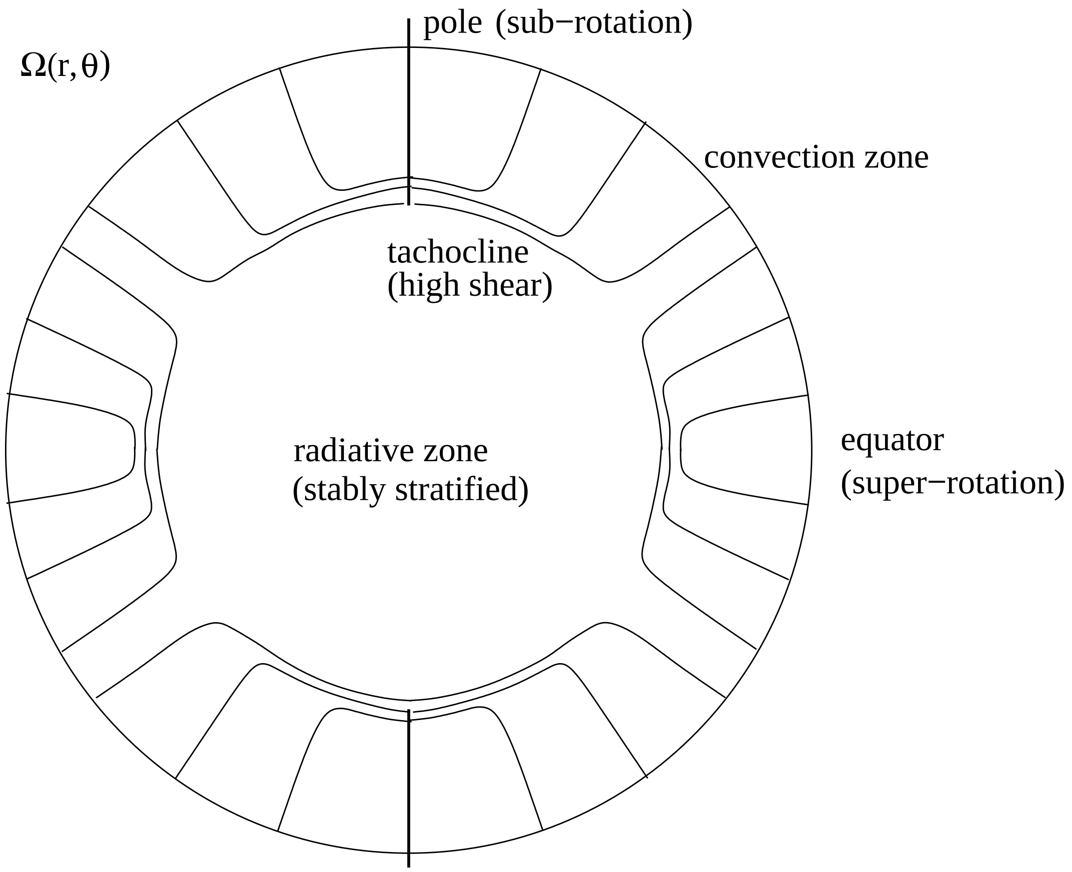

Fig. 6. Schematic Solar rotation profile. Contours of constant $\Omega(r,\theta)$ are shown; Ω is largest at the equator and smallest at the poles.

$\Omega = \Omega(\theta)$, largely independent of radius r, and in the radiative zone Ω is approximately constant. At the interface of the two zones is a thin layer, of no more than 5% of Solar radius, in which the angular velocity has large radial gradients. This is known as the *tachocline* (Spiegel & Zahn, 1992; Spiegel, 1994).

The tachocline now seems a likely location for the Solar dynamo, although the issue is far from settled, in particular how fields and fluid motions in the tachocline and convection zone interact. In the tachocline there is intense shear and an alpha effect can arise from overshooting convection or other instabilities. These processes can provide an $\alpha\omega$-dynamo giving equator-wards propagating dynamo waves. Indeed at lower latitudes and the equator $\partial\Omega/\partial r > 0$, and so a negative alpha effect $\alpha < 0$ in the Northern hemisphere would then give the correct direction of propagation. Another reason to think that much of the magnetic field is localised in a thin layer is its coherence as evidenced by the Hale polarity laws.

The new and surprising results from helioseismology have, by overturning the previous view of the Solar dynamo, acted as a stimulus to theory and numerical studies. We can only mention a few current directions of research and a few references. One important issue is: how is the tachocline maintained, and what is its structure? Spiegel & Zahn (1992) give a theory in which turbulence enhances horizontal transport of angular momentum at the top of the stably stratified radiative zone and this is responsible for maintaining the thin tachocline. On the other hand Garaud (2001) argues that the observed profile is stable and so the enhanced transport will not take place, and Gough & McIntyre (1998) suggest that the presence of the tachocline indicates that there is a magnetic field trapped in the radiative interior of the Sun. Numerical simulations of convection in rotating spheres modelling the Sun and aimed at studying the structure of the tachocline are now being undertaken by Miesch *et al.* (2000).

Assuming the existence of the tachocline, alpha effect dynamos have been constructed both as analytical models, and involving large-scale numerical simulations (DeLuca & Gilman, 1986, 1988; Parker, 1993; Prautzsch, 1993; Rüdiger & Brandenburg, 1995). A nonlinear tachocline dynamo represents a complicated fluid system, with stratification, shear, convection and magnetic fields all interacting. One important issue is, assuming the dynamo is of $\alpha\omega$ type, how is the alpha effect generated? One, traditional, possibility is simply convection. However other ways of generating complex fluid flows could include hydrodynamic instabilities of the stratified shear flow, and even instabilities of the belts of toroidal magnetic field themselves (Hughes & Proctor, 1988; Ferriz-Mas, Schmitt & Schüssler, 1994; Thelen, 2000). In the latter case the resulting alpha effect would be a nonlinear function of the field, vanishing for fields below some instability threshold, and so would not explain the growth of magnetic field from a seed field, but instead might explain its present-day structure and behaviour. Numerical simulations building in and assessing the effects of these dynamo mechanisms are under way (for example, Dikpati & Gilman, 2001). Another approach is to consider idealised fluid flows modelling the tachocline, but without building in any turbulent transport coefficients such as the alpha effect; see, for example Brandenburg *et al.* (1990), Brandenburg (1994), Ponty, Gilbert & Soward (2001), Tobias, Brummell, Clune & Toomre (2001), and the discussion of convective dynamos in the next section. Finally the study of $\alpha\omega$-dynamos in thin layers with space-dependent and nonlinear transport effects involves much interesting mathematics; see, for example Meunier *et al.* (1997), Tobias, Proctor & Knobloch (1998) and Bassom, Kuzanyan & Soward (1999).

5.4 Convective dynamos and the geodynamo

The most natural way to drive an astrophysical or planetary dynamo flow is through fluid convection. The scientific literature on convection is vast, and there are many possibilities that can be investigated. Perhaps the simplest relevant situation is a plane layer of fluid, heated from below, and rotating about a vertical axis with angular velocity Ω. This geometry was considered in the limit of rapid rotation by Childress & Soward (1972), Soward (1974) and Fautrelle & Childress (1982). These authors use multiple scale techniques, exploiting the natural scale separation between the depth, say h, of the fluid layer, and the width of the cells $E^{1/3}h$, where the Ekman number $E = \nu/2\Omega h^2 \ll 1$. A dynamo of α^2-type is then obtained. A related study of Busse (1973) includes an imposed shear, to give instead an $\alpha\omega$-dynamo. The role of rotation is important here to make the convective flow sufficiently complicated for dynamo action to take place, in particular to obtain flows with helicity. In a rotating layer even two-dimensional convecting rolls $\boldsymbol{u}(x, z, t)$ can act as a dynamo just beyond onset, provided the nonlinearity of the flow is taken into account so that the stream lines do not lie on plane surfaces, and so anti-dynamo theorem 2 of section 3.3 is avoided (Matthews, 1999). Other studies of dynamo action in rotating plane layers include St. Pierre (1993), Brandenburg (1994), Jones & Roberts (2000) and Tobias, Brummell, Clune & Toomre (2001).

From this basic situation many further ingredients can be included. The geometry can be fully spherical or a spherical annulus (for example, Zhang & Busse, 1988, 1989; Hirsching & Busse, 1995), or a cylindrical annulus. For analytical studies of convection the intermediate configuration of the *Busse annulus* has many advantages: here the fluid is confined to a cylindrical annulus with sloping top and bottom walls (Busse, 1970, 1994), and dynamo action has been studied by Kim, Hughes & Soward (1999). Many of these studies have been aimed at modelling the geodynamo, and other planetary dynamos. The most recent simulations, by Glatzmaier & Roberts (1995a,b, 1997, 2001), are beginning to resemble observations of the geomagnetic field, including reversals of the field. However the parameter space to be explored is very large, and the parameter values actually relevant to the Earth are uncertain, while at the same time unobtainable with brute force computations using current and foreseeable technology. For example the Ekman number is perhaps $E = O(10^{-15})$ (Fearn, 1994). Of course similar remarks apply about the accessibility of the parameters relevant to Solar and galactic dynamos, and even laboratory dynamos (which are characterised by a high fluid Reynolds number and so are highly turbulent).

In geodynamo theory a number of important issues arise. The first is the role of the Taylor–Proudman theorem, which tends to constrain a non-magnetic flow to be two-dimensional, independent of the coordinate along the axis of rotation, and the extent to which the magnetic field releases this constraint. A second issue is the source of energy for the geodynamo, whether arising from thermal convection, compositional convection, or from the precessional motion of the Earth. There is also the question of what role the solid iron inner core plays in the dynamo process, and its rotation rate. Finally we mention the

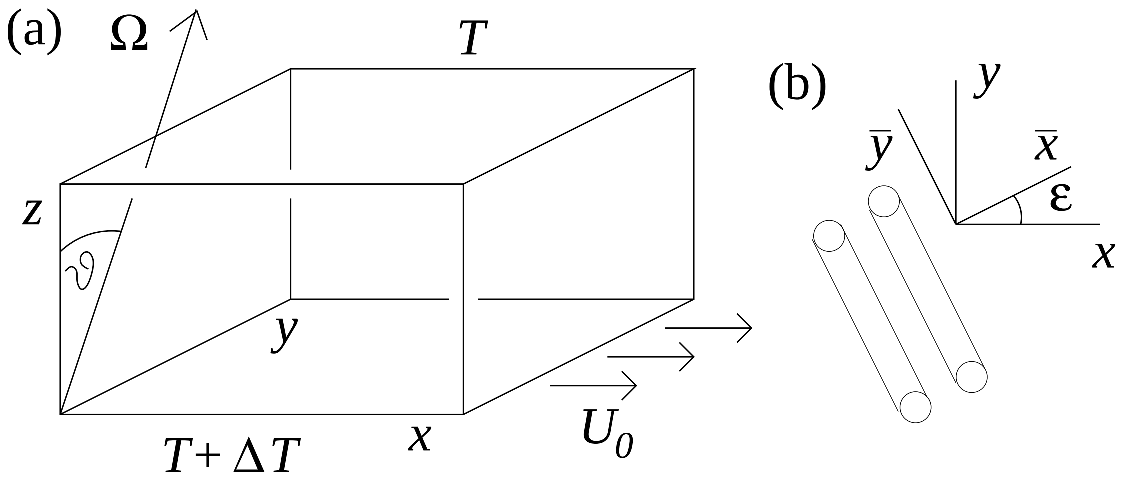

Fig. 7. Geometry of the planar fluid system. (a) The plane layer: gravity acts in the $-z$ direction. The rotation vector $\boldsymbol{\Omega}$ lies in the (y,z)-plane, making an angle ϑ with the vertical. A velocity U_0 in the x-direction is imposed at the base of the layer. (b) Rotation of axes from (x,y) to $(\bar{x},\bar{y})$, with $\bar{y}$ aligned with the roll axes.

problem of how the convection in the liquid core is coupled to the temperature distribution at the base of the mantle. We refer the reader to reviews by Roberts (1971), Busse (1983), Roberts (1987), Soward (1991), Braginsky (1994), Fearn (1994), Malkus (1994) and Hollerbach (1996) for further information on these and other topics.

To illustrate convective dynamos, and how the kinematic dynamo mechanisms that form the heart of this review can be realised in physical fluid flows, we will here briefly discuss a kinematic dynamo model studied by Ponty, Gilbert & Soward (2001). The fluid system is set up broadly to model the Solar tachocline at a co-latitude ϑ, and involves convection over a layer of concentrated shear.

A plane layer geometry is used with axes x (East), y (North) and z vertical, depicted in figure 7(a). The plane layer is of depth h, with periodic boundary conditions in x and y, and rotates about the direction

$$\boldsymbol{\Omega} = \Omega\hat{\boldsymbol{\Omega}} = \Omega(\hat{\boldsymbol{z}}\cos\vartheta + \hat{\boldsymbol{y}}\sin\vartheta) \qquad (\Omega \geq 0), \tag{5.17}$$

corresponding to co-latitude ϑ. The layer is heated from below with a temperature difference ΔT across the layer. If the system is non-dimensionalised using the layer depth and the thermal time-scale the governing equations may be written in the form

$$\partial_t\boldsymbol{u} + \boldsymbol{u}\cdot\nabla\boldsymbol{u} + \tau P\,\hat{\boldsymbol{\Omega}}\times\boldsymbol{u} = -\nabla\Pi + P\,\theta\hat{\boldsymbol{z}} + P\nabla^2\boldsymbol{u}, \tag{5.18}$$

$$\partial_t\theta + \boldsymbol{u}\cdot\nabla\theta = Ra\,u_z + \nabla^2\theta, \tag{5.19}$$

$$\partial_t\boldsymbol{B} + \boldsymbol{u}\cdot\nabla\boldsymbol{B} = \boldsymbol{B}\cdot\nabla\boldsymbol{u} + q^{-1}\nabla^2\boldsymbol{B}, \tag{5.20}$$

$$\nabla\cdot\boldsymbol{u} = \nabla\cdot\boldsymbol{B} = 0. \tag{5.21}$$

The problem is thus far specified by the five dimensionless parameters

$$\vartheta, \quad Ra = \frac{\alpha g h^3 \Delta T}{\nu\kappa}, \quad \tau = \frac{2\Omega h^2}{\nu}, \quad P = \frac{\nu}{\kappa}, \quad q = \frac{\kappa}{\eta}, \tag{5.22}$$

which are the colatitude, Rayleigh number, square root of the Taylor number, Prandtl number and Roberts number. κ is the thermal diffusivity, ν the viscosity, η the magnetic diffusivity, and α the thermal coefficient of expansion. The Boussinesq approximation has been employed, and θ is the deviation of the temperature field from a purely conductive state.

In this dimensionless framework the layer is bounded by $0 \le z \le 1$. At top and bottom boundaries $\theta = 0$ and the magnetic field is taken to obey insulating boundary conditions. So far the system is subject only to convective instabilities. However to model the tachocline a layer of shear is introduced by imposing a bottom boundary condition that $\boldsymbol{u} = U_0\hat{\boldsymbol{x}}$ in dimensional units. In the dimensionless system this velocity becomes $\boldsymbol{u} = U_0 h/\kappa\hat{\boldsymbol{x}}$; in other words we impose

$$\boldsymbol{u} = Re\, P\hat{\boldsymbol{x}} \quad (z=0), \qquad \boldsymbol{u} = 0 \quad (z=1), \qquad Re = U_0 h/\nu, \tag{5.23}$$

with the Reynolds number Re as a further, sixth parameter in our problem. This parameter can take either sign, depending on the sign of U_0 taken.

Now with these boundary conditions there is a *basic state* $\boldsymbol{u} = \boldsymbol{u}(z)$, $\theta = 0$ and $\boldsymbol{B} = 0$, corresponding to a conductive, shear flow. For large rotation $\tau \gg 1$ (and $\vartheta \neq \pi/2$), the shear becomes localised in an Ekman layer a distance of order $\tau^{-1/2}$ from the base of the plane layer,

$$\boldsymbol{u}(z) \simeq Re\, Pe^{-\mu z}(\cos\mu z, -\sin\mu z, 0), \qquad (\mu \equiv (\tfrac{1}{2}\tau\cos\vartheta)^{1/2} \gg 1). \tag{5.24}$$

There is no corresponding layer at $z = 1$.

There are then two basic mechanisms by which this basic state can bifurcate to a more complex flow (Ponty, Gilbert & Soward, 2002). The first is through fluid convection, when the Rayleigh number Ra is increased to a sufficiently large value. The second mechanism is an Ekman instability, which is a purely hydrodynamic instability that can occur when a Reynolds number $Re^* = Re\,(2/\tau\cos\vartheta)^{1/2}$, based on the thickness of the Ekman layer, is sufficiently large (Faller & Kaylor, 1966; Lilly, 1966; Leibovich & Lele, 1985).

At onset of linear instability, since the basic state is independent of x and y, the most unstable mode will have a dependence $\exp(ik_1x+ik_2y+\lambda t)$ with horizontal wave vector (k_1, k_2), consisting of rolls whose axes are in the direction $(k_2, -k_1)$. If we define new axes $(\bar{x}, \bar{y}, z)$ with $\bar{y}$ along the roll axes then the fluid flow at onset is two-dimensional, $\boldsymbol{u} = \boldsymbol{u}(\bar{x}, z, t)$, independent of $\bar{y}$; this is shown schematically in figure 7(b). In this study the fluid flow is restricted to take this two-dimensional form also into nonlinear regimes, with the angle ε between the x-axis and $\bar{x}$-axis and the wavelength $2\pi/k_c$ in the $\bar{x}$-direction fixed from the linear stability analysis. The magnetic field then can be taken to be of the form

$$\boldsymbol{B} = \boldsymbol{b}(\bar{x}, z, t)e^{il\bar{y}}, \tag{5.25}$$

allowing high-resolution, two-dimensional computations at low magnetic diffusivities. Finally note that the magnetic Reynolds number R has to be defined, not as an input parameter to the problem, but as a diagnostic, since the velocities in the fluid layer depend non-trivially on the driving from the temperature gradient $Ra > 0$ or the shear $Re > 0$. If the measured dimensionless velocity is $U = \langle \boldsymbol{u}^2 \rangle^{1/2}$, then we may define $R = qU$. The limit of large magnetic Reynolds number may be investigated by increasing q for a given flow field.

Some results are shown in figures 8 and 9. In the first of these,

$$\vartheta = 45^\circ, \quad Ra = 0, \quad \tau = 60, \quad P = 1, \quad q = 50, \quad Re = 210, \tag{5.26}$$

$$\varepsilon = 73.5^\circ, \quad k_c = 3.44. \tag{5.27}$$

The flow field is shown in figure 8(a,b) and is generated by a pure hydrodynamic instability, since $Ra = 0$. (a) shows the velocity $u_{\bar{y}}$ along the roll axes, and (b) the stream function and velocity vectors in a frame moving with the instability. In this frame the flow is steady, and it can be seen that there is a hyperbolic stagnation point and separatrices. Note the strong Ekman layer at the base of the domain. For these parameter values the magnetic Reynolds number is measured to be $R \simeq 3660$, and the magnetic field for $l = 1.2$ is shown in figure 8(c), with $|\boldsymbol{b}(\bar{x}, z, t)|$ plotted against $\bar{x}$ and z. This hides somewhat the three-dimensional nature of the field as it averages over the $\bar{y}$ direction, but it is clear that the growing mode is connected with the separatrices, as in the G.O. Roberts dynamo for large R (section 4.4). Other steady flows or values of l can also give Ponomarenko type modes, localised within the recirculating eddies.

In the second figure, 9, the parameter values are

$$\vartheta = 67.5^\circ, \quad Ra = 7.8 \times 10^5, \quad \tau = 200, \quad P = 1, \quad q = 75, \quad Re = 30, \tag{5.28}$$

$$\varepsilon = 2.33^\circ, \quad k_c = 4.3. \tag{5.29}$$

This is primarily a convective instability, modified by shear, with Ra approximately 21 times the critical value for this rotation rate. The flow is now unsteady in any frame, and a snapshot of the flow field is shown in figure 9(a,b). The magnetic Reynolds number is measured as $R \simeq 5480$ and the magnetic field is shown in 9(c) for $l = 8.5$. This now takes the form of sheets of field accumulating near to the convective roll boundaries. This is typical of a fast dynamo operating in an unsteady flow (see section 6.3 below) and there is evidence that the growth rate for $l = 8.5$ remains of order unity as

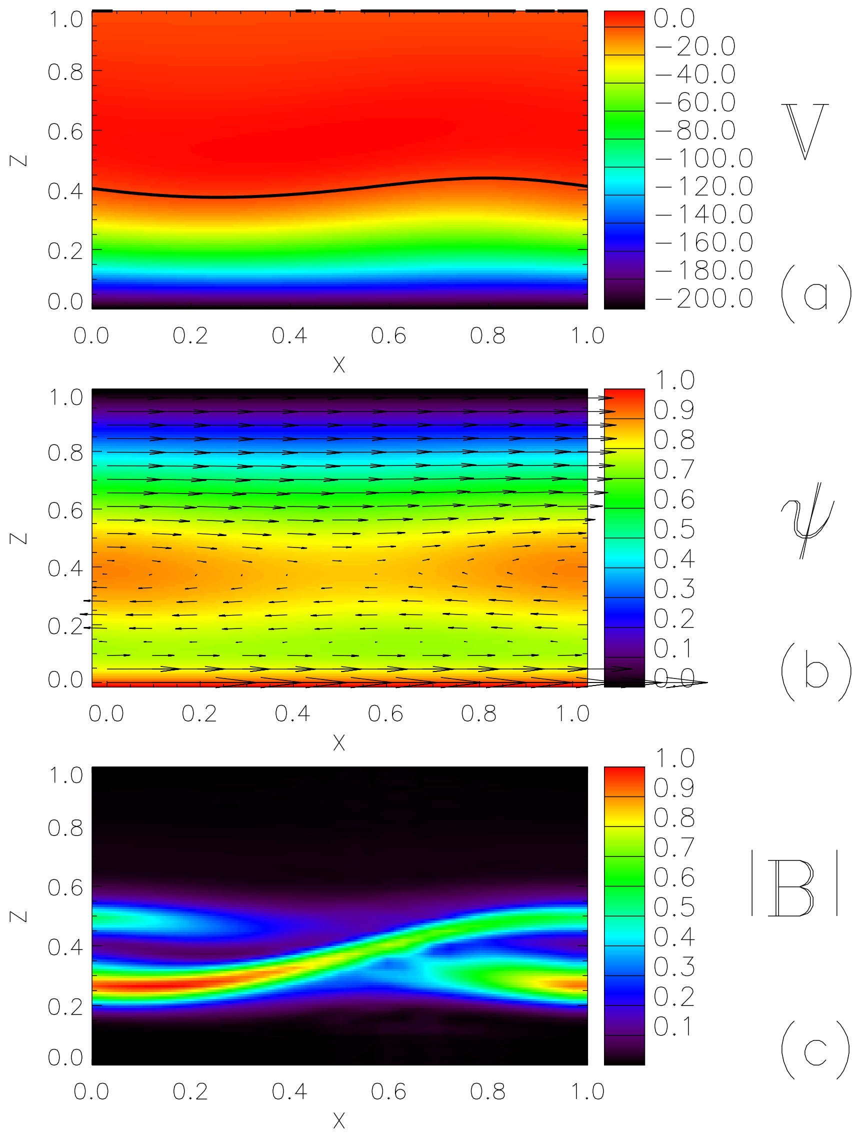

Fig. 8. Kinematic dynamo in a flow generated by a saturated Ekman instability with parameters given in (5.26), (5.27). In (a) the flow $V \equiv u_{\bar{y}}$ is shown, with the dark contour marking $u_{\bar{y}} = 0$, (b) the stream function ψ in a comoving frame is shown, with the arrows marking velocity vectors, and (c) the magnitude $|\boldsymbol{b}|$ of the magnetic field. (Reprinted from JFM, with permission of CUP.)

q, or equivalently R, is increased (Ponty, Gilbert & Soward, 2001). Another study of fast dynamo action in convective flows, this time in a Busse annulus geometry, is Kim, Hughes & Soward (1999).

5.5 Galactic and accretion disc dynamos

It is known from studies of Faraday rotation, the rotation of polarization of electromagnetic radiation as it passes through a magnetic field, that galax-

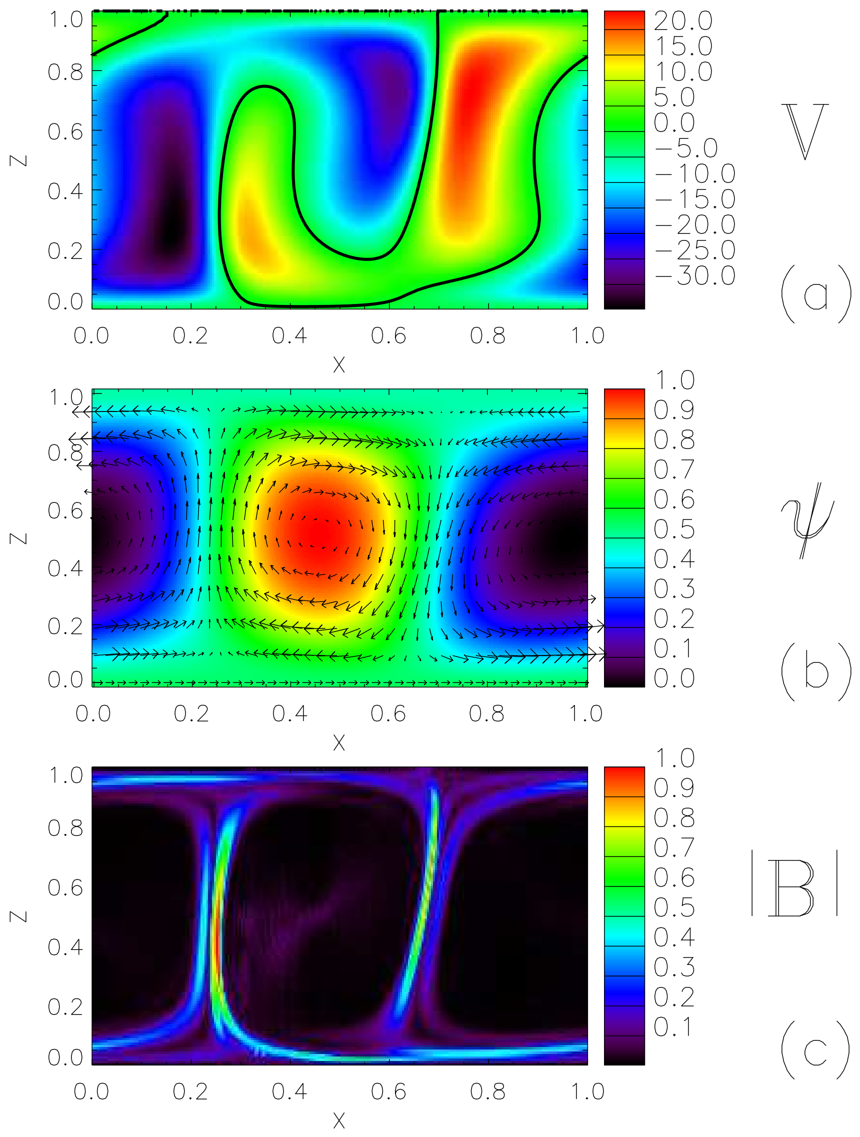

Fig. 9. Kinematic dynamo in a flow generated by a convective instability with parameters given in (5.28), (5.29). In (a) the flow $V \equiv u_{\bar{y}}$ is shown, with the dark contour marking $u_{\bar{y}} = 0$, (b) the stream function ψ in a comoving frame is shown, with the arrows marking velocity vectors, and (c) the magnitude $|\boldsymbol{b}|$ of the magnetic field. (Reprinted from JFM, with permission of CUP.)

ies possess magnetic fields. The issue of whether these fields are primordial, created when the galaxy was formed, or have been generated since remains a vexed one (Kulsrud, 1999). Nonetheless dynamo theories have been developed for galaxies, of the $\alpha\omega$ type. Here differential rotation in galaxies provides the ω-effect, while small-scale helical turbulence, arising from a combination of rotation and motion generated by supernovae explosions, provides the α effect.

At the level of $\alpha\omega$ modelling it is natural to start with a prescribed differential rotation and alpha effect, with the extra ingredient that now the geometry is that of a thin disc (Stix, 1975, 1978). Such models have been analysed in detail by Soward (1978, 1992a,b) and are now being used to model the observed magnetic fields in galaxies; see reviews in Ruzmaikin, Sokoloff & Shukurov (1988b) and Beck *et al.* (1996). Another situation in which a disc geometry is relevant is the generation of magnetic fields in accretion discs (see, for example, Brandenburg, Nordlund, Stein & Torkelsson, 1995; Campbell, 1997); such fields can contribute to instabilities, turbulence and so eddy viscosity (Balbus & Hawley, 1991). These processes can modify the structure of the disc and the inflow of accreting material.

6 Fast dynamos

We now return to kinematic dynamo theory in prescribed flows $\boldsymbol{u}$ and discuss fast dynamos, which have the property that the growth rate remains on the turn-over time-scale of the flow at large magnetic Reynolds number. An extensive review of this topic is given in Childress & Gilbert (1995).

6.1 Definitions and upper bounds

Let us consider the dimensionless magnetic induction equation in the form

$$\partial_t \boldsymbol{B} + \boldsymbol{u} \cdot \nabla \boldsymbol{B} = \boldsymbol{B} \cdot \nabla \boldsymbol{u} + \varepsilon \nabla^2 \boldsymbol{B}, \quad \nabla \cdot \boldsymbol{B} = 0, \tag{6.1}$$

where $R = \varepsilon^{-1}$ is the magnetic Reynolds number and $\boldsymbol{u}$ is a flow that is already known to be a dynamo. We let $\gamma(\varepsilon)$ be the maximum growth rate for a given ε, maximised over all sensible initial conditions. Then the flow $\boldsymbol{u}$ is a *fast dynamo* if $\gamma(\varepsilon)$ is bounded above zero as $\varepsilon \to 0$ (Vainshtein & Zeldovich, 1972). If the growth rate tends to zero in the limit, the dynamo is *slow*. More formally we define

$$\gamma(\varepsilon) = \sup_{\boldsymbol{B}_0} \limsup_{t \to \infty} t^{-1} \log \|\boldsymbol{B}\|. \tag{6.2}$$

Here $\boldsymbol{B}_0$ is the initial magnetic field, $\boldsymbol{B}(\boldsymbol{x}, t)$ is the field at time t, and $\|\boldsymbol{B}\|^2 = (\boldsymbol{B}, \boldsymbol{B})$ gives the usual L^2 or energy norm, with

$$(\boldsymbol{C}, \boldsymbol{B}) = \int_V \overline{\boldsymbol{C}} \cdot \boldsymbol{B} \, dV. \tag{6.3}$$

The initial condition should lie in L^2, that is have finite magnetic energy. The limiting *fast dynamo growth rate* is then given by

$$\gamma_0 = \liminf_{\varepsilon \to 0} \gamma(\varepsilon), \tag{6.4}$$

and the dynamo is fast if $\gamma_0 > 0$ and slow if $\gamma_0 \leq 0$.

In terms of the dynamos we have already discussed, the discontinuous Ponomarenko dynamo (section 4.1) is fast. The smooth G.O. Roberts dynamo is very close to being fast (see (4.103)). It is fast in the modified form studied by Soward (1987), but this flow field now possesses singularities and is not smooth. Note that although these two flow fields are fast dynamos, they only amplify magnetic fields on small scales of order $\varepsilon^{1/2}$, and so have been called *intermediate dynamos* by some authors (Molchanov, Ruzmaikin & Sokoloff, 1985); we shall however not make this distinction.

The key issues then are whether there are smooth flows that are fast dynamos, and whether fields on the scale of the flow can be amplified in this way. As we discussed in section 5.1, below (5.8), once one writes down an alpha effect and turbulent diffusivity that are independent of molecular values, but are based on the length and time scale of the flow, one is assuming implicitly that the flow is a fast dynamo. It therefore is incumbent on the theorist to find examples of flows $\boldsymbol{u}$ with this property. By means of additional general motivation, we note that in the Solar dynamo $R \simeq 10^8$, and the field evolves on a time scale of months and years, very much shorter than the time scale of molecular diffusion. Although the Solar dynamo is nonlinearly equilibrated, whereas we are studying kinematic regimes, it is nevertheless necessary to understand fundamental mechanisms giving fast growth and fast evolution of magnetic fields.

6.2 Stretch, twist and fold

The most famous picture of how a fast dynamo can operate is the *stretch–twist–fold* (STF) dynamo. This goes back to Vainshtein & Zeldovich (1972), Zeldovich, Ruzmaikin & Sokoloff (1983) and even Alfvén (1950), and is depicted in figure 10. We consider an initial flux tube (a) containing magnetic flux Φ_0 and energy E_0. This is stretched out (b), thus quadrupling the magnetic energy. It is then twisted (c) and folded (d), to give a doubled tube. This has energy $4E_0$, and the flux through a cross section of the doubled-up tube is now $2\Phi_0$. Plainly if the process is repeated, then after n iterations the energy will be $2^{2n}E_0$ and the total flux through a cross section of the bundle of 2^n tubes will be $2^n\Phi_0$. If we can ignore weak diffusion the growth rate would be $\gamma = \log 2$, where the time for one complete cycle is taken to be unity.

There are many comments to make. First, in drawing this picture we have not written down the flow field explicitly, although this can be done (Moffatt & Proctor, 1985; Vainshtein, Sagdeev, Rosner & Kim, 1996; Vainshtein, Sagdeev & Rosner, 1997). We have just used the fact that with $\varepsilon = 0$ field lines are

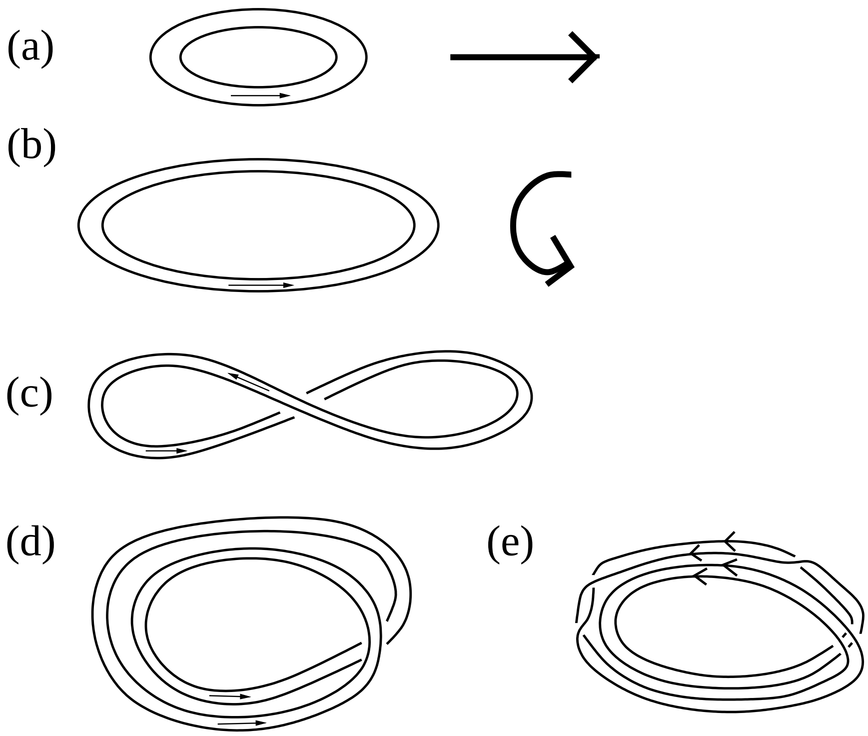

Fig. 10. The stretch–twist–fold process: an initial flux tube (a), is stretched (b), twisted (c) and folded (d), to obtain a doubled flux tube. (e) a quadrupled flux tube after 2 cycles: for clarity only the centre line of the tube is shown.

carried materially in the flow, and stretched so as to conserve fluxes. Secondly, what is the effect of diffusion and why might we expect it to be unimportant in the limit $\varepsilon \to 0$? The key aspect of the STF picture is that through three-dimensional motion magnetic field is brought into alignment. The field in the extended tube (figure 10(d,e)) has a consistent direction, and any weak diffusion, causing the field distribution to be smeared out, should make little difference to the total flux across the bundle of tubes. This should remain $\Phi \simeq 2^n\Phi_0$, corresponding to a growth rate $\gamma_0 \simeq \log 2$. The important role of flux here was stressed by Finn & Ott (1988) and Bayly & Childress (1988, 1989).

This should be contrasted with the situation for flows and magnetic fields lying in a plane with $\boldsymbol{u}(x, y, t) = (u, v, 0)$, $\boldsymbol{B}(x, y, t) = (B_x, B_y, 0)$, for which the folding is always so as to bring opposing field together and there is no amplification of a coherent and robust magnetic flux; see figure 11. In fact we know already that such a configuration cannot be a dynamo by anti-dynamo theorems 1 or 2. We can write $\boldsymbol{B} = \nabla \times (A\hat{\boldsymbol{z}})$ (cf. (3.26)) where the potential $A(x, y, t)$ obeys (3.27) (with η replaced by ε). Suppose $0 < \varepsilon \ll 1$, then from some initial condition A is advected by (3.27), with diffusion negligible at the outset. As A is transported materially gradients of A increase, and thus so

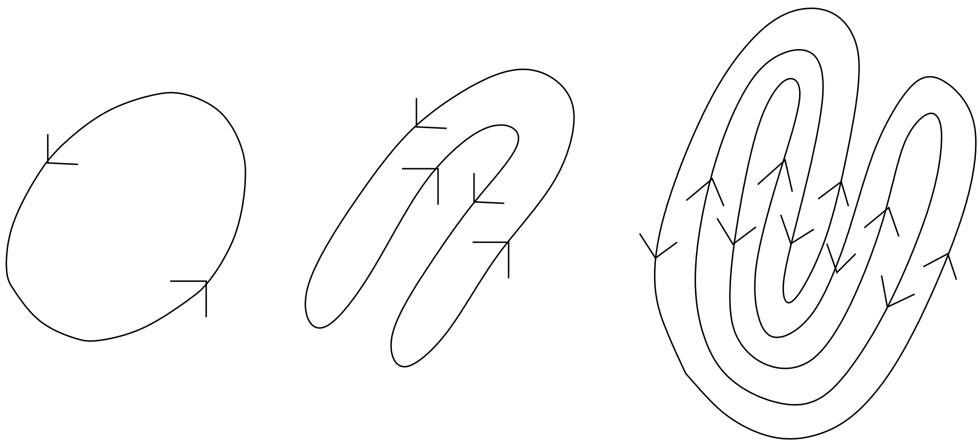

Fig. 11. Folding of magnetic field in the plane leads to opposing field which is vulnerable to diffusion, however weak.

does the corresponding magnetic field. It is important to note that although the field increases, magnetic fluxes through surfaces are bounded: this is clear pictorially from figure 11, and may be seen because fluxes are given by the difference in values of A, and these values are bounded by the initial condition.

This fine-scaling process continues until A varies on a scale of order $\varepsilon^{1/2}$, at which point A is destroyed from (3.30), together with the magnetic field. Physically, at this point weak diffusion is now acting to eliminate the opposing bands of field. Note that if however diffusion is strictly zero, $\varepsilon = 0$, then the increase of $\boldsymbol{B}$ and the magnetic energy continues indefinitely for any non-trivial flow: we can certainly have the growth rate for zero diffusion, $\gamma(0) > 0$, while the limiting growth rate for weak diffusion, $\gamma_0 \leq 0$. This highlights the singular limit of $\varepsilon \to 0$, and also the care which must be taken in applying the two non-commuting limits of large time t and small diffusivity ε. In studying fast dynamos we must take $\lim_{t\to\infty}$ first, before applying $\lim_{\varepsilon\to 0}$.

The third comment is that the STF picture is very simplified and idealised. Obviously the flow has a sense of helicity in view of the arrows giving the stretching and rotating parts of the motion in figure 10(a,b). This leads to twisting of field lines within the tube and local magnetic helicity, although the total magnetic helicity is conserved for $\varepsilon = 0$; see Moffatt & Ricca (1992) and Gilbert (2002a) for further discussion. Thus the field structure is more complicated than that depicted. The other problem is that after one STF cycle the doubled-up tube will not exactly fit into the original tube, since we have in mind a smooth volume-preserving flow with $\nabla \cdot \boldsymbol{u} = 0$. Instead with the tube of flux will be entrained flux-free fluid. As the STF process is iterated the cross section of the bundle of 2^n tubes will increase until the hole in the centre of the bundle disappears. At this point it becomes important just how the STF flow is defined more globally. This problem arises in Vainshtein, Sagdeev, Rosner & Kim (1996), where a flow modelling the STF moves is simulated numerically.

Thus the STF dynamo is at this point only a picture of how fast dynamo action can occur. It is nonetheless a very attractive picture, with all the correct ingredients. In particular it stresses the importance of alignment of field lines so as to build up coherent magnetic flux, which is robust to the effects of weak diffusion. It also highlights the importance of chaotic stretching in the flow: the length of the tube doubles on each iteration of the STF moves, and this corresponds to a *line-stretching exponent* $h_{\rm line} = \log 2$.

6.3 Fast dynamo action in flows

Before discussing further theory and conjectures on fast dynamos, we will consider some examples that have been studied numerically. We will assume that Lagrangian chaos, that is the exponential stretching of magnetic field in finite volumes, is important and this means that the flow must depend on at least three of the coordinates (x, y, z, t). The class of flows that are best studied, and easiest to simulate numerically, are those taking the form $\boldsymbol{u}(x, y, t)$. We can think of such a flow as comprising two components: the horizontal part $\boldsymbol{u}_{\rm H} = (u_x, u_y, 0)$ and the z-independent vertical component u_z.

Examples of such flows have been studied by Galloway & Proctor (1992), Klapper (1992), Otani (1993), Childress & Gilbert (1995), Hollerbach, Galloway & Proctor (1995) and Ponty, Pouquet & Sulem (1995), and numerical evidence for fast dynamo action obtained. We shall focus on an example of Otani (1993), which we refer to as the *MW+ flow*,

$$\boldsymbol{u}(x, y, t) = 2\cos^2 t\,(0, \sin x, \cos x) + 2\sin^2 t\,(\sin y, 0, -\cos y), \tag{6.5}$$

short for 'modulated waves, positive helicity'. This flow is obviously closely related to the G.O. Roberts dynamo flow given in equation (4.45) (with a translation in y). However whereas the two Beltrami waves composing $\boldsymbol{u}$ in (4.45) are steady, now they are smoothly switched off and on, that is modulated. Otani's example is based on earlier dynamo models of Bayly & Childress (1988, 1989), in which Beltrami waves and diffusion were applied alternately to the magnetic field.

Focussing only on the horizontal component of these flows, the effect of introducing weak time-dependence to the steady G.O. Roberts flow (4.45) would be to break up the network of separatrices shown in figure 3. These would be replaced by a network of chaotic layers. When the time-dependence is as strong as in (6.5), the network is rather wide, and the only obvious remnant of the original cellular flow is modest islands of regularity. This is shown on a Poincaré section in figure 12, where the positions of advected markers are

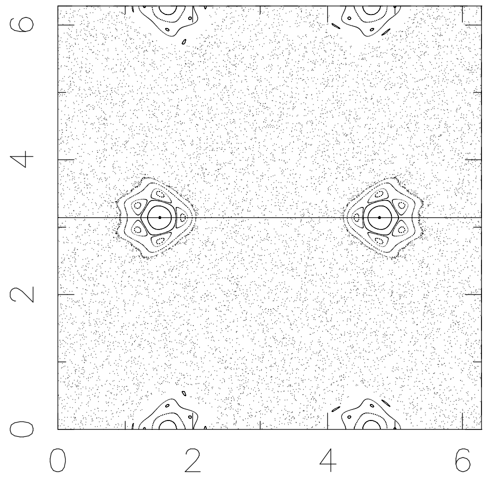

Fig. 12. Poincaré section of the flow MW+, with $0 \le x, y \le 2\pi$. The horizontal line shown is C, used for averaging field.

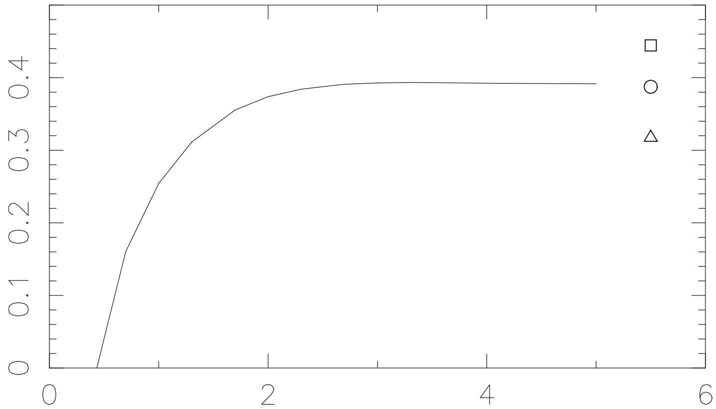

Fig. 13. Growth rate $\gamma(\varepsilon, k)$ plotted against $\log_{10} \varepsilon^{-1}$ for MW+ with $k = 0.8$. Also shown are Γ (circle), h_{line} (square) and Λ_{L} (triangle).

plotted every period of the flow.

Because the flow is independent of z we can take out a normal mode in the magnetic field with z-wave number k, and since the flow field is time-periodic a growing magnetic mode will take the Floquet form

$$\boldsymbol{B}(x, y, z, t) = \boldsymbol{b}(x, y, t)e^{ikz} = \boldsymbol{c}(x, y, t)e^{ikz+\lambda t}, \tag{6.6}$$

where $\boldsymbol{c}$ is periodic in t with period 2π, and λ is the kinematic dynamo growth rate. We take the magnetic field to have the same periodicity in space as the underlying flow, and figure 13 shows maximum magnetic growth rates $\gamma = \operatorname{Re} \lambda$ plotted against $\log_{10} \varepsilon^{-1}$ with $k = 0.8$ (Otani, 1993; Childress & Gilbert, 1995). The growth rate appears to saturate at around $\gamma_0 \simeq 0.39$ as the diffusivity $\varepsilon \to 0$.

There is thus clear evidence of fast dynamo action, with growth rates apparently bounded above zero in the limit of large magnetic Reynolds number

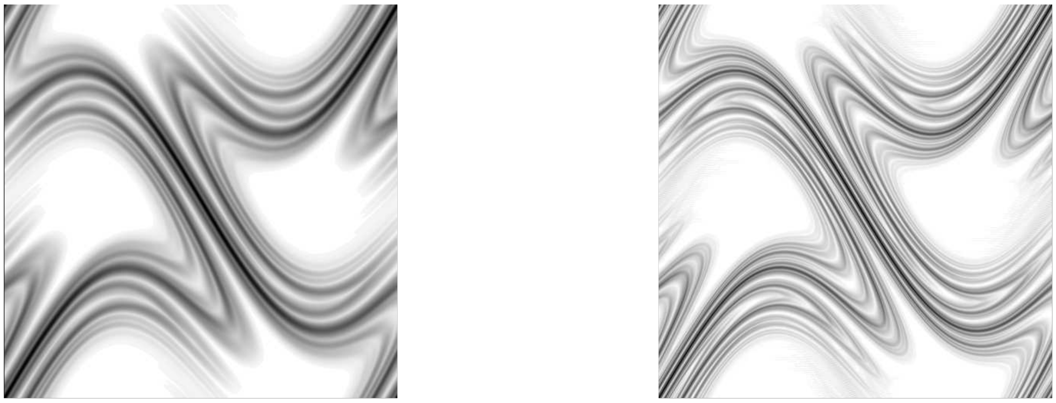

Fig. 14. Eigenfunctions for $k = 0.8$ and (a) $\varepsilon = 5 \times 10^{-4}$ (left) and (b) $\varepsilon = 5 \times 10^{-5}$ (right). The quantity $(|b_x|^2 + |b_y|^2)^{1/4}$ is plotted for $0 \le x, y \le 2\pi$.

$R = \varepsilon^{-1} \to \infty$. Note also that this is for fixed wave number k, and so the field amplified has a large-scale component. Although the maximum growth rate saturates cleanly as $\varepsilon \to 0$, the eigenfunctions become ever more complicated. Figure 14 shows the eigenfunctions at a given instant, for $\varepsilon = 5 \times 10^{-4}$ (left) and $\varepsilon = 5 \times 10^{-5}$ (right); the numerical resolution of 512^2 is becoming evident on the second picture. Plotted is $(|b_x|^2 + |b_y|^2)^{1/4}$ (see (6.6)) as a grey-scale graph with white for zero and black for the maximum value.

As the diffusion is decreased the eigenfunctions gain finer and finer structure. The field takes the form of piles of sheets, which accumulate in the form of *tendrils* about what was originally a hyperbolic stagnation point of the G.O. Roberts flow, in the centre of figure 12. From further analysis of the data (see Childress & Gilbert, 1995, section 2.3) it can be seen that the field direction in the central pile of sheets is largely coherent and directed along the sheets, although there are some sheets of opposite sign there also. The flow is thus bringing largely like-signed horizontal field together. The vertical component u_z of the flow is playing an important role here in largely avoiding the accumulation of fine opposing fields that would occur in its absence. The folding and vertical motion do not give perfect alignment of field, as in the idealised STF picture, but still do rather well.

In fact the dynamo mechanism is rather like that for the steady G.O. Roberts flow discussed in section 4.4, and is known as the *stretch–fold–shear mechanism* (Bayly & Childress, 1988, 1989). Recall from figure 4 that in this flow tongues of field are pulled out and then sheared by the component u_z to reinforce a large-scale z-dependent field, in fact a helical wave. These tongues are narrow, of order $R^{-1/2} = \varepsilon^{1/2}$. Now in the chaotic MW+ flow folds of field are also pulled out, but now by the chaotic stretching and folding. These can then be sheared in z. The difference, though, is that the chaotic stretching and folding operates on space and time scales of order unity (independent of ε) and so the field that is reinforced has scales of order unity in z, and growth rates of order unity: a fast dynamo with a coherent large scale field. The value of k can be fixed to optimise this effect, $k \simeq 0.8$, and give the maximum growth rate. In addition there are fluctuations, which contribute to the complexity of the field seen in figure 14. However these are really just a distraction: the actual mechanism is reinforcing a large-scale field and these fluctuations are part of what is essentially a passive cascade of magnetic energy to diffusive scales of order $\varepsilon^{1/2}$ (Moffatt & Proctor, 1985).

What determines the asymptotic growth rate γ_0? The markers on the right-hand side of figure 13 give some points of comparison. The lowest, triangle marker gives the Liapunov exponent $\Lambda_{\rm L}$ of the flow, measured in the main chaotic region, and this, surprisingly, appears to lie below the asymptotic dynamo growth rate. The uppermost, square marker is the rate of stretching of material lines in the chaotic region, $h_{\rm line}$, and this exceeds γ_0, in keeping with a rigorous upper bound that we discuss below.

The middle, circle marker in figure 13 gives the growth rate Γ of magnetic flux in the absence of diffusion, $\varepsilon = 0$. Recall that for the STF model above it was helpful to think in terms of the amplification of coherent fluxes, as these would be robust to weak diffusion. For the MW+ flow with $\varepsilon = 0$ and a suitable initial condition, the flux $\Phi_C(t)$ was measured through a surface marked by the line C in figure 12 and extending in the z-direction (see Childress & Gilbert, 1995, for further details). This flux shows exponential growth and its growth rate Γ, obtained with *zero* diffusion, appears to agree with the asymptotic growth rate γ_0 in the *limit* of weak diffusion, in agreement with conjectures of Finn & Ott (1988), Bayly & Childress (1988, 1989), Bayly (1992) and Childress & Gilbert (1995). It is important to stress that this agreement, although physically reasonable, is mathematically non-trivial. With $\varepsilon > 0$ any suitable measurement of the field will give the same growth rate $\gamma(\varepsilon)$, because the field takes the form of a growing eigenfunction (6.6) with an underlying time-periodic spatial form. This eigenfunction is smooth on scales of order $\varepsilon^{1/2}$ (Moffatt & Proctor, 1985), given by the balance of exponential stretching and diffusion. However for $\varepsilon = 0$, the field never settles down, but is cascaded to finer and finer scales in the flow; in this case different quantities will generally have different growth rates. For example, for planar flow energy can grow exponentially, but fluxes cannot grow as they are bounded by initial conditions, as discussed in section 6.2.

We will return to discuss conjectures about magnetic flux and dynamo mechanisms below; here we finish the section by remarking on other studies and simulations. The above flows of the form $\boldsymbol{u}(x, y, t)$ have received most attention as they are easy to simulate; furthermore the geometry of the flow field is not too difficult to understand, being based on $\boldsymbol{u}_{\rm H}$. The first flows to be studied for fast dynamo action however were steady three-dimensional ABC flows $\boldsymbol{u}(x, y, z)$, which we defined in equation (4.44). Growth rates for $\mathcal{A} = \mathcal{B} = \mathcal{C} = 1$ are summarised in figure 15. Arnold & Korkina (1983) studied

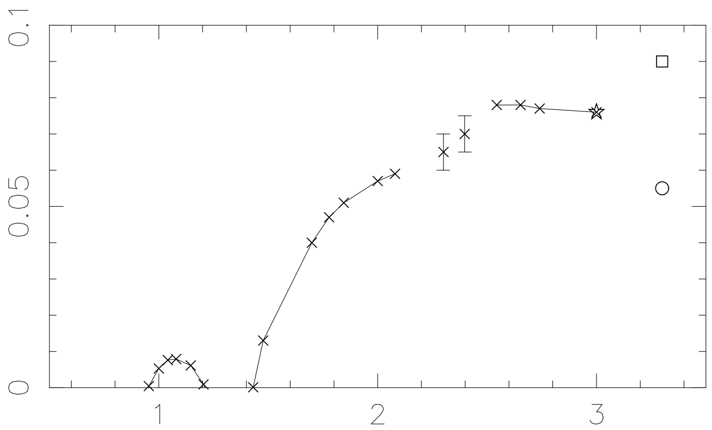

Fig. 15. Dynamo growth rate γ plotted against $\log_{10} R$ for the $\mathcal{A} = \mathcal{B} = \mathcal{C} = 1$ flow. The data points for $R \leq 550$ (times signs) are from Galloway & Frisch (1986) and Arnold & Korkina (1983), and the $R = 1000$ point (star) is from Lau & Finn (1993). The flux growth rate Γ is shown by a circle and h_{line} by a square.

this case and exploited symmetry to reduce the scale of the numerical eigenvalue problem for dynamo growth rates. They found a window of dynamo action for $8.9 \lesssim R \lesssim 17.5$ (with $R \equiv \varepsilon^{-1}$); further simulations by Galloway & Frisch (1986) found a second window of dynamo action for $R \gtrsim 27$ which has been traced up to $R = 1000$ by Lau & Finn (1993). Growth rates appear to asymptote around $\gamma_0 \simeq 0.77$; which is less than measurements of the line-stretching exponent h_{line} (square on figure 15), and *greater* than measurements of the flux growth rate Γ (circle) (Gilbert, 1991; Childress & Gilbert, 1995). This apparent lack of agreement appears to exist because the limit $R \to \infty$ is numerically very delicate for this flow. The bands of chaos happen to be very fine in scale (Dombre *et al.*, 1986), and it is far from clear that even $R \simeq 1000$ is yet in the asymptotic regime of large R. Clearer evidence for fast dynamo action in a steady three-dimensional flow, a Kolmogorov flow, has been obtained by Galloway & Proctor (1992), with reasonable agreement between flux growth rates and γ_0 (Childress & Gilbert, 1995). Other studies of possible fast dynamos include a steady Beltrami flow in a sphere by Zheligovsky (1993) and a flow $\boldsymbol{u}(x, y, z, t)$, which is of ABC type but with additional time-dependence, by Brummell, Cattaneo & Tobias (2001) (see section 6.6).

6.4 Upper bounds

Taking the limit of large magnetic Reynolds number brings the presence or otherwise of chaos in the fluid flow $\boldsymbol{u}$ into sharp focus. In the perfectly conducting limit $R = \infty$, magnetic field is carried as a passive vector field, and magnetic field lines are stretched in the same way as are material lines. This suggests that there may be upper bounds on the fast dynamo exponent γ_0 involving the chaotic properties of the fluid flow. The first of such bounds was proved by Oseledets (1984) and Vishik (1989) (see also Latushkin & Stepin, 1991) and is that γ_0 cannot exceed the *maximum Liapunov exponent* $\Lambda_{\max}$ of the flow. To define this quantity consider a vector $\boldsymbol{v}_0$ located at some initial point $\boldsymbol{x}_0$ in the flow. It is carried, stretched and rotated by the flow and at time t is $\boldsymbol{v}(t)$, having length $|\boldsymbol{v}(t)|$. We then define

$$\Lambda_{\max} = \sup_{\boldsymbol{v}_0, \boldsymbol{x}_0} \limsup_{t \to \infty} t^{-1} \log |\boldsymbol{v}(t)|. \tag{6.7}$$

Now as this is maximised over all initial vectors $\boldsymbol{v}_0$ and initial points $\boldsymbol{x}_0$, a positive value does not indicate the presence of chaos in the flow. Indeed in the G.O. Roberts cellular flow depicted in figure 3, $\Lambda_{\max}$ is positive because a vector $\boldsymbol{v}_0$ located at a hyperbolic stagnation point $\boldsymbol{x}_0$, and pointing in the stretching direction there, increases exponentially in time.

This bound does therefore not necessitate a chaotic flow $\boldsymbol{u}$ for fast dynamo action. Chaos is however required by the tighter upper bound, conjectured by Finn & Ott (1988) and proved by Klapper & Young (1995), that for smooth flows γ_0 is no greater than the *topological entropy* h. This is an appealing result, because for two-dimensional flows $\boldsymbol{u}(x, y, t)$, such as MW+ above, the topological entropy is equal to the line-stretching exponent, $h = h_{\text{line}}$. To define h_{line} more formally, let L_0 be an initial material line of finite length in the fluid flow. We let it evolve, carried passively, for time t to give a line $L(t)$ of length $|L(t)|$. Then we may define

$$h_{\text{line}} = \sup_{L_0} \limsup_{t \to \infty} t^{-1} \log |L(t)|. \tag{6.8}$$

This bound, $\gamma_0 \leq h = h_{\text{line}}$, for smooth two-dimensional flows indicates that strong magnetic field line stretching is an essential part of any fast dynamo process. In three dimensions h is whichever is greater: the rate of growth of lines or of surface areas, in the fluid flow.

We may also define the most commonly used measure of chaos, the Liapunov exponent Λ_{L}. Here we take an initial vector $\boldsymbol{v}_0$ defined at a *typical* point $\boldsymbol{x}_0$ and measure

$$\Lambda_{\text{L}} = \sup_{\boldsymbol{v}_0} \limsup_{t \to \infty} t^{-1} \log |\boldsymbol{v}(t)|. \tag{6.9}$$

Because this is not maximised over all initial points $\boldsymbol{x}_0$ it is obviously less than (or possibly equal to) $\Lambda_{\max}$.

The Liapunov exponent Λ_{L} is also less than or equal to the line-stretching exponent h_{line}: the reason is that different averaging processes are occurring (Finn & Ott, 1988). For Λ_{L} the notion of a typical point involves an average, over points in the chaotic volume under consideration. For h_{line}, we take the average length of a line $L(t)$ which we can consider as composed of many vectors. Because we compute its length we are weighting the longer, more stretched vectors. This extra weighting gives a greater growth rate, $h_{\text{line}} \geq$

$\Lambda_{\rm L}$ (with equality only if the stretching is uniform). Alternatively note that in computing $\log|L(t)|$ we sum the lengths of many vectors composing the line $L(t)$ and then take the logarithm, whereas in computing $\Lambda_{\rm L}$ we take the logarithm of lengths of vectors first, and then average. The fact that the operations of averaging and taking logarithms do not commute explains why $h_{\rm line}$ and $\Lambda_{\rm L}$ generally differ.

The result that $h_{\rm line}$ is an upper bound on fast dynamo growth rates is confirmed for the MW+ flow in figure 13 above and for other models (see Childress & Gilbert, 1995). On the other hand a positive Liapunov exponent $\Lambda_{\rm L}$ tells us nothing about γ_0.

6.5 Flux conjectures

We know that the topological entropy h is an upper bound on γ_0, or for two-dimensional flows $\boldsymbol{u}(x,y,t)$ simply the line-stretching exponent $h_{\rm line}$. Measuring h or $h_{\rm line}$ does not involve diffusion, just the chaotic properties of the flow field. The question then is: can the fast dynamo exponent γ_0 itself somehow be related to the properties of the chaotic flow, without explicitly considering the limit $\varepsilon \to 0$? Bearing in mind the STF picture, the natural quantity on which to focus is magnetic flux. The intuition here is that fluxes should be robust to diffusion, which will tend only to smear out magnetic field locally. There are two approaches here: in the first we take the asymptotic growth rate Γ_S of magnetic flux

$$\Phi_S = \int_S \boldsymbol{B}\cdot\boldsymbol{n}\,dS \tag{6.10}$$

through an open surface S in the flow. If this growth rate Γ_S is maximised over initial conditions $\boldsymbol{B}_0$ and surfaces S, then we obtain a flux growth exponent Γ. The conjecture of Finn & Ott (1988) is that $\Gamma = \gamma_0$.

The second, related approach of Bayly & Childress (1988, 1989) and Bayly (1994) is to measure smooth linear functionals of the field. Let $\boldsymbol{B}(\boldsymbol{x},t)$ be an evolving field, from some initial condition $\boldsymbol{B}_0(\boldsymbol{x})$. Let us take a fixed smooth test function $\boldsymbol{f}(\boldsymbol{x})$ and define

$$\Phi_{\boldsymbol{f}}(t) = (\boldsymbol{f},\boldsymbol{B}) \equiv \int_V \overline{\boldsymbol{f}}\cdot\boldsymbol{B}\,dV \tag{6.11}$$

(V being the volume in which the flow is defined). We then may define a flux growth rate by

$$\Gamma = \sup_{\boldsymbol{f},\boldsymbol{B}_0}\limsup_{t\to\infty} t^{-1}\log|\Phi_{\boldsymbol{f}}(t)|. \tag{6.12}$$

One may then conjecture that provided $\Gamma>0$, $\Gamma=\gamma_0$ for smooth flows. There are a number of other conjectures that can be made, depending on whether the flow is smooth or not (see section 4.1 of Childress & Gilbert, 1995). Little has been proved mathematically, although Klapper (1993) has used the idea of *shadowing* to prove results for hyperbolic systems.

Finally, given that the fast dynamo growth rate is less than the topological entropy, it is of interest to try to quantify the difference $h - \gamma_0 \geq 0$ in terms of the flow properties. Clearly this difference is related to the folding of field in the fluid flow, and how far short the flow falls of the idealised STF picture, which we recall had perfect alignment with $h = \gamma_0 = \log 2$. There have been two approaches here: one is to define a *cancellation exponent*, which captures the tendency of the magnetic field to have alternating directions on fine scales for $\varepsilon = 0$ and large time t (Du & Ott, 1993; Du, Tél & Ott, 1994; Ott, 1998).

The second approach is to use methods based on periodic orbit sums. In a chaotic system there are many periodic orbits, and studying orbits of increasing period reveals increasingly detailed information about the properties of the flow. It is possible to recast the dynamo problem in terms of sums over periodic orbits (Aurell & Gilbert, 1993; Balmforth *et al.*, 1993; Soward, 1994b); there is little rigorous theory as yet, but good numerical agreement in some examples. This approach has also led to some interesting conjectures by Oseledets (1993) about the relationship of γ_0 with the ergodic properties of the fluid flow.

Much of our limited theory on fast dynamos comes from the study of evolution of magnetic field under mappings, rather than fluid flows. Unfortunately we do not have space to do more than list a number of studies here. The simplest maps considered are baker's maps, and these can be used to model the STF dynamo picture (Finn & Ott, 1988). To model the fast dynamo seen in Otani's flow above, Bayly & Childress (1988, 1989) introduced the idea of the stretch–fold–shear (SFS) dynamo mechanism and illustrated it with a very simple model based on a baker's map in the (x, y)-plane and shear in the z-direction. This model is tantalisingly difficult to analyse, but progress has been made using the setting of Rugh (1992); see Gilbert (2002b). Other dynamos that have been studied include maps on a two-torus (Oseledets, 1993) and dynamos based on pseudo-Anosov maps with vertical shear (Gilbert, 1993). Further studies are reviewed in Childress & Gilbert (1995).

6.6 Nonlinear fast dynamos

While much is understood about fast dynamos in kinematic regimes, little is known about how they equilibrate in a nonlinear framework. Indeed it is unclear whether there is any meaningful distinction between slow and fast dynamos in a nonlinear regime: the definitions refer to kinematic growth rates, and in a saturated regime the growth rate is zero regardless of how the field grew in the first place! Nonetheless the study of fast dynamos has highlighted the importance of Lagrangian chaos in fluid flows and consideration of dynamo mechanisms at large R, and these form a basis for understanding nonlinear regimes. Here we highlight the issues and discuss the results of two recent numerical studies.

The first issue is that of setting up a suitable model. The flow is no longer prescribed but must be driven somehow. Possibilities include convective driving (see section 5.4) or imposing a given body force, which is convenient especially when periodic geometry is used. Once the model is specified, a flow $\boldsymbol{u}$ will be driven; if it is sufficiently complicated and R is large enough, a magnetic field will increase until the Lorentz force becomes important and the growth ceases. We may then list a number of questions that can be asked:

(1) What is the saturation level of the magnetic energy? If the magnetic field has structure over a range of scales, how much energy is in the large-scale field, and how much at the smallest scales? This latter issue is important in comparing with observations, for example the magnitude of the observed large-scale galactic and Solar fields (Vainshtein & Cattaneo, 1992; Gilbert, Otani & Childress, 1993; Vainshtein, Parker & Rosner, 1993).

(2) What is the mechanism for the equilibration of the magnetic field? For example, does equilibration occur because the magnetic field suppresses the fluid flow entirely, or because the stretching in the fluid flow is suppressed (Cattaneo, Hughes & Kim, 1996; Maksymczuk & Gilbert, 1998), or because the folding of field in a fast dynamo is modified to be less constructive? Or is it some messy combination of these processes?

(3) What is the time scale of evolution of a large-scale magnetic field in a saturation regime? This is a crucial question, and perhaps the possibility of fast evolution of a large-scale magnetic field is the only sensible counterpart to a fast dynamo in a nonlinear equilibrated regime. Can an equilibrated magnetic field substantially change its structure through reconnection on a fast advective time-scale? The question is important as the Solar field evolves on a rapid 11-year time-scale, and in this sense is a nonlinear fast dynamo.

(4) Tied up with these earlier issues is: to what extent can the evolution of the saturated magnetic field be described by a nonlinear α effect (for example, (5.10)) and eddy diffusion, or other transport effects (Cattaneo & Hughes, 1996; Gruzinov & Diamond, 1996)?

(5) Another set of problems involves spatially extended systems, again relevant to modelling astrophysical dynamos. For a fast dynamo, magnetic field is amplified with most rapid growth for fields on the same scale as the fluid flow (sometimes this is called the *small-scale dynamo*). If this

fluid flow is of small scale in a spatially extended system (for example small-scale convection or turbulence), the question then is how do fields evolve over these larger scales? One mechanism that has been observed is an inverse cascade (Pouquet, Frisch & Léorat, 1976; Gilbert & Sulem, 1990; Brandenburg, 2001), whereby after initial saturation on the scale of the flow, fields evolve to larger and larger scales until finally the dominant field is at the largest scale available in the system. Again there are important issues of time scales and saturation levels in such an inverse cascade.

(6) The final question is: how do all these mechanisms and results depend on the magnetic Reynolds number R and the fluid Reynolds number Re, bearing in mind that both are very large in astrophysical applications, with $1 \ll R \ll Re$ for the Sun and $1 \ll Re \ll R$ for the galaxy? Also how much do they depend on the model and the forcing adopted?

The problems of handling nonlinearity, as well as spatially extended systems and large parameters, R and Re, make this research area mostly the domain of numerical simulations. We shall focus on two studies to illustrate recent results and some of the problems of dealing with nonlinear dynamos. Our first study is that of Brummell, Cattaneo & Tobias (2001), who solve the equations

$$\partial_t \boldsymbol{u} + \boldsymbol{u} \cdot \nabla \boldsymbol{u} = -\nabla p + Re^{-1} \nabla^2 \boldsymbol{u} + \boldsymbol{J} \times \boldsymbol{B} + \boldsymbol{F}, \tag{6.13}$$

$$\partial_t \boldsymbol{B} + \boldsymbol{u} \cdot \nabla \boldsymbol{B} = \boldsymbol{B} \cdot \nabla \boldsymbol{u} + R^{-1} \nabla^2 \boldsymbol{B}, \tag{6.14}$$

$$\nabla \cdot \boldsymbol{u} = \nabla \cdot \boldsymbol{B} = 0. \tag{6.15}$$

The flow is driven by a prescribed body force $\boldsymbol{F}$ which is chosen so that in the absence of magnetic field, the flow is

$$\begin{aligned} \boldsymbol{u}_0 = (\, & \sin(z + \varepsilon \sin \Omega t) + \cos(y + \varepsilon \sin \Omega t), \\ & \sin(x + \varepsilon \sin \Omega t) + \cos(z + \varepsilon \sin \Omega t), \\ & \sin(y + \varepsilon \sin \Omega t) + \cos(x + \varepsilon \sin \Omega t)). \end{aligned} \tag{6.16}$$

In fact the force is simply $\boldsymbol{F} = (\partial_t - Re^{-1} \nabla^2) \boldsymbol{u}_0$ (as the flow is Beltrami, $\boldsymbol{u}_0 \times \boldsymbol{\omega}_0 = 0$). Note that this force is Reynolds number dependent; for steady flow $\varepsilon\Omega = 0$, $\boldsymbol{F} = O(Re^{-1})$ for all Re, while for unsteady flow $\varepsilon\Omega \neq 0$, $\boldsymbol{F} = O(Re^{-1})$ in the viscous limit $Re \to 0$ and $\boldsymbol{F} = O(1)$ in the inviscid limit $Re \to \infty$.

The flow is parameterised by ε and Ω, and reduces to a steady ABC flow (4.44) for $\varepsilon\Omega = 0$. Other studies of nonlinear ABC and related flows include Galanti, Sulem & Pouquet (1992), Vainshtein & Cattaneo (1992), Cattaneo, Hughes & Kim (1996) and Maksymczuk & Gilbert (1998). This steady flow has only thin bands of chaos and small Liapunov exponents; however as ε and Ω are increased the chaos fills out more and more of the $(2\pi)^3$ domain, and fills the whole region for $\varepsilon = \Omega = 1$. These flows appear to show fast dynamo action, given the numerical limitations on the magnetic Reynolds number, $R \le 170$, and the growing magnetic field has a tube structure with a magnetic length-scale

$$l_B \equiv (<|\boldsymbol{B}|^2> / <|\nabla \times \boldsymbol{B}|^2>)^{1/2} \propto R^{-1/2}, \tag{6.17}$$

as R is increased.

The authors then explore the dynamical regime for R and Re varying up to 100. It is found that members of the above family of flows exhibit hydrodynamic instability for moderate values of Re; however this instability is slowly growing compared with the kinematic evolution of the magnetic field, and so need not be considered. Runs show rapid growth and equilibration of magnetic field for $\varepsilon = \Omega = 1$. When growth saturates, in physical space the magnetic field takes the form of tubes and sheets with a greater filling factor than in the kinematic regime. The length scale of the field increases, but still scales as $l_B \propto R^{-1/2}$ (independently of Re). This indicates that the fine scales of the magnetic field are still controlled by a balance between advection and diffusion.

One important quantity to measure is the magnitude of the equilibrated magnetic energy. This shows two regimes,

$$\mathcal{E} \propto R^{1/2} Re^{-1} \quad (R \le 50), \qquad \mathcal{E} \propto Re^{-1} \quad (R \ge 50). \tag{6.18}$$

In both cases the scaling is with Re^{-1} suggesting that the primary balance is between the Lorentz force and the viscous term in the Navier–Stokes equation (6.13). The $O(Re^{-1})$ scaling law is very reasonable in the viscous limit $Re \to 0$ in view of the scaling $\boldsymbol{F} = O(Re^{-1})$ of the driving force. However a transition to an Re-independent scaling, in which the Lorentz force balances inertial terms, would be expected at some point as Re is increased to large values; recall that for large Re the forcing is $\boldsymbol{F} = O(1)$ for the case of an unsteady driven flow. A similar scaling to (6.18) is found in the theoretical study of the Ponomarenko dynamo (Bassom & Gilbert, 1997), with $\mathcal{E} \propto R^{2/5} Re^{-1}$ for $1 \ll R \ll Re$, resulting from the same balance. Numerical simulations of this Ponomarenko dynamo show a similar behaviour but with shallower power laws (Dobler, Shukurov & Brandenburg, 2002).

As for the dependence on R in (6.18), in the first regime the energy increases with R suggesting a balance between the flows driven by the Lorentz force on small scales of size l_B and the driven flow $\boldsymbol{u}_0$, with $\boldsymbol{J} \times \boldsymbol{B} \sim Re^{-1} \nabla^2 \boldsymbol{u}$ and $\nabla \sim l_B^{-1} \sim R^{1/2}$. In short the field is acting primarily to suppress the fluid flow and this is the equilibration mechanism. In the second regime, the saturation independent of R is interpreted by the authors as the magnetic field acting to suppress the Lagrangian chaos in the flow. In nonlinear regimes the magnetic field lines must be considered as elastic and resist stretching through the Lorentz force feedback on the flow. This in turn suppresses the separation of neighbouring fluid elements and so the Liapunov exponents of the flow. (Note that this refers to Lagrangian chaos, the separation of material particles carried in the flow, and is independent of the notion of Eulerian chaos, whereby the components of the flow at a given point in space may be chaotic functions of time.) Similar suppression of chaos has been studied by Cattaneo & Vainshtein (1991) and Cattaneo, Hughes & Kim (1996). Maksymczuk & Gilbert (1998) found this mechanism in a truncated, viscous model but also found evidence of an inverse cascade, whereby after kinematic growth, large-scale magnetic field modes tended to become dominant and saturate through flow suppression rather than suppression of chaos, in the framework of Gilbert & Sulem (1990). It remains to be seen whether these results carry over to more realistic models.

Another situation studied by Brummell, Cattaneo & Tobias (2001) is the case $\varepsilon = 1$, $\Omega = 2.5$ in (6.16) and $Re = R = 100$, in which case kinematic growth is seen and there is an initial phase of magnetic saturation. However the field then decays exponentially. As a result the simulation is left with a flow field $\boldsymbol{u}_1$, forced by $\boldsymbol{F}$, which is not a kinematic dynamo for these parameter values. The system has evolved from one purely hydrodynamic branch to another, mediated by a transitory magnetic field. The fact that nonlinear dynamos are nonlinear magnetohydrodynamic systems with many degrees of freedom means that there can be many solution branches and bifurcations, and this is what makes their study in any generality difficult and numerically time-consuming, especially in the demanding and important limits of large R and large Re.

The second study we discuss is that of Brandenburg (2001), who considers evolution of magnetic field in a compressible flow. The aim is to study the effects of scale separation between the kinematic dynamo modes and the scale of the system, as far as this can currently be achieved numerically. The fields are governed by

$$\partial_t \boldsymbol{A} = \boldsymbol{u} \times \boldsymbol{B} - \eta\mu \boldsymbol{J}, \tag{6.19}$$

$$(\partial_t + \boldsymbol{u}\cdot\nabla)\log\rho = -\nabla\cdot\boldsymbol{u}, \tag{6.20}$$

$$\rho(\partial_t + \boldsymbol{u}\cdot\nabla)\boldsymbol{u} = -c_{\mathrm{s}}^2\rho\nabla\log\rho + \boldsymbol{J}\times\boldsymbol{B} + \mu_{\mathrm{visc}}(\nabla^2\boldsymbol{u} + \tfrac{1}{3}\nabla\nabla\cdot\boldsymbol{u}) + \rho\boldsymbol{F}. \tag{6.21}$$

Here ρ is the density, $\boldsymbol{A}$ is the vector potential for the magnetic field, c_{s} is the sound speed, and μ_{visc} the dynamical viscosity. The domain is a $(2\pi)^3$ periodic box, and the forcing employed is

$$\boldsymbol{F}(\boldsymbol{x},t) = N\boldsymbol{f}_{\boldsymbol{k}(t)}\exp(i\boldsymbol{k}(t)\cdot\boldsymbol{x} + i\phi(t)) + \mathrm{c.c.} \tag{6.22}$$

Without going into the details, we mention that $\boldsymbol{k}(t)$ is a time-dependent wave-vector, which varies in direction but whose magnitude is in the band $4.5 < |\boldsymbol{k}| < 5.5$, and the forcing is designed to be maximally helical, with

$i\boldsymbol{k} \times \boldsymbol{f}_{\boldsymbol{k}} = |\boldsymbol{k}|\boldsymbol{f}_{\boldsymbol{k}}$ at any time. In this way energy and helicity are injected into the flow field at wave numbers $k = |\boldsymbol{k}| \simeq 5$.

In one set of runs the magnetic and fluid Reynolds numbers are increased from $R = Re = 16$ to 120, these values being based on the scale and magnitude of the forcing at $k \simeq 5$; the values are $R = Re = 80$ to 600 based on the scale of the system. The kinematic growth rate increases as $R = Re$ is increased. During the kinematic regime most of the magnetic energy is in scales $k = 5$ and smaller. However as the Lorentz force becomes important, the magnetic energy transfers to larger scales in a (non-local) inverse cascade, and the energy in the smaller scales declines. This is even more pronounced in a further run when the forcing wave number is increased to $k \simeq 30$; there is a clear wave packet of magnetic energy travelling to larger scales. In both cases the field in the final state has a strong helical component on the scale $k = 1$, and smaller scale excitation around the forcing wave numbers. The final state is similar to an alpha-effect dynamo in which a large-scale field is maintained by a mean emf. Measurements of the alpha effect suggest strong R-dependent quenching as in (5.10), together with quenching of the turbulent magnetic diffusivity. The magnitude of the large-scale field in the final state appears to increase slowly with R.

Although the kinematic growth of magnetic field occurs on rapid time-scales, during the saturation phase the large-scale field evolves much more slowly. For increasing values of R, the time scale of evolution of the large-scale field increases. This has been interpreted as a consequence of a magnetic helicity constraint. Magnetic helicity is an invariant for a perfectly conducting fluid, for which $R = \infty$, and can only be destroyed by diffusive processes. In the limit of large R it is found that helicity is increasingly well conserved in MHD systems. Thus to generate a dominant helical large-scale field, which appears to be the ultimate steady state of these systems, much helicity must be dissipated and this takes an increasing length of time. (The alternative that helicity of the opposite sign is stored in other scales of the field, does not seem to be realised.) We refer the reader to Brandenburg (2001), Brandenburg & Dobler (2001), Vishniac & Cho (2001), Brandenburg, Dobler & Subramanian (2002) and Gilbert (2002a) for further discussion.

These and other simulations give interesting pointers to phenomena in the nonlinear regime. However the reader should always be aware that Reynolds numbers may be far from asymptotic even in the largest current simulations. There is still much uncertainty about dynamo behaviour for large R and large Re, as studied in the computer laboratory. We only have observations of stellar and galactic dynamos. One important point is that in a simulation such as Brandenburg (2001) the large-scale fields, once generated, appear to be dominant and evolve very slowly, over scales closer to the diffusive time-scale R^{-1} than the turn-over time-scale. There is little evidence yet of strong magnetic fields showing significant dynamical behaviour on an advective time-scale in such simulations, even though this appears to be the case in the Sun, with the field reversing each 11 years.

Note that for a comparison between different numerical studies the precise definition of the magnetic Reynolds number $R = \mathcal{L}\mathcal{V}/\eta$ (and Re) may be important: for example the length scale of a 2π-periodic box could be taken as $\mathcal{L} = 1$ (the inverse of the smallest wave number) (for example, Brummell, Cattaneo & Tobias, 2001) or $\mathcal{L} = 2\pi$ (for example, Brandenburg, 2001), and this can make a large and subjectively important difference in quoted values of R or Re. Also there may be different ways of defining $\mathcal{V}$. To further complicate matters, in a nonlinear simulation with a body force, it may be convenient to define a magnetic Reynolds number based on the magnitude $\mathcal{F}$ of the forcing, $R_F = \mathcal{F}\mathcal{L}^3/\eta\nu$. This is based on the flow that would be driven in a balance between viscous terms and the forcing, and is a control parameter for the experimentalist. Alternatively one could define $R_F = \sqrt{\mathcal{F}\mathcal{L}^3}/\eta$, based on a balance between forcing and inertial terms; in hydrodynamics the strength of a given forcing is similarly sometimes measured by a Grashof number, $G = \mathcal{F}\mathcal{L}^3/\nu^2$; see Childress, Kerswell & Gilbert (2001).

For the same forcing there may also be many different flows (for example with or without a magnetic field present), giving different values for an effective magnetic Reynolds number $R = \mathcal{L}\mathcal{V}/\eta$, based on the magnitude $\mathcal{V}$ of the actual flow $\boldsymbol{u}$ that is realised. Such an effective magnetic Reynolds number is now a diagnostic, to be measured in the simulation. Similarly in a convective simulation, the control parameters might include a Rayleigh number, and the effective magnetic Reynolds number is then a diagnostic that depends on the form of the convection realised in a given run.

7 Open issues

In this final section we set out a few open issues, based mostly on fast and Solar dynamos.

(1) *Laminar dynamos*: are there general formulae for alpha effects and growth rates at large R for laminar two-dimensional flows with hyperbolic stagnation points joined by a network of separatrices? What about networks of separatrices in a bounded plane layer, as depicted in figure 8? This would generalise the results for the G.O. Roberts (1970) flow (section 4.3) to stream line configurations that arise naturally in flows driven by convection or other instabilities.

(2) *Fast dynamos*: can fast dynamo action be proved for a given smooth flow or class of flows? Recently Dr. Oleg Kozlovsky (personal communication) has proved rigorous results for fast dynamo action in a steady three-dimensional flow with a pretzel configuration. This smooth flow is carefully designed to allow field vectors to be always brought into alignment, using rows of stagnation points to cut and glue together field, and create what is basically a baker's map as a return map. A picture of how such a dynamo might operate is given in figure 7.11 of Childress & Gilbert (1995); as with STF, it is easy to draw the picture but much more difficult to go from this to a precise mathematical result.

(3) *Fast dynamos*: can fast dynamo action be shown to be a generic property in certain classes of flows $\boldsymbol{u}$? For example, if a two-dimensional time-dependent flow $\boldsymbol{u}(x, y, t)$ (section 6.3) fails to be a fast dynamo, with $\gamma_0 \leq 0$, is there a nearby flow which is a fast dynamo? This has been conjectured (see Finn & Ott, 1988; Childress & Gilbert, 1995) and is true for many simplified models but, mathematically, little is known and obviously the word 'nearby' above needs to be specified.

(4) *Fast dynamos*: what can usefully be said in general about the nonlinear saturation of fast dynamos, or is this process highly model-dependent? What are the answers to the questions in section 6.6, in particular how do saturation processes depend on the hydrodynamic Reynolds number?

(5) *Folding*: in the STF picture (figure 10) a tube of field is doubled up at each iteration to create a bundle of 2^n subtubes arranged with a consistent orientation. Plainly this cannot be done indefinitely, as $n \to \infty$, for an initial tube of *finite volume* and volume-preserving periodic flow $\boldsymbol{u}$. As the STF process is iterated, field-free fluid is entrained and the bundle of field becomes thicker until at some point the picture breaks down. However can the STF process be achieved repeatedly with a *single* magnetic field line?

In other words is the following possible? There is a volume preserving periodic flow $\boldsymbol{u}$ (or if preferred a volume-preserving map M) defined inside the interior V of a sphere S, a solid torus $T \subset V$ and an initial closed curve $C_0 \subset T$ which wraps once round the hole in T. Let the image of C_0 after n periods of the flow $\boldsymbol{u}$ be called C_n. Can it be the case that for all n, C_n lies wholly inside T and wraps 2^n times around T with consistent orientation?

This is a question about the kinds of folding that are allowed in three dimensions, and we note that if the condition that the flow is volume-preserving is dropped, then this can be achieved by a map known as the *solenoid*.

(6) *Solar dynamo*: why is the Solar magnetic field so coherent, obeying the Hale polarity laws to such a high degree, when usually at large magnetic Reynolds numbers dynamos tend to have strong fluctuating fields? Is this because the tachocline is a thin layer dynamo, with an effectively rather reduced value of the magnetic Reynolds number?

(7) *Solar dynamo*: how does the Solar magnetic field evolve so rapidly, on the 11-year time-scale? Although fast dynamo theory shows that kinematic dynamos can evolve on the turn-over time-scale of the fluid motion, there is some evidence that nonlinearity through the Lorentz force tends to suppress reconnection. The very dramatic suppression of the alpha effect that has been proposed (see (5.10)) would tend to slow down the evolution of a large-scale equilibrated magnetic field.

    Put differently, the Hale polarity laws indicate strong coherent belts of toroidal field, of opposite signs in the two hemispheres, presumably located deep down in the tachocline. How are these destroyed in a matter of a few years, every 11 years when the fields in the dynamo cycle reverse?

    One possibility is that the dramatic suppression of the alpha effect that has been proposed and observed at large magnetic Reynolds number becomes modified when the fluid Reynolds number is also large. In this case the magnetic field may drive small-scale fluid flows that can tap magnetic energy, lead to accelerated reconnection processes and so an enhanced alpha effect. This regime is however difficult to study analytically or numerically.

(8) *Paradigms*: how do we go beyond the alpha effect? This is beginning perhaps to outlive its usefulness, and it is now clear that to model the Solar dynamo and geodynamo it is necessary to take into account the actual fluid motions and the form of the convection. This is now becoming possible, in restricted regimes, in numerical simulations but we are lacking the theoretical tools to really understand the results.

    For example, consider the Solar dynamo: is it best to think of this as an $\alpha\omega$-dynamo, parameterising turbulent convection and large-scale circulations? Or are we now reaching the point where we should be considering a given, organised large-scale flow, for example a few giant convective cells overshooting into the tachocline, and trying to understand the effect of these flows on the field?

    Here the philosophy is more aligned with the study of laminar and fast dynamos, but based on realistic flows and ultimately bringing in the nonlinear feedback through the Lorentz force. On the positive side, such a fluid dynamical viewpoint may get around issues such as the suppression of the alpha effect (see (5.10)); however the mathematical analysis or numerical study of such models remains challenging.

Acknowledgements

I am grateful to Axel Brandenburg, Steve Childress, Chris Jones, Isaac Klapper, Paul Matthews, Helmut Moritz, Yannick Ponty, Andrew Soward, Andreas Tilgner, Steve Tobias and Keke Zhang for useful references and discussions. The pictures in figures 8, 9 and 14 were obtained using the parallel computer 'ceres' at the University of Exeter, supported by the HEFCE JREI. Also, figures 8 and 9 were kindly provided by Yannick Ponty, whose work with the author and Andrew Soward was funded by the Leverhulme Trust.

References

M. Abramowitz & I.A. Stegun, *Handbook of mathematical functions.* Dover (1972).

H. Alfvén, *Discussion of the origin of the terrestrial and solar magnetic fields.* Tellus 2 (1950), 74–82.

A.P. Anufriyev & V.M. Fishman, *Magnetic field structure in the two-dimensional motion of a conducting fluid.* Geomag. Aeron. 22 (1982), 245–248.

V.I. Arnold, *Sur la topologie des écoulements stationnaires des fluides parfaits.* C. R. Acad. Sci. Paris 261 (1965), 17–20.

V.I. Arnold & E. Korkina, *The growth of a magnetic field in a three-dimensional steady incompressible flow.* Vest. Mosk. Un. Ta. Ser. 1, Matem. Mekh., no. 3 (1983), 43–46.

V.I. Arnold, Ya.B. Zeldovich, A.A. Ruzmaikin & D.D. Sokoloff, *A magnetic field in a stationary flow with stretching in Riemannian space.* Sov. Phys. JETP 54 (1981), 1083–1086.

V.I. Arnold, Ya.B. Zeldovich, A.A. Ruzmaikin & D.D. Sokoloff, *Steady-state magnetic field in a periodic flow.* Sov. Phys. Dokl. 27 (1982), 814–816.

E. Aurell & A.D. Gilbert, *Fast dynamos and determinants of singular integral operators.* Geophys. Astrophys. Fluid Dynam. 73 (1993), 5–32.

G. Backus, *A class of self-sustaining dissipative spherical dynamos.* Ann. Physics 4 (1958), 372–447.

S.A. Balbus & J.F. Hawley, *Powerful local shear instability in weakly magnetized disks 1. Linear analysis.* Astrophys. J. 376 (1991), 214–222.

N.J. Balmforth, P. Cvitanović, G.R. Ierley, E.A. Spiegel & G. Vattay, *Advection of vector fields by chaotic flows.* In: Stochastic Processes in Astrophysics, pp. 148–160. Annals New York Acad. Sci., vol. 706 (1993).

A.P. Bassom & A.D. Gilbert, *Nonlinear equilibration of a dynamo in a smooth helical flow.* J. Fluid Mech. 343 (1997), 375–406.

A.P. Bassom, K.M. Kuzanyan & A.M. Soward, *A nonlinear dynamo wave* *riding on a spatially varying background.* Proc. R. Soc. Lond. A 455 (1999), 1443–1481.

G.K. Batchelor, *An introduction to fluid mechanics.* Cambridge University Press (1967).

B.J. Bayly, *Infinitely conducting dynamos and other horrible eigenproblems.* In: Nonlinear phenomena in atmospheric and oceanic sciences (ed. G.F. Carnevale, R.T. Pierrehumbert), pp. 139–176, IMA Series in Mathematics and its Applications, vol. 40. Springer–Verlag (1992).

B.J. Bayly, *Maps and dynamos.* In: Lectures on Solar and planetary dynamos (ed. M.R.E. Proctor, A.D. Gilbert), pp. 305–329. Cambridge University Press (1994).

B.J. Bayly & S. Childress, *Construction of fast dynamos using unsteady flows and maps in three dimensions.* Geophys. Astrophys. Fluid Dynam. 44 (1988), 211–240.

B.J. Bayly & S. Childress, *Unsteady dynamo effects at large magnetic Reynolds numbers.* Geophys. Astrophys. Fluid Dynam. 49 (1989), 23–43.

R. Beck, A. Brandenburg, D. Moss, A.M. Shukurov & D.D. Sokoloff, *Galactic magnetism: recent developments and perspectives.* Ann. Rev. Astron. Astrophys. 34 (1996), 155–206.

E. Beltrami, *Opera Matematiche*, vol. 4 (1889), p. 304.

E.R. Benton, *Kinematic dynamo action with helical symmetry in an unbounded fluid conductor. Part 1: Formulation and survey of low order cases.* Geophys. Astrophys. Fluid Dynam. 12 (1979a), 313–44.

E.R. Benton, *Kinematic dynamo action with helical symmetry in an unbounded fluid conductor. Part 2: Further development of an explicit solution for the prototype case of Lortz.* Geophys. Astrophys. Fluid Dynam. 12 (1979b), 345–358.

E.G. Blackman & G.B. Field, *Constraints on the magnitude of α in dynamo theory.* Astrophys. J. 534 (2000), 984–988.

S.I. Braginsky, *Self excitation of a magnetic field during the motion of a highly conducting fluid.* Sov. Phys. JETP 20 (1964a), 726–735.

S.I. Braginsky, *Theory of the hydromagnetic dynamo.* Sov. Phys. JETP 20 (1964b), 1462–1471.

S.I. Braginsky, *The nonlinear dynamo and model-Z.* In: Lectures on Solar and planetary dynamos (ed. M.R.E. Proctor, A.D. Gilbert), pp. 267–304. Cambridge University Press (1994).

A. Brandenburg, *Solar dynamos: computational background.* In: Lectures on Solar and planetary dynamos (ed. M.R.E. Proctor, A.D. Gilbert), pp. 117–159. Cambridge University Press (1994).

A. Brandenburg, *The inverse cascade and nonlinear alpha-effect in simulations of isotropic helical hydromagnetic turbulence.* Astrophys. J. 550 (2001), 824–840.

A. Brandenburg & W. Dobler, *Large scale dynamos with helicity loss through boundaries.* Astron. Astrophys. 369 (2001), 329–338.

A. Brandenburg & E.G. Zweibel, *Effects of pressure and resistivity on the* *ambipolar diffusion singularity: too little, too late?* Astrophys. J. 448 (1995), 734–741.

A. Brandenburg, W. Dobler & K. Subramanian, *Magnetic helicity in stellar dynamos: new numerical experiments.* Astr. Nachr. 323 (2002), 99–122.

A. Brandenburg, Å. Nordlund, P. Pulkkinen, R.F. Stein & I. Tuominen, *3D simulation of turbulent cyclonic magnetoconvection.* Astron. Astrophys. 232 (1990), 277–291.

A. Brandenburg, Å. Nordlund, R.F. Stein & U. Torkelsson, *Dynamo-generated turbulence and large-scale magnetic-fields in a Keplerian shear-flow.* Astrophys. J. 446 (1995), 741–754.

T.M. Brown, J. Christensen–Dalsgaard, W.A. Dziembowski, P. Goode, D.O. Gough, *Inferring the Sun's internal angular velocity from observed p-mode frequency splittings.* Astrophys. J. 343 (1989), 526–546.

N.H. Brummell, F. Cattaneo & S.M. Tobias, *Linear and nonlinear dynamo properties of time-dependent ABC flows.* Fluid Dyn. Res. 28 (2001), 237–265.

E.C. Bullard & H. Gellman, *Homogeneous dynamos and terrestrial magnetism.* Phil. Trans. R. Soc. Lond. A 247 (1954), 213–278.

F.H. Busse, *Thermal instabilities in rapidly rotating systems.* J. Fluid Mech. 44 (1970), 441–460.

F.H. Busse, *Generation of magnetic fields by convection.* J. Fluid Mech. 57 (1973), 529–544.

F.H. Busse, *A necessary condition for the geodynamo.* J. Geophys. Res. 80 (1975), 278–280.

F.H. Busse, *Recent developments in the dynamo theory of planetary magnetism.* Ann. Rev. Earth Planet. Sci. 11 (1983), 241–268.

F.H. Busse, *Convection driven zonal flows and vortices in the major planets.* Chaos 4 (1994), 123–134.

F.H. Busse, *Homogeneous dynamos in planetary cores and in the laboratory.* Ann. Rev. Fluid Mech. 32 (2000), 383–408.

C.G. Campbell, *Magnetohydrodynamics of binary stars.* Kluwer (1997).

F. Cattaneo & D.W. Hughes, *Nonlinear saturation of the turbulent alpha effect.* Phys. Rev. E 54 (1996), 4532–4535.

F. Cattaneo & S.I. Vainshtein, *Suppression of turbulent transport by a weak magnetic field.* Astrophys. J. 376 (1991), L21–L24.

F. Cattaneo, D.W. Hughes & E.-J. Kim, *Suppression of chaos in a simplified nonlinear dynamo model.* Phys. Rev. Lett. 76 (1996), 2057–2060.

P. Chen & J.L. Milovich, *An explicit solution for static unbounded helical dynamos.* Geophys. Astrophys. Fluid Dynam. 30 (1984), 343–353.

S. Childress, *Construction of steady-state hydromagnetic dynamos. I. Spatially periodic fields.* Report MF–53, Courant Institute of Mathematical Sciences (1967).

S. Childress, *Théorie magnetohydrodynamique de l'effet dynamo.* Report: Departement Mécanique de la Faculté des Sciences. Université de Paris (1969).

S. Childress, *New solutions of the kinematic dynamo problem.* J. Math. Phys.

11 (1970), 3063–3076.
S. Childress, *Alpha-effect in flux ropes and sheets.* Phys. Earth Planet. Int. 20 (1979), 172–180.
S. Childress, *Fast dynamo theory.* In: Topological aspects of the dynamics of fluids and plasmas (ed. H.K. Moffatt, G.M. Zaslavsky, P. Comte, M. Tabor), pp. 111–147. Kluwer Academic Publishers (1992).
S. Childress & A.D. Gilbert, *Stretch, twist, fold: the fast dynamo.* Lecture Notes in Physics: Monographs. Springer–Verlag (1995).
S. Childress & A.M. Soward, *Convection driven hydromagnetic dynamos.* Phys. Rev. Lett. 29 (1972), 837–839.
S. Childress & A.M. Soward, *Scalar transport and alpha-effect for a family of cat's-eyes flows.* J. Fluid Mech. 205 (1989), 99–133.
S. Childress, R.R. Kerswell & A.D. Gilbert, *Bounds on dissipation for Navier–Stokes flow with Kolmogorov forcing.* Physica D 158 (2001), 105–128.
T.G. Cowling, *The magnetic field of sunspots.* Mon. Not. R. Astr. Soc. 140 (1934), 39–48.
T.G. Cowling, *Magnetohydrodynamics.* Interscience (1957).
E.E. DeLuca & P.A. Gilman, *Dynamo theory for the interface between the convection zone and the radiative interior of a star. Part I: Model equations and exact solutions.* Geophys. Astrophys. Fluid Dynam. 37 (1986), 85–127.
E.E. DeLuca & P.A. Gilman, *Dynamo theory for the interface between the convection zone and the radiative interior of a star. Part II: Numerical solutions of the nonlinear equations.* Geophys. Astrophys. Fluid Dynam. 43 (1988), 119–148.
M. Dikpati & P.A. Gilman, *Flux-transport dynamos with α-effect from global instability of tachocline differential rotation: a solution for magnetic parity selection in the Sun.* Astrophys. J. 559 (2001), 428–442.
W. Dobler, A.M. Shukurov & A. Brandenburg, *Nonlinear states of the screw dynamo.* Phys. Rev. E 65 (2002), 036311.
T. Dombre, U. Frisch, J.M. Greene, M. Hénon, A. Mehr & A.M. Soward, *Chaotic streamlines in the ABC flows.* J. Fluid Mech. 167 (1986), 353–391.
E.M. Drobyshevski & V.S. Yuferev, *Topological pumping of magnetic flux by three-dimensional convection.* J. Fluid Mech. 65 (1974), 33–44.
Y. Du & E. Ott, *Growth rates for fast kinematic dynamo instabilities of chaotic fluid flows.* J. Fluid Mech. 257 (1993), 265–288.
Y. Du, T. Tél & E. Ott, *Characterization of sign singular measures.* Physica D 76 (1994), 168–180.
M.L. Dudley & R.W. James, *Time-dependent kinematic dynamos with stationary flows.* Proc. R. Soc. Lond. A 425 (1989), 407–429.
W. Dziembowski, P.H. Goode & K.G. Libbrecht, *The radial gradient in the Sun's rotation.* Astrophys. J. 337 (1989), L53–L57.
W.M. Elsasser, *Induction effects in terrestrial magnetism, I. Theory.* Phys. Rev. 69 (1946), 106–116.
A.J. Faller & R.E. Kaylor, *A numerical study of the instability of laminar Ekman boundary layer flow.* J. Atmos. Sci. 23 (1966), 466–480.

Y. Fautrelle & S. Childress, *Convective dynamos with intermediate and strong fields.* Geophys. Astrophys. Fluid Dynam. 22 (1982), 235–279.

D.R. Fearn, *Nonlinear planetary dynamos.* In: Lectures on Solar and planetary dynamos (ed. M.R.E. Proctor, A.D. Gilbert), pp. 219–244. Cambridge University Press (1994).

D.R. Fearn, P.H. Roberts & A.M. Soward, *Convection, stability and the dynamo.* In: Energy stability and convection (ed. G.P. Galdi, B. Straughan), pp. 60–324. Longman (1988).

A. Ferriz-Mas, D. Schmitt & M. Schüssler, *A dynamo effect due to instability of magnetic flux tubes.* Astron. Astrophys. 289 (1994), 949–956.

J.M. Finn & E. Ott, *Chaotic flows and fast magnetic dynamos.* Phys. Fluids 31 (1988), 2992–3011.

U. Frisch, Z.S. She & P.-L. Sulem, *Large-scale flow driven by the anisotropic kinetic alpha effect.* Physica D 28 (1987), 382–392.

A.K. Gailitis, *Experimental aspects of a laboratory scale liquid sodium dynamo model.* In: Solar and planetary dynamos (ed. M.R.E. Proctor, P.C. Matthews, A.M. Rucklidge), pp. 91–98. Cambridge University Press (1993).

A.K. Gailitis & Ya.G. Freiberg, *Non-uniform model of a helical dynamo.* Magnetohydrodynam. 16 (1980), 11–15.

A.K. Gailitis, O.A. Lielausis, S. Dement'ev, E. Platacis, A. Cifersons, G. Gerbeth, T. Gundrum, F. Stefani, M. Christen, H. Hänel & G. Will, *Detection of a flow induced magnetic field eigenmode in the Riga dynamo facility.* Phys. Rev. Lett. 84 (2000), 4365–4368.

B. Galanti, N. Kleeorin & I. Rogachevskii, *Nonlinear dynamo in the ABC flow: the Hall effect.* Phys. Plasmas 1 (1994), 3843–3849.

B. Galanti, P.-L. Sulem & A. Pouquet, *Linear and nonlinear dynamos associated with ABC flows.* Geophys. Astrophys. Fluid Dynam. 66 (1992), 183–208.

D.J. Galloway & U. Frisch, *Dynamo action in a family of flows with chaotic streamlines.* Geophys. Astrophys. Fluid Dynam. 36 (1986), 53–83.

D.J. Galloway & M.R.E. Proctor, *Numerical calculations of fast dynamos for smooth velocity fields with realistic diffusion.* Nature 356 (1992), 691–693.

P. Garaud, *Latitudinal shear instability in the Solar tachocline.* Mon. Not. R. Astr. Soc. 324 (2001), 68–76.

R.D. Gibson & P.H. Roberts *The Bullard–Gellman dynamo.* In: The application of modern physics to the Earth and planetary interiors (ed. S.K. Runcorn), pp. 577–601. Wiley Interscience (1969).

A.D. Gilbert, *Fast dynamo action in the Ponomarenko dynamo.* Geophys. Astrophys. Fluid Dynam. 44 (1988), 214–258.

A.D. Gilbert, *Fast dynamo action in a steady chaotic flow.* Nature 350 (1991), 483–485.

A.D. Gilbert, *Magnetic field evolution in steady chaotic flows.* Phil. Trans. R. Soc. Lond. A 339 (1992), 627–656.

A.D. Gilbert, *Towards a realistic fast dynamo: models based on cat maps and pseudo-Anosov maps.* Proc. R. Soc. Lond. A 443 (1993), 585–606.

A.D. Gilbert, *Magnetic helicity in fast dynamos.* Geophys. Astrophys. Fluid Dynam. 96 (2002a), 135–151.

A.D. Gilbert, *Advected fields in maps: I. Magnetic flux growth in the stretch–fold–shear map.* Physica D, 166 (2002b), 167–196.

A.D. Gilbert & Y. Ponty, *Dynamos on stream surfaces of a highly conducting fluid.* Geophys. Astrophys. Fluid. Dynam. 93 (2000), 55–95.

A.D. Gilbert & P.-L. Sulem, *On inverse cascades in alpha effect dynamos.* Geophys. Astrophys. Fluid Dynam. 51 (1990), 243–261.

A.D. Gilbert, U. Frisch & A. Pouquet, *Helicity is unnecessary for alpha effect dynamos, but it helps.* Geophys. Astrophys. Fluid Dynam. 42 (1988), 151–161.

A.D. Gilbert, N.F. Otani & S. Childress, *Simple dynamical fast dynamos.* In: Solar and Planetary Dynamos (ed. M.R.E. Proctor, P.C. Matthews, A.M. Rucklidge), pp. 129–136. Cambridge University Press (1993).

P.A. Gilman, *Dynamically consistent nonlinear dynamos driven by convection in a rotating spherical shell. II. Dynamos with cycles and strong feedbacks.* Astrophys. J. Suppl. 53 (1983), 243–268.

P.A. Gilman & J. Miller, *Dynamically consistent nonlinear dynamos driven by convection in a rotating spherical shell.* Astrophys. J. Suppl. 46 (1981), 211–238.

G.A. Glatzmaier, *Numerical simulations of stellar convective dynamos. I. The model and method.* J. Comput. Phys. 55 (1984), 461–484.

G.A. Glatzmaier, *Numerical simulations of stellar convective dynamos. II. Field propagation in the convection zone.* Astrophys. J. 192 (1985a), 300–307.

G.A. Glatzmaier, *Numerical simulations of stellar convective dynamos. III. At the base of the convection zone.* Geophys. Astrophys. Fluid Dynam. 31 (1985b), 137–150.

G.A. Glatzmaier & P.H. Roberts, *A 3-dimensional self-consistent computer simulation of a geomagnetic-field reversal.* Nature 377 (1995a), 203–209.

G.A. Glatzmaier & P.H. Roberts, *A 3-dimensional convective dynamo solution with rotating and finitely conducting inner core and mantle* Phys. Earth Planet. Inter. 91 (1995b), 63–75.

G.A. Glatzmaier & P.H. Roberts, *Simulating the geodynamo.* Contemp. Phys. 38 (1997), 269–288.

G.A. Glatzmaier & P.H. Roberts, *The geodynamo, past, present and future.* Geophys. Astrophys. Fluid Dynam. 94 (2001), 47–84.

D.O. Gough & M.E. McIntyre, *Inevitability of a magnetic field in the Sun's radiative interior.* Nature 394 (1998), 755–757.

D.O. Gough, T. Sekii & P.B. Stark, *Inferring spatial variation of Solar properties from helioseismic data.* Astrophys. J. 459 (1996), 779–791.

A.V. Gruzinov & P.H. Diamond, *Nonlinear mean field electrodynamics of turbulent dynamos.* Phys. Plasmas 3 (1996), 1853–1857.

A. Herzenberg, *Geomagnetic dynamos.* Phil. Trans. R. Soc. Lond. A 250 (1958), 543–583.

W. Hirsching & F.H. Busse, *Stationary and chaotic dynamos in rotating spherical shells*. Phys. Earth Planet. Int. 90 (1995), 243–254.

R. Hollerbach, *On the theory of the geodynamo.* Phys. Earth Planet. Int. 98 (1996), 163–185.

R. Hollerbach, D.J. Galloway & M.R.E. Proctor, *Numerical evidence of fast dynamo action in a spherical shell.* Phys. Rev. Lett. 74 (1995), 3145–3148.

P. Hoyng, *Turbulent transport of magnetic fields. III. Stochastic excitation of global magnetic modes.* Astrophys. J. 332 (1988), 857–871.

D.W. Hughes & M.R.E. Proctor, *Magnetic fields in the Solar convection zone: magnetoconvection and magnetic buoyancy.* Ann. Rev. Fluid Mech. 20 (1988), 187–223.

D.J. Ivers & R.W. James, *Axisymmetric anti-dynamo theorems in compressible non-uniform conducting fluids.* Phil. Trans. R. Soc. Lond. A 312 (1984), 179–218.

C.A. Jones & P.H. Roberts, *Convection driven dynamos in a rotating plane layer.* J. Fluid Mech. 404 (2000), 311–331.

R. Kaiser, *Towards a poloidal magnetic field theorem.* Geophys. Astrophys. Fluid Dynam. 80 (1995), 129–144.

R. Kaiser, B.J. Schmitt & F.H. Busse, *On the invisible dynamo.* Geophys. Astrophys. Fluid Dynam. 77 (1994), 93–109.

A.P. Kazantsev, *Enhancement of a magnetic field by a conducting fluid.* Sov. Phys. JETP 26 (1968), 1031–1034.

E.-J. Kim, D.W. Hughes & A.M. Soward, *An investigation into high conductivity dynamo action driven by rotating convection.* Geophys. Astrophys. Fluid Dynam. 91 (1999), 303–339.

I. Klapper, *A study of fast dynamo action in chaotic helical cells.* J. Fluid Mech. 239 (1992), 359–381.

I. Klapper, *Shadowing and the diffusionless limit in fast dynamo theory.* Nonlinearity 6 (1993), 869–884.

I. Klapper & L.-S. Young, *Bounds on the fast dynamo growth rate involving topological entropy.* Comm. Math. Phys. 173 (1995), 623–646.

R.H. Kraichnan, *Diffusion of weak magnetic fields by isotropic turbulence.* J. Fluid Mech. 75 (1976a), 657–676.

R.H. Kraichnan, *Diffusion of passive-scalar and magnetic fields by helical turbulence.* J. Fluid Mech. 77 (1976b), 753–768.

F. Krause & R. Meinel, *Stability of simple nonlinear α^2-dynamos.* Geophys. Astrophys. Fluid Dynam. 43 (1988), 95–117.

F. Krause & K.-H. Rädler, *Mean-field magnetohydrodynamics and dynamo theory.* Pergamon Press (1980).

R.M. Kulsrud, *A critical review of galactic dynamos.* Ann. Rev. Astron. Astrophys. 37 (1999), 37–64.

L.D. Landau & E.M. Lifshitz, *The classical theory of fields.* Pergamon Press (1975).

A. Lanotte, A. Noullez, M. Vergassola & A. Wirth, *Large-scale dynamo by negative magnetic eddy diffusivities.* Geophys. Astrophys. Fluid Dynam. 91

(1999), 131–146.

J. Larmor, *How could a rotating body such as the Sun become a rotating magnet?* Rep. Brit. Assoc. Adv. Sci. (1919), 159–160.

Yu.D. Latushkin & A.M. Stepin, *Weighted translation operators and linear extensions of dynamical systems.* Russian Math. Surveys 46(2) (1991) 95–165.

Y.-T. Lau & J.M. Finn, *Fast dynamos with finite resistivity in steady flows with stagnation points.* Phys. Fluids B 5 (1993), 365–375.

S. Leibovich & S.K. Lele, *The influence of the horizontal component of Earth's angular velocity on the instability of the Ekman layer.* J. Fluid Mech. 150 (1985), 41–87.

D.K. Lilly, *On the instability of Ekman boundary flow.* J. Atmos. Sci. 23 (1966), 481–494.

D. Lortz, *Exact solutions of the hydromagnetic dynamo problem.* Plasma Phys. 10 (1968), 967–972.

F.J. Lowes & I. Wilkinson, *Geomagnetic dynamo: a laboratory model.* Nature 198 (1963), 1158–1160.

F.J. Lowes & I. Wilkinson, *Geomagnetic dynamo: an improved laboratory model.* Nature 219 (1968), 717–718.

J. Maksymczuk & A.D. Gilbert, *Remarks on the equilibration of high conductivity dynamos.* Geophys. Astrophys. Fluid Dynam. 90 (1998), 127–137.

W.V.R. Malkus, *Energy sources for planetary dynamos.* In: Lectures on Solar and planetary dynamos (ed. M.R.E. Proctor, A.D. Gilbert), pp. 161–179. Cambridge University Press (1994).

P.C. Matthews, *Dynamo action in simple convective flows.* Proc. R. Soc. Lond. A 455 (1999), 1829–1840.

N. Meunier, M.R.E. Proctor, D.D. Sokoloff, A.M. Soward & S.M. Tobias, *Asymptotic properties of a nonlinear $\alpha\omega$-dynamo wave: period, amplitude and latitudinal dependence.* Geophys. Astrophys. Fluid Dynam. 86 (1997), 249–285.

M.S. Miesch, J.R. Elliott, J. Toomre, T.L. Clune, G.A. Glatzmaier & P.A. Gilman, *Three-dimensional spherical simulations of Solar convection. I. Differential rotation and pattern evolution achieved with laminar and turbulent states.* Astrophys. J. 532 (2000), 593–615.

H.K. Moffatt, *The degree of knottedness of tangled vortex lines.* J. Fluid Mech. 35 (1969), 117–129.

H.K. Moffatt, *Magnetic field generation in electrically conducting fluids.* Cambridge University Press (1978).

H.K. Moffatt & M.R.E. Proctor, *Topological constraints associated with fast dynamo action.* J. Fluid Mech. 154 (1985), 493–507.

H.K. Moffatt & R.L. Ricca, *Helicity and the Călugăreanu invariant.* Proc. R. Soc. Lond. A 439 (1992), 411–429.

S.A. Molchanov, A.A. Ruzmaikin & D.D. Sokoloff, *Kinematic dynamo in random flow.* Sov. Phys. Usp. 28 (1985) 307–327.

V.I. Oseledets, *Liapunov entropy and the spectral radius of the dynamo op-*

erator. Sixth International Symposium on Information Theory, Tashkent, 1984, Abstracts, Part 3, pp. 162–163. IPI (1984).

V.I. Oseledets, *Fast dynamo problem for a smooth map on a two-torus.* Geophys. Astrophys. Fluid Dynam. 73 (1993), 133–145.

N.F. Otani, *A fast kinematic dynamo in two-dimensional time-dependent flows.* J. Fluid Mech. 253 (1993), 327–340.

E. Ott, *Chaotic flows and kinematic magnetic dynamos: A tutorial review.* Phys. Plasmas 5 (1998), 1636–1646.

E.N. Parker, *Hydromagnetic dynamo models.* Astrophys. J. 122 (1955), 293–314.

E.N. Parker, *Cosmical magnetic fields.* Clarendon Press (1979).

E.N. Parker, *A Solar dynamo surface wave at the interface between convection and non-uniform rotation.* Astrophys. J. 408 (1993), 707–719.

R.L. Parker, *Reconnexion of lines of force in rotating spheres and cylinders.* Proc. R. Soc. Lond. A 291 (1966), 60–72.

F.W. Perkins & E.G. Zweibel, *A high magnetic Reynolds number dynamo.* Phys. Fluids 30 (1987), 1079–1084.

F. Plunian, P. Marty & A. Alemany, *Kinematic dynamo action in a network of screw motions; application to the core of a fast breeder reactor.* J. Fluid Mech. 382 (1999), 137–154.

Yu.B. Ponomarenko, *On the theory of hydromagnetic dynamos.* Zh. Prikl. Mekh. & Tekh. Fiz. (USSR) 6 (1973), 47–51.

Y. Ponty, A.D. Gilbert & A.M. Soward, *Kinematic dynamo action in large magnetic Reynolds number flows driven by shear and convection.* J. Fluid Mech. 435 (2001), 261–287.

Y. Ponty, A.D. Gilbert & A.M. Soward, *The onset of thermal convection in Ekman–Couette shear flow with oblique rotation.* J. Fluid Mech.487 (2003), 91–123.

Y. Ponty, A. Pouquet & P.-L. Sulem, *Dynamos in weakly chaotic two-dimensional flows.* Geophys. Astrophys. Fluid Dynam. 79 (1995), 239–257.

A. Pouquet, U. Frisch & J. Léorat, *Strong MHD turbulence and the nonlinear dynamo effect.* J. Fluid Mech. 77 (1976), 321–354.

T. Prautzsch, *The dynamo mechanism in the deep convection zone of the Sun.* In: Solar and planetary dynamos (ed. M.R.E. Proctor, P.C. Matthews, A.M. Rucklidge), pp. 249–256. Cambridge University Press (1993).

M.R.E. Proctor, *On Backus' necessary condition for dynamo action in a conducting sphere.* Geophys. Astrophys. Fluid Dynam. 9 (1977), 89–93.

M.R.E. Proctor, *Convection and magnetoconvection in rapidly rotating spheres.* In: Lectures on Solar and planetary dynamos (ed. M.R.E. Proctor & A.D. Gilbert), pp. 97–115, Cambridge University Press (1994).

M.R.E. Proctor & A.D. Gilbert (eds.), *Lectures on Solar and planetary dynamos.* Cambridge University Press (1994).

M.R.E. Proctor & N.O. Weiss, *Magnetoconvection.* Rep. Prog. Phys. 45 (1982), 1317–1379.

G.O. Roberts, *Spatially periodic dynamos.* Phil. Trans. R. Soc. Lond. A 266

(1970), 535–558.

G.O. Roberts, *Dynamo action of fluid motions with two-dimensional periodicity.* Phil. Trans. R. Soc. Lond. A 271 (1972), 411–454.

P.H. Roberts, *An introduction to magnetohydrodynamics.* Elsevier (1967).

P.H. Roberts, *Dynamo theory.* In: Mathematical problems in the geophysical sciences, vol. 2 (ed. W.H. Reid), pp. 129–206. Lectures in Applied Mathematics, vol. 14. AMS Publications (1971).

P.H. Roberts, *Dynamo theory.* In: Irreversible phenomena and dynamical systems analysis in geosciences (ed. C. Nicolis, G. Nicolis), pp. 73–133. Reidel (1987).

P.H. Roberts, *Fundamentals of dynamo theory.* In: Lectures on Solar and planetary dynamos (ed. M.R.E. Proctor, A.D. Gilbert), pp. 1–58. Cambridge University Press (1994).

P.H. Roberts & A.M. Soward, *Dynamo theory.* Ann. Rev. Fluid Mech. 24 (1992), 459–512.

M.N. Rosenbluth, H.L. Berk, I. Doxas & W. Horton, *Effective diffusion in laminar convective flows.* Phys. Fluids 30 (1987), 2636–2647.

G. Rüdiger & A. Brandenburg, *A Solar dynamo in the overshoot layer: cycle period and butterfly diagram.* Astron. Astrophys. 296 (1995), 557–566.

H.H. Rugh, *The correlation spectrum for hyperbolic analytic maps.* Nonlinearity 5 (1992), 1237–1263.

A.A. Ruzmaikin, D.D. Sokoloff & A.M. Shukurov, *A hydromagnetic screw dynamo.* J. Fluid Mech. 197 (1988a), 39–56.

A.A. Ruzmaikin, D.D. Sokoloff & A.M. Shukurov, *Magnetism of spiral galaxies.* Nature 336 (1988b), 341–347.

G.R. Sarson, C.A. Jones & K. Zhang, *Dynamo action in a uniform ambient field.* Phys. Earth Planet. Int. 111 (1999), 47–68.

B.I. Shraiman, *Diffusive transport in a Rayleigh–Bénard convection cell.* Phys. Rev. A 36 (1987), 261–267.

A.M. Shukurov & D.D. Sokoloff, *Evolution of magnetic fields in a swirling jet.* In: Solar and planetary dynamos (ed. M.R.E. Proctor, P.C. Matthews, A.M. Rucklidge), pp. 271–274. Cambridge University Press (1993).

A.A. Solovyev, *Excitation of magnetic field by the axisymmetric motion of a conducting fluid.* Izv. Akad. Nauk USSR, Fiz. Zemli, no. 4 (1985), 101–103.

A.A. Solovyev, *Magnetic field excitation by conducting fluid flow at high magnetic Reynolds numbers.* Izv. Akad. Nauk USSR, Fiz. Zemli, no. 5 (1987), 77–80.

A.M. Soward, *A convection driven dynamo I. The weak field case.* Phil. Trans. R. Soc. Lond. A 275 (1974), 611–651.

A.M. Soward, *A thin disc model of the galactic dynamo.* Astron. Nachr. 299 (1978), 25–33.

A.M. Soward, *Fast dynamo action in a steady flow.* J. Fluid Mech. 180 (1987), 267–295.

A.M. Soward, *A unified approach to a class of slow dynamos.* Geophys. Astrophys. Fluid Dynam. 53 (1990), 81–107.

A.M. Soward, *The Earth's dynamo.* Geophys. Astrophys. Fluid Dynam. 62 (1991), 191–209.

A.M. Soward, *Thin disc kinematic $\alpha\omega$-models I. Long length scale modes.* Geophys. Astrophys. Fluid Dynam. 64 (1992a), 163–199.

A.M. Soward, *Thin disc kinematic $\alpha\omega$-models II. Short length scale modes.* Geophys. Astrophys. Fluid Dynam. 64 (1992b), 201–225.

A.M. Soward, *Fast dynamos.* In: Lectures on Solar and planetary dynamos (ed. M.R.E. Proctor, A.D. Gilbert), pp. 181–217. Cambridge University Press (1994a).

A.M. Soward, *On the role of stagnation points and periodic particle paths in a two-dimensional pulsed flow fast dynamo model.* Physica D 76 (1994b), 181–201.

A.M. Soward & S. Childress, *Large magnetic Reynolds number dynamo action in spatially periodic flow with mean motion.* Phil. Trans. R. Soc. Lond. A 331 (1990), 649–733.

E.A. Spiegel, *The chaotic Solar cycle.* In: Lectures on Solar and planetary dynamos (ed. M.R.E. Proctor, A.D. Gilbert), pp. 245–265. Cambridge University Press (1994).

E.A. Spiegel & J.-P. Zahn, *The Solar tachocline.* Astron. Astrophys. 265 (1992), 106–114.

M. Steenbeck, F. Krause & K.-H. Rädler, *A calculation of the mean electromotive force in an electrically conducting fluid in turbulent motion, under the influence of Coriolis forces.* Z. Naturforsch. 21a (1966), 369–376.

R. Stieglitz & U. Müller, *Experimental demonstration of a homogeneous two-scale dynamo.* Phys. Fluids 13 (2001), 561–564.

M. Stix, *The galactic dynamo.* Astron. Astrophys. 42 (1975), 85–89.

M. Stix, *Erratum: the galactic dynamo.* Astron. Astrophys. 68 (1978), 459.

M.G. St. Pierre, *The strong field branch of the Childress–Soward dynamo.* In: Solar and planetary dynamos (ed. M.R.E. Proctor, P.C. Matthews, A.M. Rucklidge), pp. 295–302. Cambridge University Press (1993).

J.-C. Thelen, *A mean electromotive force induced by magnetic buoyancy instabilities.* Mon. Not. R. Astr. Soc. 315 (2000), 155–164.

A. Tilgner, *Towards experimental fluid dynamos.* Phys. Earth Planet. Int. 117 (2000), 171–177.

S.M. Tobias, N.H. Brummell, T.L. Clune & J. Toomre, *Transport and storage of magnetic field by overshooting turbulent compressible convection.* Astrophys. J. 549 (2001), 1183–1203.

S.M. Tobias, M.R.E. Proctor & E. Knobloch, *Convective and absolute instabilities of fluid flows in finite geometry.* Physica D 113 (1998), 43–72.

S.I. Vainshtein & F. Cattaneo, *Nonlinear restrictions on dynamo action.* Astrophys. J. 393 (1992), 199–203.

S.I. Vainshtein & Ya.B. Zeldovich, *Origin of magnetic fields in astrophysics.* Sov. Phys. Usp. 15 (1972) 159–172.

S.I. Vainshtein, E.N. Parker & R. Rosner, *On the generation of 'strong' magnetic fields.* Astrophys. J. 404 (1993), 773–780.

S.I. Vainshtein, R.Z. Sagdeev, R. Rosner & E.-J. Kim, *Fractal properties of the stretch–twist–fold magnetic dynamo.* Phys. Rev. E 53 (1996), 4729–4744.

S.I. Vainshtein, R.Z. Sagdeev & R. Rosner, *Stretch–twist–fold and ABC nonlinear dynamos: restricted chaos.* Phys. Rev. E 56 (1997), 1605–1622.

M.M. Vishik, *Magnetic field generation by the motion of a highly conducting fluid.* Geophys. Astrophys. Fluid Dynam. 48 (1989), 151–167.

E.T. Vishniac & J. Cho, *Magnetic helicity conservation and astrophysical dynamos.* Astrophys. J. 550 (2001), 752–760.

N.O. Weiss, *The expulsion of magnetic flux by eddies.* Proc. R. Soc. Lond. A 293 (1966), 310–328.

N.O. Weiss, *Solar and stellar dynamos.* In: Lectures on Solar and planetary dynamos (ed. M.R.E. Proctor, A.D. Gilbert), pp. 59–95. Cambridge University Press (1994).

L. Woltjer, *A theorem on force-free magnetic fields.* Proc. Nat. Acad. Sci. USA 44 (1958), 489–491.

H. Yoshimura, *Solar cycle dynamo wave propagation.* Astrophys. J. 201 (1975), 740–748.

Ya.B. Zeldovich, *The magnetic field in the two-dimensional motion of a conducting turbulent liquid.* Sov. Phys. JETP 4 (1957), 460–462.

Ya.B. Zeldovich, A.A. Ruzmaikin & D.D. Sokoloff, *Magnetic Fields in Astrophysics.* The fluid mechanics of astrophysics and geophysics, vol. 3. Gordon & Breach (1983).

Ya.B. Zeldovich, S.A. Molchanov, A.A. Ruzmaikin & D.D. Sokoloff, *Intermittency, diffusion, and generation in a nonstationary medium.* Sov. Sci. Rev. C Math. Phys. 7 (1988), 1–110.

K. Zhang & F.H. Busse, *Finite amplitude convection and magnetic field generation in a rotating spherical shell.* Geophys. Astrophys. Fluid Dynam. 44 (1988), 33–53.

K. Zhang & F.H. Busse, *Convection driven magnetohydrodynamic dynamos in rotating spherical shells.* Geophys. Astrophys. Fluid Dynam. 49 (1989), 97–116.

V.A. Zheligovsky, *A kinematic magnetic dynamo sustained by a Beltrami flow in a sphere.* Geophys. Astrophys. Fluid Dynam. 73 (1993), 217–254.

E.G. Zweibel, *Ambipolar diffusion drifts and dynamos in turbulent gases.* Astrophys. J. 329 (1988), 384–391.